

## Durham E-Theses

---

### *Measurements on the growth of gaseous ionization at ultra high frequencies*

Nicholls, M.J.

#### How to cite:

---

Nicholls, M.J. (1978) *Measurements on the growth of gaseous ionization at ultra high frequencies*, Durham theses, Durham University. Available at Durham E-Theses Online:  
<http://etheses.dur.ac.uk/9325/>

#### Use policy

---

The full-text may be used and/or reproduced, and given to third parties in any format or medium, without prior permission or charge, for personal research or study, educational, or not-for-profit purposes provided that:

- a full bibliographic reference is made to the original source
- a [link](#) is made to the metadata record in Durham E-Theses
- the full-text is not changed in any way

The full-text must not be sold in any format or medium without the formal permission of the copyright holders.

Please consult the [full Durham E-Theses policy](#) for further details.

**MEASUREMENTS ON THE GROWTH OF GASEOUS IONIZATION  
AT ULTRA HIGH FREQUENCIES**

by

**M.J. Nicholls, B.Sc.,**

**Being an account of the work carried  
out at the University of Durham during  
the period Sept. 1956 to Sept. 1959.**

**Thesis submitted to the University of Durham  
in support of an application for a Degree of Ph.D.**

The copyright of this thesis rests with the author.  
No quotation from it should be published without  
his prior written consent and information derived  
from it should be acknowledged.



## PREFACE

An apparatus has been built to study ionization by collision in a gas under ultra high frequency fields and especially the conditions covering the transition to the conducting state. The u.h.f. field is developed between two Rogowski profiled electrodes incorporated into a tuned quarter wave transmission line which is loosely coupled to the main oscillator. The u.h.f. field has a frequency of 106 Mc/sec. and its magnitude is measured by its effect on the frequency of oscillation of a small metal disc suspended in the gap. This instrument is used as a step-over so that a rectifying circuit loosely coupled to the transmission line can be calibrated. The disc can be removed from the gap during the experiments.

Electrons are emitted from a thermionic cathode situated inside one of the electrodes and diffuse out into the gap through small holes in the electrode shell where they are moved across the gap by a small unidirectional field. The large u.h.f. field is superimposed on this field so that the electrons acquire enough energy to ionize the gas by collision; the resulting electron current to the far electrode is measured by a galvanometer.

With this arrangement the amplification resulting from collision ionization can be measured and its dependence on the life-time of the electron in the gap can be studied. The

measurements can be carried right up to breakdown conditions, and the results can be expressed in terms of the number of ionizing collisions per second in the life of one electron, a coefficient closely related to Townsend's  $\alpha$  .

It is shown that the lifetime of the electrons not only depends on the drift under the direct field but also on the process of diffusion out of the gap and two methods of evaluating it are given.

Although only preliminary results have been obtained these are sufficient to indicate that a useful contribution to ionization studies can be made by investigations with this apparatus.

## CONTENTS

	Page.	
CHAPTER 1	INTRODUCTION	1
CHAPTER II	THE DESIGN AND THEORETICAL ASPECTS OF THE PROBLEM.	12
CHAPTER III	A BRIEF DESCRIPTION OF THE APPARATUS.	19
CHAPTER IV	THE ULTRA HIGH FREQUENCY OSCILLATOR.	23
CHAPTER V	THE PRODUCTION OF THE U.H.F. FIELD BETWEEN THE TEST ELECTRODES.	26
CHAPTER VI	THE ELECTRODE ASSEMBLY.	31
CHAPTER VII	THE MEASUREMENT OF THE U.H.F. FIELD.	39
CHAPTER VIII	THE DETERMINATION OF THE TRANSIT TIME.	51
CHAPTER IX	THE DIRECT CURRENT MEASURING SYSTEM.	55
CHAPTER X	THE EVACUATING AND GAS CONTROL SYSTEM.	60
CHAPTER XI	MEASUREMENT OF THE PRE-BREAKDOWN IONIZATION IN HYDROGEN.	63
CHAPTER XII	A DISCUSSION OF THE POSSIBLE CAUSES OF THE REDUCTION OF THE ELECTRON CURRENT TO THE COLLECTING ELECTRODE.	68
CHAPTER XIII	THE DETERMINATION OF THE AVERAGE LIFETIME OF AN ELECTRON IN THE ELECTRODE GAP.	80
CHAPTER XIV	RESULTS AND DISCUSSION.	91
	ACKNOWLEDGEMENTS.	96
	REFERENCES.	97
APPENDIX I.	CALIBRATION OF THE DIRECT CURRENT MEASURING GALVANOMETERS.	99

CHAPTER I  
INTRODUCTION.

Investigations into the nature of the breakdown of gases by high frequency fields have afforded much evidence for determining the operative mechanisms before and after breakdown, not only for this type of field but for direct fields as well. Apart from the theoretical aspects of the investigations there are the more practical aspects such as the determination of the limiting power carried by wave guides and aerials, (Paska 1955 and McDonald 1959), ion sources for nuclear physics and thermonuclear physics, and the detection of ionising radiation. Most practical cases of gas breakdown under both high frequency fields and direct fields depend on so many parameters that investigations tend to be meaningless. It is only by investigating the breakdown phenomena in pure gases under controlled conditions that the possible mechanism of the change of a gas, from behaving as a near perfect insulator before breakdown, to a near perfect conductor afterwards, can be determined.

D.C. Breakdown.

Of the many investigations made of the breakdown mechanism in uniform and non uniform direct fields, perhaps the most notable are those of Townsend, 1910, and latterly Llewellyn Jones and others, 1950. It has been established that under steady direct fields two conditions have to be fulfilled before



the onset of a discharge. These conditions are, firstly, that an electron moving through the gas shall produce an avalanche of further electrons by collision processes and secondly, that as a result of this avalanche further electrons shall be generated in the gap or at the cathode in order to replace those electrons arriving at the anode, and hence continue the transfer of charge. Townsend showed that at low gas pressures in air, nitrogen and hydrogen the amplification of a photoelectric current by a uniform direct field at constant  $E/p$ , where  $E$  is the field and  $p$  the pressure, resulted initially from collision ionisation in the gap. If one electron produces  $\alpha$  ion pairs by collision with gas atoms in travelling one cm., then in moving a distance  $x$  cm. from the cathode it will produce  $n$  electrons, where  $n = e^{\alpha x}$ . Furthermore, if  $I_0$  is the initial photoelectric current generated at the cathode, and  $I$  the current arriving at the anode a distance  $d$  cm. away, then  $I = I_0 e^{\alpha d}$ . The coefficient  $\alpha$  is known as Townsend's first coefficient and is dependent on the energy of the electrons which is a function of  $E/p$ . For increasing gap widths and constant  $E/p$ , i.e. large  $d$  and constant  $\alpha$ , the increase in  $I$  at gap widths slightly smaller than the gap width for breakdown, is more than exponential because secondary processes come into operation and fulfil the second condition as outlined above. Fig. 1.1 shows curves relating the amplification to the gap width for various gases. These

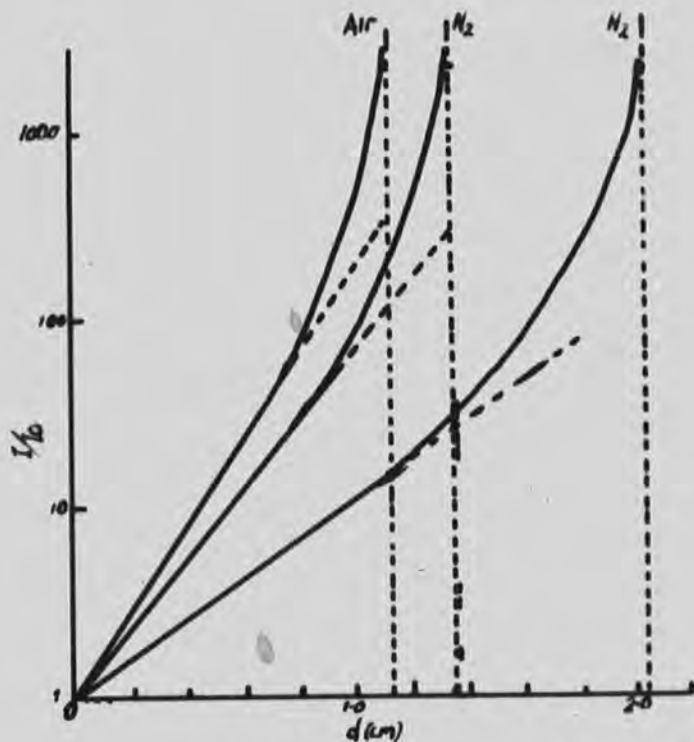


FIG.1.1 TYPICAL  $\log I/I_0$  vs. CURVES FROM LEWELLYN JONES 1951.

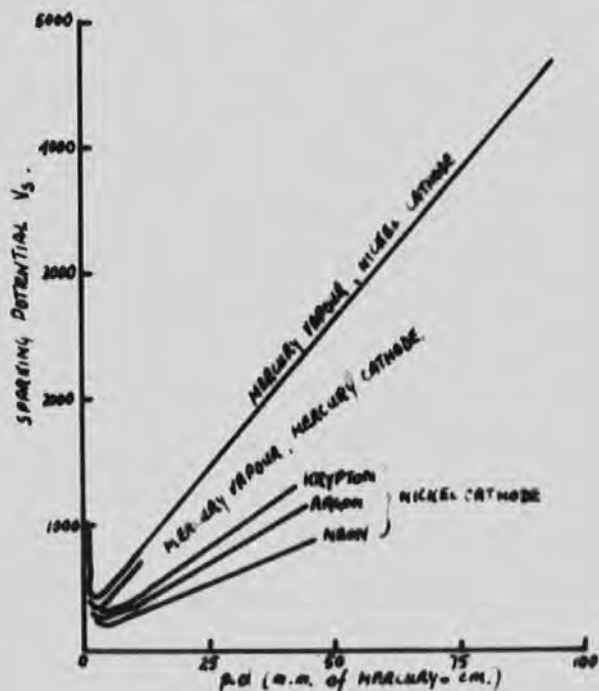


FIG.1.2 PASCHEN CURVES FROM LEWELLYN JONES 1951.



relationships can be fully represented by the equation:

$$\frac{I}{I_0} = \frac{e^{\alpha d}}{1 - \frac{w}{\alpha} e^{\alpha d - 1}}$$

where  $w$  is the number of secondary electrons produced at the cathode by an electron in the gap; the breakdown condition is represented by the denominator approaching zero, i.e.  $\frac{w}{\alpha} e^{\alpha d - 1} = 1$

The secondary processes are consistent with the assumption of extra cathode emission caused by the incidence of positive ions and photons; collision ionization being relatively slight.

Since both  $\alpha/p$  and  $w$  are functions of  $E/p$ , i.e.  $V/p.d$ , where  $V$  is the voltage applied to the gap, it follows from the above criterion for breakdown that  $V_B$ , the breakdown voltage, is a function of  $p.d_B$ , where  $d_B$  is the minimum gap width that will break down under  $V_B$ . This was established experimentally by Paschen, 1889 and is known as Paschen's Law. Fig. 1.2 shows a graphical example of this type of function, where the minima correspond to the transition from relatively few electron-molecule, or electron-atom collisions per second to many collisions per second. Both these conditions result in fewer ionizing events due in the first case to the low probability of collision, and in the second to the high energy loss in the elastic collisions.

It was natural to assume that this type of mechanism would be operative at higher pressures but subsequent experiments tended to conflict with the argument. Rogowski, 1926 had

found that on applying a voltage pulse to a gap the voltage collapsed in  $10^{-6}$  to  $10^{-7}$  seconds, a very much faster time than the transit time of the positive ions. This indicated the possible absence of any secondary processes if the effect of photons was ignored. This was supported by the fact that several workers, e.g. Loeb, 1939, had found that the graphs of  $\text{Log } I/I_0$  versus  $d$  seemed to be linear even when the electrode separation was very near to that at which breakdown occurred. If this were the case some other mechanism must have acted quite rapidly under breakdown conditions. This led to many theories of breakdown such as the Loeb streamer Theory, 1928, 1939, to replace the Townsend mechanism. The Streamer Theory suggests that additional electrons are produced in the gap ahead of the main avalanche by photoionization.

Explanations of breakdown based on the Streamer Theory continued to be favoured because the experiments were not accurate enough to show that the Townsend mechanism might operate after all. However, careful thought by Llewellyn Jones at Swansea, 1950, 1952, resulted in the design of experiments which showed that the breakdown mechanism was of the Townsend type over a very wide range, and that there was no significant effect due to space charge between the current limits of  $10^{-16}$  and  $10^{-7}$  amps.

#### A.C. Breakdown.

With low frequency fields the effect of each half cycle

will be similar to that of applying a direct voltage pulse across the gap in question, in which case the peak field will determine whether the gap will break down. When breakdown takes place under these conditions it is said to be in the low frequency breakdown region, (l.f.).

At very much higher frequencies, as the electron swarm approaches the anode the field changes and reverses the direction of motion of the electrons and an avalanche continues to build up due to the general drift velocity in each direction. It is possible even at high stresses for the electron movement to be limited to the inter-electrode space and consequently the rate of removal of the electrons to the electrodes will be less than the corresponding D.C. case and the breakdown stress will be smaller. This frequency region is known as the ultra high frequency region and although large electron or ion currents are not collected by the electrodes, breakdown does occur in the sense that the energy supplied by the high frequency field generator is dissipated by the electrons in the gap.

At frequencies between the low frequency case and the ultra high frequency case, reductions in breakdown stress have been observed and associated with the positive ions not being swept to the electrodes during a half cycle of the field. Although positive ions do not appreciably contribute to the increase in electron and ion population by collision ionization

the non-removal of the ions result in a residual positive space charge which enhances the value of the field (Reukema, 1927).

However Fucks and others, 1957, using low values of p.d. have found that the breakdown stress actually increases above the D.C. breakdown stress for frequencies in this region, and have observed two maxima, as shown in Fig. 1.3. Their explanation of these maxima is that the first maximum is due to the finite transit time of the positive ions affecting the secondary emission at the electrodes, and the second maximum to the transit time of the electrons, reducing the mean velocity attainable, and hence their ionizing efficiency. At higher frequencies they observed a reduction in the breakdown stress associated with the usual ultra high frequency conditions. It is apparent that at the low values of p.d. used by Fucks et.al. there was no space charge in the gap, and their results can be reconciled with the other results described above. This frequency region, between the low frequency and the ultra high frequency region, is known as the high frequency region.

When the frequency is high or the pressure very low, the field frequency approaches the collision frequency of the electrons so that there is a transition from a state of many collisions per oscillation to a state of many oscillations per collision, resulting in fewer ionizations. In this region the electrons tend to oscillate out of phase with the

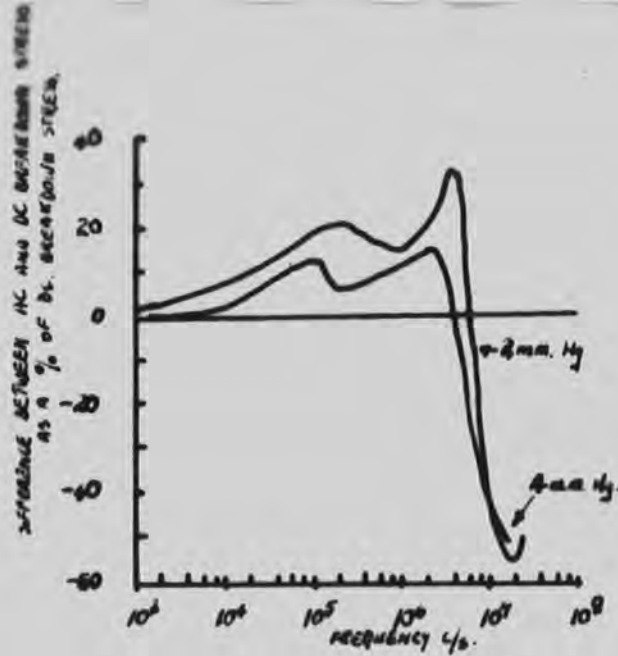


FIG. 1.3

DIFFERENCE BETWEEN AC AND DC BREAKDOWN STRESS AS A % OF DC BREAKDOWN STRESS AS A FUNCTION OF FREQUENCY. GAP BOTH 208  $\mu\text{m}$ .

*not used because - from 20 regions see Fig 1.3 and pg. 17*

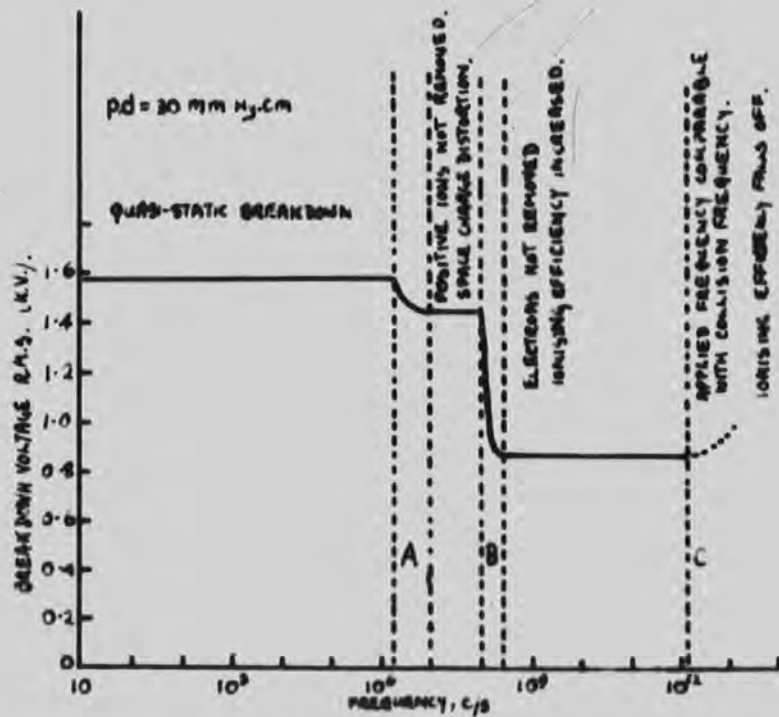


FIG. 1.4

BREAKDOWN VOLTAGE FOR A 20 mm. GAP AT ATMOSPHERIC PRESSURE.

TRANSITION A BASED ON LAGER, 1931.

TRANSITION B BASED ON GILL + DORRINGTON, 1931.

TRANSITION C BASED ON LAGER, 1931.

FROM PROJE, 1950

field and Margenau, 1946, has calculated the effective field causing ionization which is given by:

$$E_e^2 = \frac{\nu_c^2}{\nu_c^2 + \omega^2} \cdot E_u^2$$

where  $\nu_c$  is the collision frequency and  $\omega$  the angular frequency of the field. Consequently the necessary stress that has to be applied to produce breakdown increases at high frequencies, the transition being marked by a minimum in the breakdown characteristic provided that the dimensions of the gas vessel and the electrode separation are large compared with the electron orbit under the applied field.

The various frequency regions are represented graphically in Fig. 1.4. This curve is not plotted from observations made in one experiment as the techniques differ for particular frequencies but is merely an indication of the frequency regions assembled from the results of many observers.

#### Ultra High Frequency Breakdown.

The nature of the transition to the ultra high frequency breakdown region from the high frequency region was investigated by C. and H. Gutton, 1928, and later by Gill and Donaldson, 1931, who observed under certain conditions a minimum in the breakdown characteristic,  $p$  against  $V$ . The position of this minimum was shown to be dependent on the field frequency and corresponded to the pressure at which the electrons were just being swept to the electrodes for that particular frequency,

Fig. 1.5. Further experiments of this type have been conducted by Gill and von Engel, 1949, who showed that an abrupt variation of breakdown potential occurs when electrons can just traverse the distance between opposite electrodes.

When the conditions are such that the electrons do not reach the electrodes or the vessel walls, the action of the secondary processes plays no part in the breakdown and the breakdown stress is independent of the nature of the electrodes. This was shown to be the case by Llewellyn Jones and Morgan, 1951, using both clean and oxidised electrodes, when considerable difference could be expected in any secondary emission, but they observed that both breakdown characteristics were identical.

In this region the mechanism of breakdown consists of two processes; the generation of electrons, usually by single electron collisions with gas atoms or molecules, and the loss of electrons by diffusion, attachment and recombination. The generation of electrons is of the type involving Townsend's coefficient  $\alpha$ , so that the breakdown field can be calculated if the value of  $\alpha$ , the energy distribution function and the rate of loss are known.

This has been further developed by Holstein, 1946, and Herlin and Brown, 1948, for a gas in which the electron attachment and recombination are negligible, when the criterion can be taken as the condition that the rate of electron

TRANSVERSE  
(FULL LINES)

LONGITUDINAL  
(DOTTED LINE)

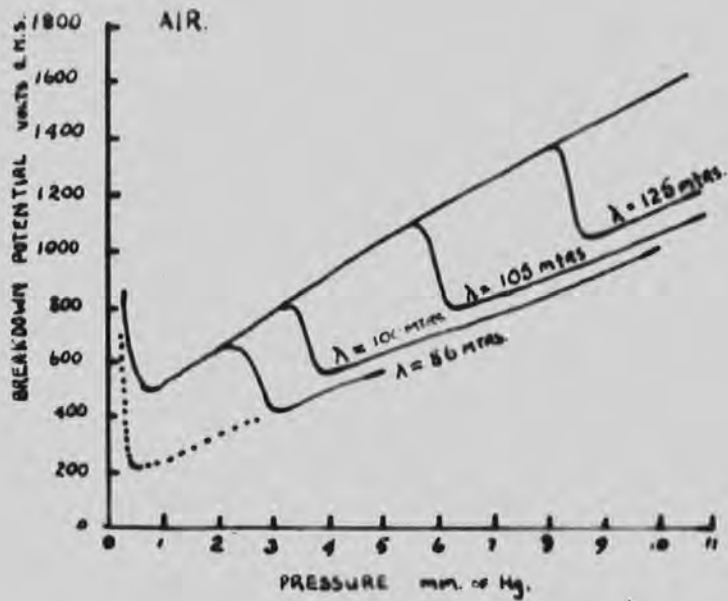
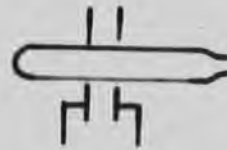


FIG. 1.5

BREAKDOWN VOLTAGE AND  
PRESSURE FOR TWO DIFFERENT  
ELECTRODE ARRANGEMENTS AT  
DIFFERENT FIELD FREQUENCIES,  
WAVELENGTH IN MICRONS.  
FROM GILL AND DONALDSON '33



production is equal to, or just greater than, the rate of loss by diffusion from the highly stressed region of the gas. This condition is expressed mathematically and solved for the boundary conditions involved. MacDonald and Brown, 1949, have further shown that this theory is limited to the cases where the gap length is small compared with the wavelength of the applied field and the mean free path of the electrons is not comparable with the dimensions of the electrodes or containing vessel. They have examined the published data of breakdown under these conditions and show that they conform to a self consistent set of results from 1 Mc/sec to 3000 Mc/sec

Clark and Prowse, 1958, have established further the validity of the diffusion theory at frequencies of 5 and 10 Mc/sec. Using electrodes of different diameters and different electrode separations they showed that a unique curve could be plotted similar to the E.d; p.d. Paschen curve, provided that  $d$ , the electrode separation, was replaced by  $\Lambda$ , the diffusion length of the inter-electrode space, which depended simply on the dimensions of the space and is given by;

$$\frac{1}{\Lambda^2} = \left(\frac{\pi}{d}\right)^2 + \left(\frac{2.405}{r}\right)^2$$

where  $r$  is the radius of the plane portion of the electrodes.

For sustained u.h.f. fields the breakdown mechanism is controlled by diffusion so that a discharge will occur if an electron produces at least one other electron during its

lifetime as limited by diffusion. Consequently, it can be expected that the time taken to build up the electron population to a concentration which constitutes breakdown will be greater than the mean lifetime of the electrons.

Oscillographic measurements of the time lag to breakdown have been made by Prowse and Jasinski, 1952, in both monatomic and polyatomic gases using pulses of 2800 Mc/sec. microwave fields. They showed that breakdown in a polyatomic gas can occur in time intervals of less than  $10^{-7}$  seconds, much smaller than the lifetime of the electrons as controlled by diffusion.

Pulsed measurements by Labrum, 1947, on Neon, showed that relatively long time lags are associated with the formation of the discharge and that there is a dependence of breakdown stress on pulse duration. This led Labrum to suggest a mechanism whereby the conditions for breakdown are governed simply by the increase in the electron population to a certain critical value without removal taking place.

Following Labrum's work, Prowse, 1957, has shown theoretically that the value of  $\alpha$  needed for breakdown under sustained conditions and pulsed conditions is affected in the same manner by the electron lifetime as controlled by diffusion and as controlled by pulse length respectively. However, this is not supported experimentally.

In view of the difficulties experienced in establishing the operative mechanisms of breakdown for both sustained and

and pulsed u.h.f. fields, a less ambiguous method than the measurement of breakdown stresses is necessary for a direct study of the ionization processes at u.h.f.

The fact that the careful extension of Townsend's work by Llewellyn Jones at Swansea had showed that the Townsend mechanism did suffice to explain the breakdown conditions for direct fields over a wide range, indicated that in the more difficult u.h.f. case the nearest type of experiment to that of Townsend should be attempted.

This thesis describes the design of such an experiment and the construction of the necessary apparatus. It includes an analysis of the preliminary results of pre-breakdown amplification and shows that it will be possible to obtain such useful evidence.

## CHAPTER II

### THE DESIGN AND THEORETICAL ASPECTS OF THE PROBLEM

Many direct investigations, as outlined in the introduction, have been made into the development of a current up to breakdown under direct field conditions, but very few, investigations, if any, when the breakdown takes place under u.h.f. conditions. Fatechang, 1951 conducted an experiment at atmospheric pressure to investigate the onset of high frequency breakdown when the positive ion orbit is less than the gap width. Although this was not concerned with the u.h.f. region it is quite likely that the frequency of the field could have been increased until the electron orbit was smaller than the gap width. In this experiment he found that there was considerable growth of current in the high frequency region when the applied potential was near the breakdown value.

Francis and von Engel, 1953-54, have measured high frequency ionization currents in an electrodeless discharge when the pressure was such that the electron mean free path was greater than the size of the vessel containing the gas under test so that there was very little ionization caused by electron-atom or electron-molecule collisions. The field frequency was low enough for the electrons to be swept to the vessel walls each half cycle and the discharge started when the applied field was large enough to cause multiplication of

electrons by secondary emission from the end walls of the vessel. The discharge chamber was connected into one arm of a balanced bridge which became unbalanced as the current built up to breakdown. The amount of this unbalance was amplified electronically and displayed oscillographically.

Both these experiments are in the high frequency range but Biendi and Brown, 1949, with their investigations of the ambipolar diffusion coefficient of electrons and ions produced by a u.h.f. discharge in helium, have shown that it is possible to determine the conditions in a u.h.f. discharge from external parameters. They determined the change in the resonant frequency of a cavity in which a vessel containing the helium was situated, as an effect of the charge distribution in the gas. With this method they determined that the stationary charge distribution reached in the vessel during a microwave pulse producing breakdown was in the region of  $10^{10}$  to  $10^{11}$  electrons or ions per cc.

In view of the absence of experiments in the u.h.f. region to determine breakdown currents directly, an apparatus was designed similar to the apparatus of Townsend, 1910, for determining  $\alpha$ , so that the onset of breakdown in the u.h.f. region could be studied quantitatively. Townsend's method involved the release of electrons photoelectrically at a cathode so that they move to an anode under a steady direct field, at the same time acquiring energy from the field to ionise the gas.

It was envisaged that for u.h.f. conditions a similar small current could be released at an electrode and be moved across to another electrode under the influence of a small direct field, which would not be large enough to cause any appreciable ionization of its own accord. Whilst the electrons move across the gap between the electrodes, a large u.h.f. field can be applied at a frequency high enough to restrict the size of the electron orbit to a small fraction of the electrode separation. Under the influence of this u.h.f. field the electrons will ionize the gas and produce an amplified current. This amplification can be determined by measuring the electron current to the collecting electrode with and without the applied u.h.f. field.

This arrangement affords a method of varying the lifetime of electrons, which was initially assumed to be equal to the crossing time of the electrons, by varying both the small direct field and the electrode separation. The transit time could be separately measured by using a system of electron gates incorporated in the electrodes and similar to those in the experiments of Bradbury and Nielson, 1936, on the drift velocity of electrons.

*electron  
Shutter  
method* ←

#### The design of the apparatus.

A diagram of the electrode system indicating the necessary conditions is in Fig. 2.1. It can be seen that it was decided to use a thermionic source of electrons on account

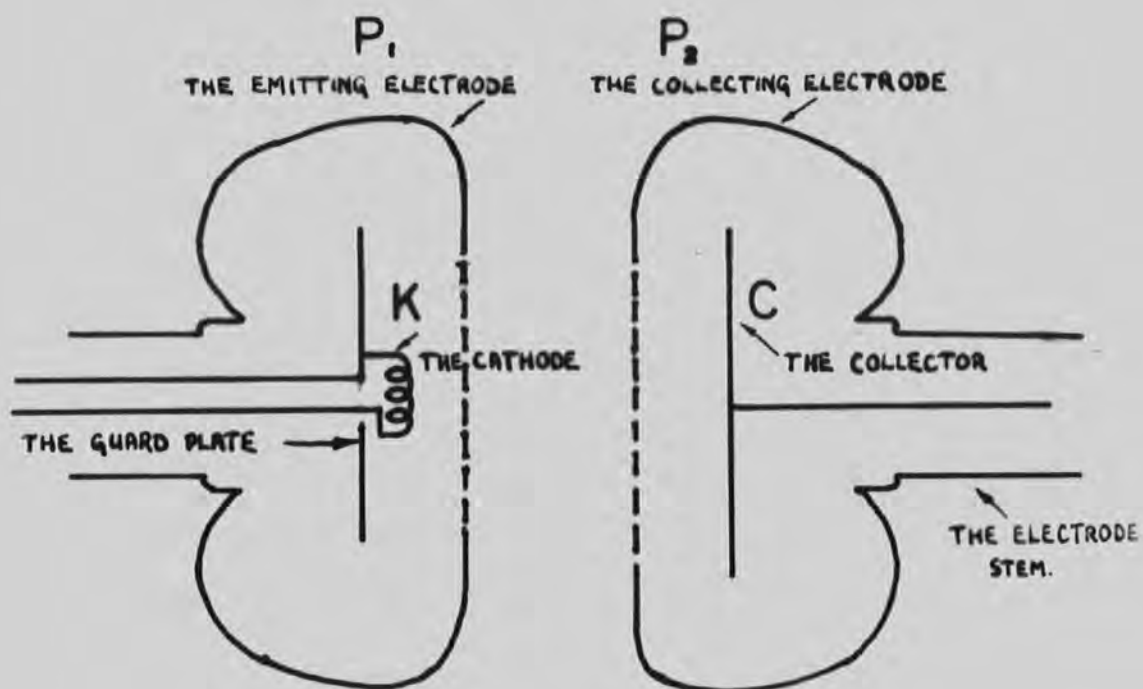


FIG. 2.1

A SCHEMATIC DIAGRAM OF THE ELECTRODE SYSTEM.

of it being a steady, and as shown later, a copious supply.

In Fig. 2.1,  $P_1$  and  $P_2$  are a pair of plane parallel electrodes which are immersed in the gas to be studied. They are perforated so that electrons from the cathode, K, diffuse out into the gap between  $P_1$  and  $P_2$ , and at  $P_2$  diffuse into the space between  $P_2$  and the collector, C. Suitable potentials are applied to the electrodes so as to produce fields as follows:

a). between  $P_1$  and  $P_2$ , a strong u.h.f. field which confers ionizing energy on the electrons in the gap,  $P_1$  to  $P_2$ .

b). between  $P_1$  and  $P_2$  a weak unidirectional field to control the lifetime of the electrons in the gap.

c). between K and  $P_1$ , an oscillating field to modulate the current of electrons emerging through  $P_1$ .

d). between  $P_2$  and C, an oscillating field of the same frequency and at a known phase with respect to that in (c), in order to modulate the distribution of the electron stream reaching C. If this phasing is such that  $P_1$  and  $P_2$  are at the same potential with respect to the oscillating field then a current maximum will be observed in the collector if the transit time is approximately the time of half a cycle, or of one and a half cycles etc. By determining the necessary modulation frequencies for succeeding maxima to the collector, an estimation of the transit time can be made.

If the current arriving at  $P_2$  without an applied u.h.f.



field is  $i_0$ , then that reaching  $P_2$  with the u.h.f. field applied will ideally be  $i_0 e^{\psi T}$  where  $\psi$  is the number of ionizing collisions made by one electron per second, and  $T$  the transit time,  $\psi$  is related to  $\alpha$ , the number of ionizing collisions per centimetre of drift in the field direction by the expression:

$$\psi = \alpha W.$$

where  $W$  is the drift velocity of the electron in the field direction. It is assumed that the unidirectional field in (b) above may be neglected in comparison with the u.h.f. field in computing  $W$ .

The object of the experiment is to measure  $\psi$  as a function of the field strength, pressure and nature of the gas, and especially to study in this way, how ionization proceeds when the transition to the conducting state is approached. Because the lifetime of the electrons can be varied without altering the u.h.f. energising field it should be possible to see how the value of  $\psi$  is affected by the concentration of the electrons and ions in the gap.

#### Consideration of the exact experimental conditions.

It is worth considering a set of likely conditions in order that the approximate field frequencies may be calculated. It was decided that the u.h.f. field should have a frequency of about 100 Mc/sec., which is low enough for a diode voltmeter to be used as a voltage measuring instrument, and satisfies

the condition that there shall be many electron-atom or electron-molecule collisions per oscillation.

Consider a gap width of 0.635 cm., i.e.  $P_1$  to  $P_2$ , in an atmosphere of hydrogen, at a pressure of 8 mm. of Hg., and a direct field of 10 volts/cm. Under these conditions the number of electron-molecule collisions per oscillation is about 500. Initially without a u.h.f. field, the transit time is  $0.5 \mu$  sec. but as the u.h.f. field is increased, the average electron energy increases and the mobility of the electrons decreases, so that the crossing time becomes longer, e.g.  $1.9 \mu$  sec. when  $E_{\perp} = 200$  volts/cm. Thus without the u.h.f. field the necessary modulating frequency for the first current maximum to the collector to be observed, is approximately 1 Mc/sec. and when a u.h.f. field is applied, as low as 250 Kc/sec. The next maximum will be observed when the frequency is trebled. When the crossing time is of the order of  $1 \mu$  sec. the electrons will execute about 100 orbits whilst they are in the gap.

The effect of the electron energy on the transit time.

It was later realised that at high electron energies, (high u.h.f. fields), there is competition for the control of the electron lifetime by two processes, one being diffusion and the other being the removal by drifting to the electrodes under the small direct field. This complicates the determination of the lifetime of the electron as diffusion

will affect both the accuracy of any transit time as measured with the modulating field, and the meaning of such a time once its determination has been achieved.

However, Brown and Varnerin, 1950, have derived an expression for the lifetime of electrons under these circumstances so that it can be calculated from the conditions of the experiment. Failing this a method has been developed to determine the lifetime using the results obtained from breakdown conditions in the experiment. As shown later, both these methods are essentially similar in that they both depend on the validity of the diffusion theory for the conditions of the experiment. This indicates that the modulation of the electron current may produce evidence on the diffusion of high energy electrons rather than a measurement of the lifetime.

Having considered the design of the experiment the necessary apparatus was developed and constructed as described in the following chapters.

## CHAPTER III

### A BRIEF DESCRIPTION OF THE APPARATUS

The main requirement of the apparatus is that sufficient u.h.f. power is obtainable at the test electrodes so that the gap can be stressed to breakdown. With this in mind an oscillator was built which oscillates in the 100 Mc/sec. region. This frequency region allows the power to be carried by transmission lines and accordingly the tuned elements of the oscillator, which is of the tuned anode, tuned grid type, are quarter wave transmission lines.

The closed end of the anode quarter wave line is loosely coupled to the closed end of another quarter wave line which is terminated at its open end by the test electrodes, see Fig. 3.1. The loop of this second line is split by a mica condenser in order to isolate the separate electrodes for D.C. measurements. The u.h.f. voltage across the electrodes can be varied by altering either the coupling between the line and the oscillator or the anode potential of the oscillator.

The test electrodes are enclosed in a 'Pyrex' glass chamber designed so that the quarter wave line passes through tubes in its side. By this means, as little as possible of the line need be in the enclosure and a variable condenser can be attached externally across the line near to the electrodes, so that any variation in the separation of the electrodes can be compensated for, and the line retuned.

Scale 1/5 full size.

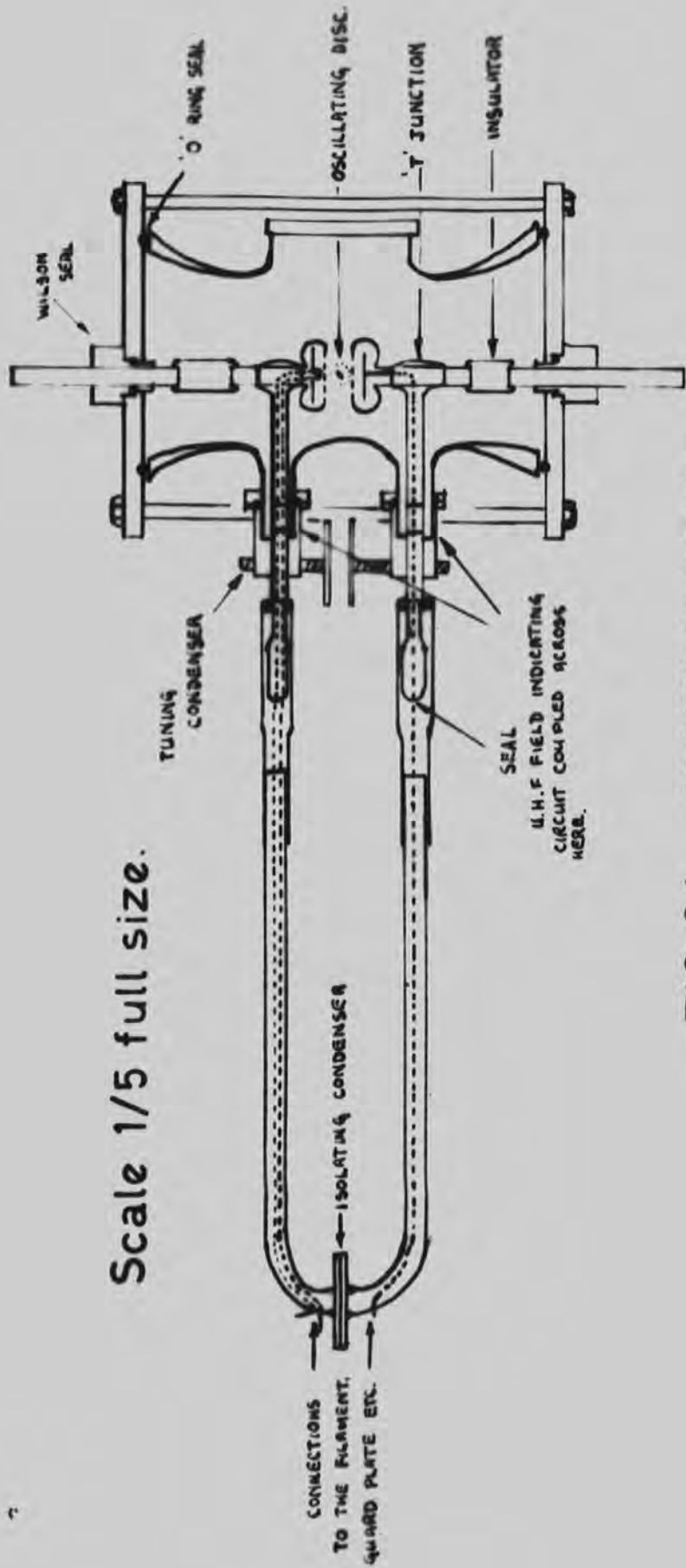


FIG. 3.1

THE QUARTER WAVE TRANSMISSION LINE AND CHAMBER.

Electrons are emitted from an oxide coated cathode situated inside one of the test electrodes, (Fig. 2.1), and they move through small holes in the electrode,  $P_1$ , under the influence of a direct field. This direct field is necessary in order to cause a measurable number of electrons to move into the main gap but it must be small so that it does not appreciably affect the energy of the electrons and in effect they arrive in the gap as if they have diffused through the holes.

A modulating field of variable frequency can be superimposed on the direct field so that the electrons move into the gap in bursts. A similar modulating field can be applied across the collecting electrode,  $P_2$ , and an internal collecting plate as in Fig. 2.1.

The oscillator providing the modulating potential is of the single valve, tuned anode, tuned grid, type. This has a wide frequency range (200 Kc/sec. to 7 Mc/sec.) achieved by using five coils. A tuned circuit is loosely coupled to the anode coil of the oscillator and the output fed through a filter system to the respective electrodes on both sides of the transmission line. This filter system is necessary to prevent the direct current paths through the galvanometers which measure the ionization currents, from short circuiting the modulating inputs to the electrodes.

The small direct fields can be determined using a D.C.

meter and the modulating potential by using a valve voltmeter, but the measurement of the ultra high frequency field presents a problem on account of the small amount of power available. This is overcome by using a symmetrical type valve voltmeter loosely coupled to the line external to the chamber by small capacitances. The rectified output of this voltmeter is displayed on a sensitive galvanometer the deflection of which is a measure of the voltage across the electrodes. Because the voltmeter is neither connected to the line directly nor across the end of the line, the potential corresponding to a particular deflection cannot be determined directly. This is overcome by using a stepover instrument.

This consists of a small disc of metal which is suspended in the electrode gap from its edge by a quartz fibre. If the position of rest of the disc is such that its diameter lies along the field, any small oscillations the disc may execute about its position of rest will have a frequency which will depend on the strength of the field and will be independent of the polarity of the field. This means that the disc can be calibrated with low frequency or unidirectional fields and then be used to calibrate the valve voltmeter for ultra high frequency fields. The disc is small enough not to affect the tuning of the line and can be removed during the experiment.

The chamber is made from a piece of standard 'Pyrex' pipeline with steel plates clamped to the ends and sealed by

'O' ring seals. A 'T' junction electrically connects each end of the transmission line to the appropriate electrode stem which is supported by a rod passing through a rubber seal in the centre of the end plates, see Fig. 3.1. The gap width can be altered by adjusting the position of the rods from outside the chamber.

The chamber is connected to a 'Pyrex' vacuum line which incorporates facilities for pipetting small quantities of spectroscopically pure gas into the chamber or more particularly, pure hydrogen which has passed through the walls of a hot Palladium tube. The line is evacuated by means of an oil diffusion pump backed by a rotary backing pump and the pressure may be measured by a Pirani gauge, a dial gauge and a differential gauge. The pressure of the gas under test is measured by the differential gauge which is calibrated against a mercury manometer; the other two gauges are used merely to determine the pressure conditions in the chamber.

This apparatus enables the ionization and breakdown characteristics of various gases to be studied under conditions which can be easily controlled and determined.



## CHAPTER IV

### THE ULTRA HIGH FREQUENCY OSCILLATOR

Two types of oscillator might be used to provide the u.h.f. power, one a two stage oscillator and the other a free running oscillator. A two stage oscillator would consist of a master oscillator feeding into a high frequency amplifier; this would be the more complicated to build but could be expected to have a greater frequency stability. The most likely disadvantage of the free running oscillator is that the frequency may vary with the applied load, but should not be apparent if the load is small, i.e. the oscillator is loosely coupled to the load.

Bearing these arguments in mind, a free running oscillator was built in order to test its performance. As shown by subsequent references this oscillator proved to be adequate for the experimental conditions described in this thesis. This free running oscillator is a tuned anode, tuned grid type, using two power tetrodes working in push-pull, Fig. 4.1. It is designed to operate in the frequency region of 100 Mc/sec. ; the two power tetrodes having a maximum dissipation of 60 watts each. This frequency range enables the tuned elements to be of the transmission line type such that the anode and the grid elements are quarter wave lines with the valves connected to the open ends. The anode line which takes the

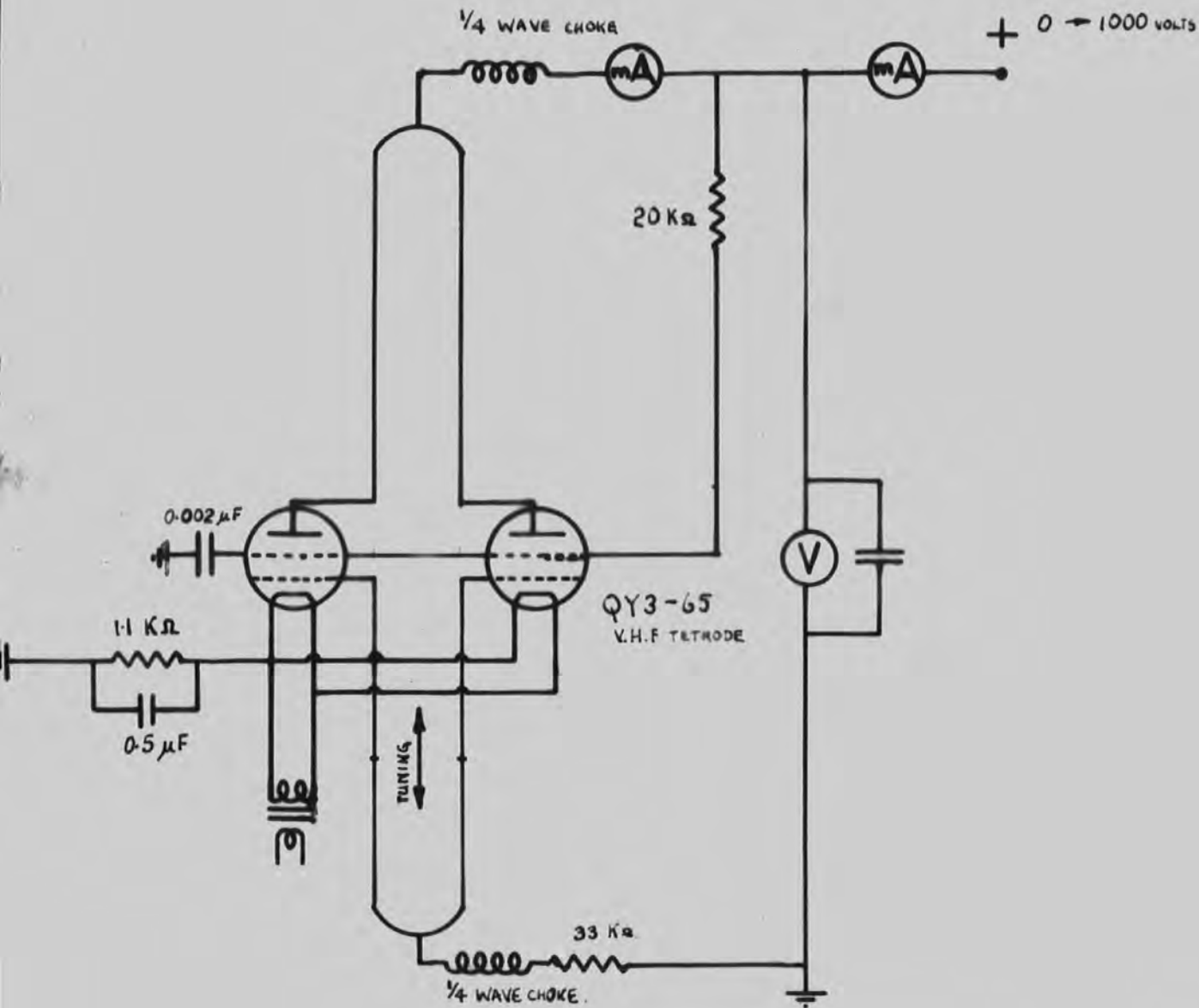


FIG. 4.1

U.H.F. OSCILLATOR CIRCUIT  
DIAGRAM.

form of a hairpin, is constructed from copper tubing 0.95 cm. in diameter, and is 75 cms. long with the limbs separated by 7.5 cm. The loop of the grid line is made from solid rod which slides inside two tubes forming the rest of the line. This allows it to be tuned. The normal working position of the oscillator is such that the valves have their base uppermost, the grid line being above the anode line to give adequate coupling. The oscillator is enclosed by an aluminium shield, save for a space immediately below the anode to allow for coupling between it and the main line.

The main transmission line which operates under resonant conditions is constructed from similar tubing to that used in the anode line. This has a high Q factor and has the advantages listed below:

- a) Maximum voltage is developed when the coupling is loose.
- b) The line is relatively noiseless because the Q factor is a measure of the discrimination against other frequencies.
- c) The energy input to the line for a given voltage is low and a low conductance across the electrodes produces a sharp voltage collapse so that sensitive measurement is achieved.
- d) The energy available for electrode damage, gas dissociation and over heating etc. is small.

The power in the transmission line can be varied either by altering the coupling or by varying the anode voltage.

The variation of coupling is a rough control achieved by mounting the oscillator with a counterbalance in a rack, so that it may slide up and down above the loop of the line thus varying the distance between them. Variation of the anode voltage controls the output of the oscillator smoothly and thus the power in the line. This is achieved by supplying the 1000 volt power pack with the output from a Variac.

This in turn was fed from a constant voltage transformer to reduce the effects of mains fluctuations.

A determination of the frequency was made using a set of Lecher wires loosely coupled to the oscillator. Successive positions of a short circuiting bridge for resonance, were found, and the frequency indicated was 106.8 Mc/sec. to within 0.1%. The frequency was found to lie within this accuracy for an anode voltage range of 250 to 1000 volts. Such a stability indicates that the performance of the oscillator satisfies the experimental requirements.

## CHAPTER V

### THE PRODUCTION OF THE U.H.F. FIELD BETWEEN THE TEST ELECTRODES

The electrodes are incorporated into a resonant quarter wave line, the greater part of which is constructed from copper tube as described in the previous chapter. It is necessary that there is a means of immersing the electrodes in the gas to be studied and of altering their separation. The capacitance across the end of the line will vary with the separation but can be compensated for, either by altering the length of the line or by altering the capacitance across the end of the line by means of the tuning plates shown in Fig.3.2. It had to be recognised that the apparatus might only be the prototype of a more elaborate set-up which could be baked out etc., and consequently it would be advantageous for the apparatus to be dismantled and assembled with ease, to facilitate modification. With these points in mind the transmission line and chamber was constructed as follows.

The chamber is made from a piece of 'Pyrex' pipe line of 3 inches internal diameter and 9 inches in length. The ends of the pipe are thickened and are ground flat and parallel so that two steel end plates, through which the supports for the electrodes pass, can be sealed to them. The transmission line passes through two glass tube stubs, 7.5 cms. apart in the side of the chamber and is sealed to

these by means of 'O' ring seals. The line is soft soldered into the brass body of these seals and is cut off near them on the outside of the chamber. This enables a small copper to glass seal to be soldered into the ends of the projecting tubes so that the connections to the filament and the internal electrodes can be sealed through the glass of the seal, see Fig. 5.1. Both these arrangements provide a vacuum tight seal whilst allowing electrical connections to be made to the parts of the line inside the chamber. A metal sleeve fits over the copper to glass seal in order to complete the electrical continuity of the line, the loop of which slides into these sleeves so that its total length can be varied for preliminary tuning. This loop is split by a mica condenser which insulates the two test electrodes from one another for D.C. measurements. This does not affect the line appreciably for the ultra high frequency conditions.

The wires to the internal electrodes are led down the centre of the separate limbs of the 'hairpin' coming out at holes near the isolating condenser. When the line is tuned the u.h.f. current maximum is situated at the loop, so that any capacitance between the leads and earth has little effect on the line.

To allow for the movement of the electrodes along their axes, (variation of gap width) they are supported by the shafts of two Wilson rotary seals which allow both lateral

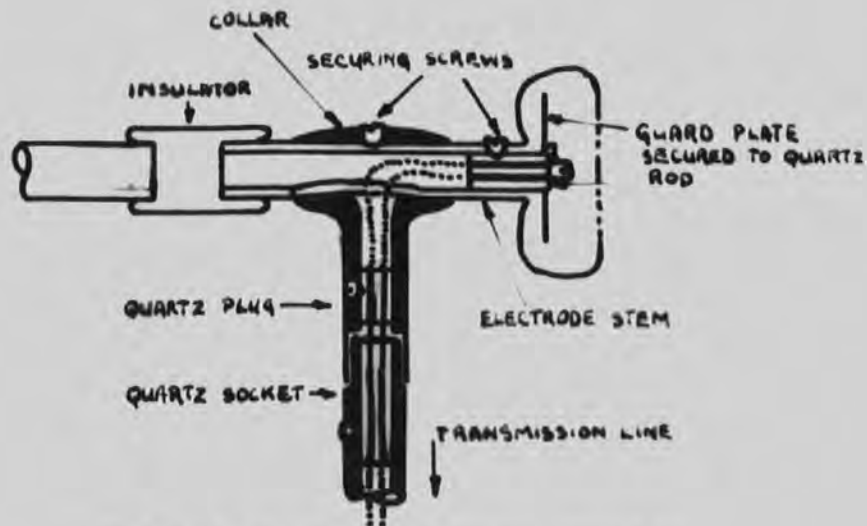


FIG. 5.1 METHOD OF MAKING CONNECTIONS TO THE EMITTING ELECTRODE

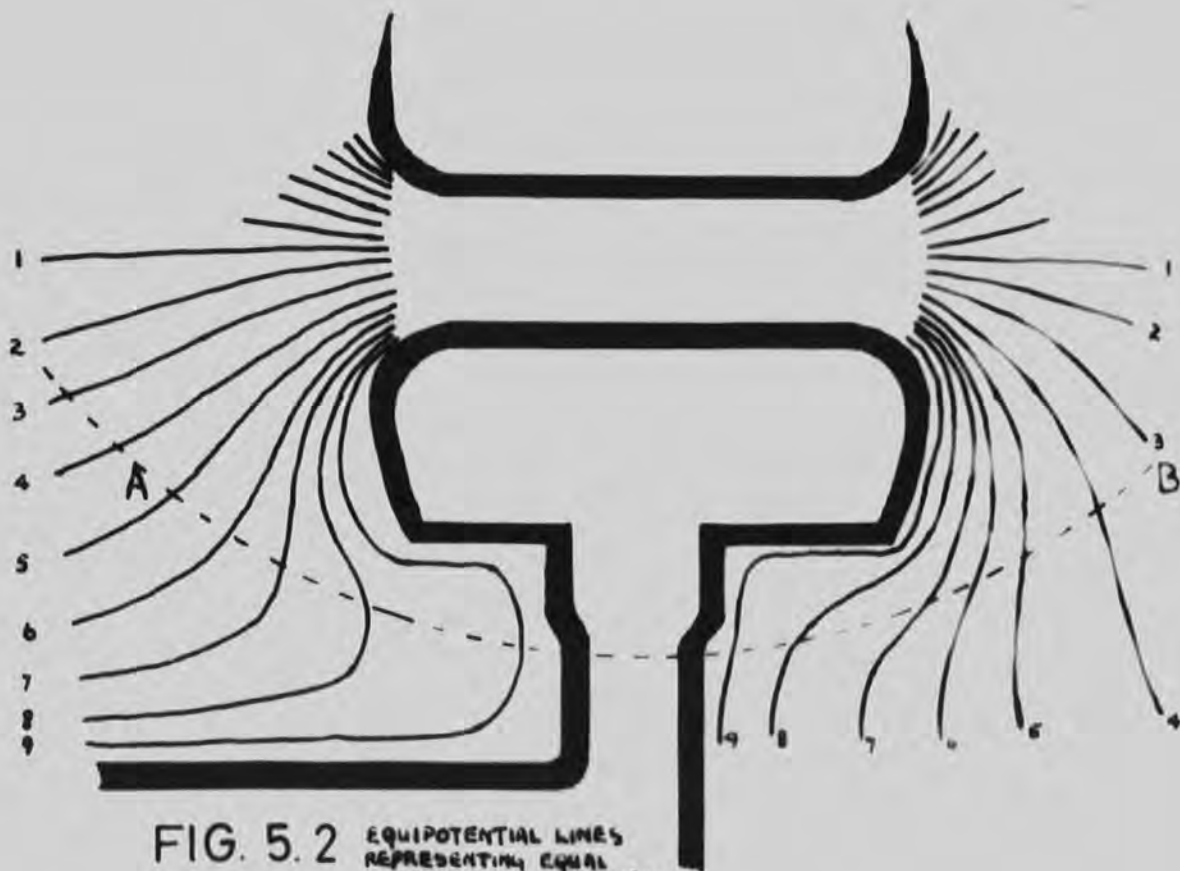


FIG. 5.2 EQUIPOTENTIAL LINES REPRESENTING EQUAL INCREMENTS OF POTENTIAL FOR ELECTRODE CONFIGURATION. NUMBERED FOR COMPARISON.

and rotary movement. The shafts of the seals are insulated from the electrode stems by polystyrene insulators so that both the Wilson seal and the end plate can be at earth potential. The seals themselves are bored through the end plates and sealed with 'O' ring seals and the end plates in turn are sealed to the ground ends of the chamber by 3 inch 'O' rings inserted into a specially machined groove in the surface of the plate. This design was preferred to a bellows system because it was easier to assemble and allowed the electrodes greater freedom of movement.

The connections between the ends of the line and the electrodes are made by means of collars soldered onto the line at right angles, see Fig. 5.1. These collars fit over the electrode stems so that the junctions do not give rise to corona discharges whilst allowing a movement of each electrode of 1 cm. The collars also cover slots in the electrode stems through which pass the leads to the internal electrodes etc. These leads, which are insulated by small ceramic beads are flexible enough not to constrain the electrode movement.

Should these junctions or electrodes need modifying or repairing, they can be unscrewed from the polystyrene insulator, unplugged from a special quartz insulated plug built into the transmission line and removed from the chamber through a 3 inch diameter inspection aperture. During the experiment this aperture can be sealed with a greased ground-glass plate.



The assembly is mounted so that the axis lies in a horizontal plane in order that the oscillating-disc field-meter can be lowered into the gap.

Two micrometer screw heads determine the position of the electrode supports at a position outside the chamber. Thus, once the readings for a particular separation of the electrodes as determined by a flat parallel plate inserted between them, has been established, any subsequent separation can be found.

The chamber and transmission line is screened with tin-plate except for the loop and under these conditions the tuning of the line is very sensitive to movement of the tuning condenser plates (Fig. 3.1) which are screwed into the bosses on the body of the 'O' ring seals.

It was thought that the position of the transmission line with respect to the electrodes might affect the field distribution between them and a plot of the equipotential surfaces was made for such a configuration using a model of the electrodes in an electrolytic tank. Fig. 5.2 shows the result of this investigation, where it can be seen that above the line AB. there is no appreciable difference between the pattern to the right of the electrodes and that to the left. From this it was concluded that the affect was negligible. The equipotential lines in the gap are so close together that they are not drawn.

The maximum field strength attainable is greater than 1000 volts/cm. for a gap width of 1 cm. This is in excess of the present requirements but may be useful for future experiments.

CHAPTER VI  
THE ELECTRODE ASSEMBLY

Preliminary investigations were made on two electrodes of approximately the same size as envisaged in the main apparatus, these being mounted in a small evacuated enclosure which was easily accessible, Fig. 6.1. These investigations were made in the absence of the 100 Mc/sec. field with the object of designing an efficient cathode and studying the general behaviour of such an electrode system.

At an early stage in the design considerations it was decided that the cathode would have to be of the thermionic type rather than the photoelectric type used by some workers in this field (e.g. Llewellyn Jones et al 1957). The objection to the photo-electric type of emission was the difficulty of illuminating a surface inside the electrodes so that the resultant electron beam could be modulated as it passed into the gap. Admittedly there is an objection to the thermionic type of emission in that the necessary heat will cause the temperature of electrodes to rise and cause convection currents in the gas. However, if a good emitter can be made that will dissipate little power for the required emission this can be discounted.

With this in mind the emission properties of both a plain platinum wire and a platinum wire coated with the mixed



FIG. 6.1 PRELIMINARY EVALUATION CHAMBER.

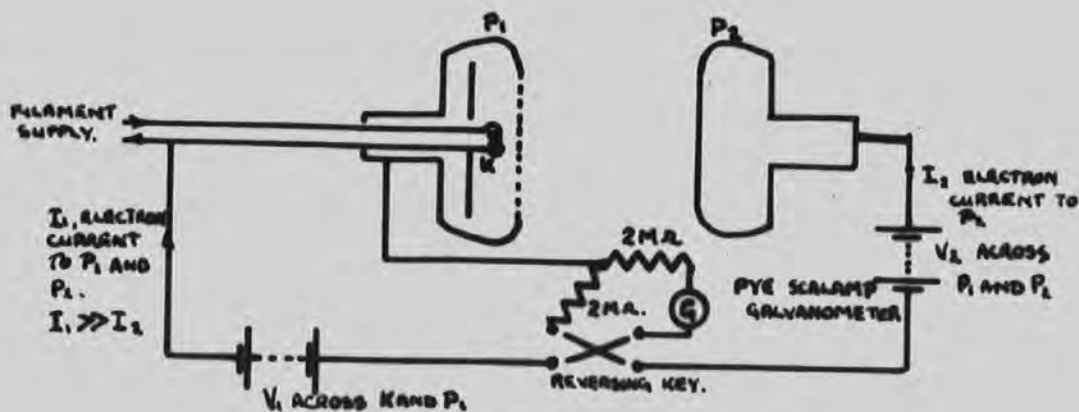


FIG. 6.2 CURRENT MEASURING CIRCUIT FOR PRELIMINARY INVESTIGATION.

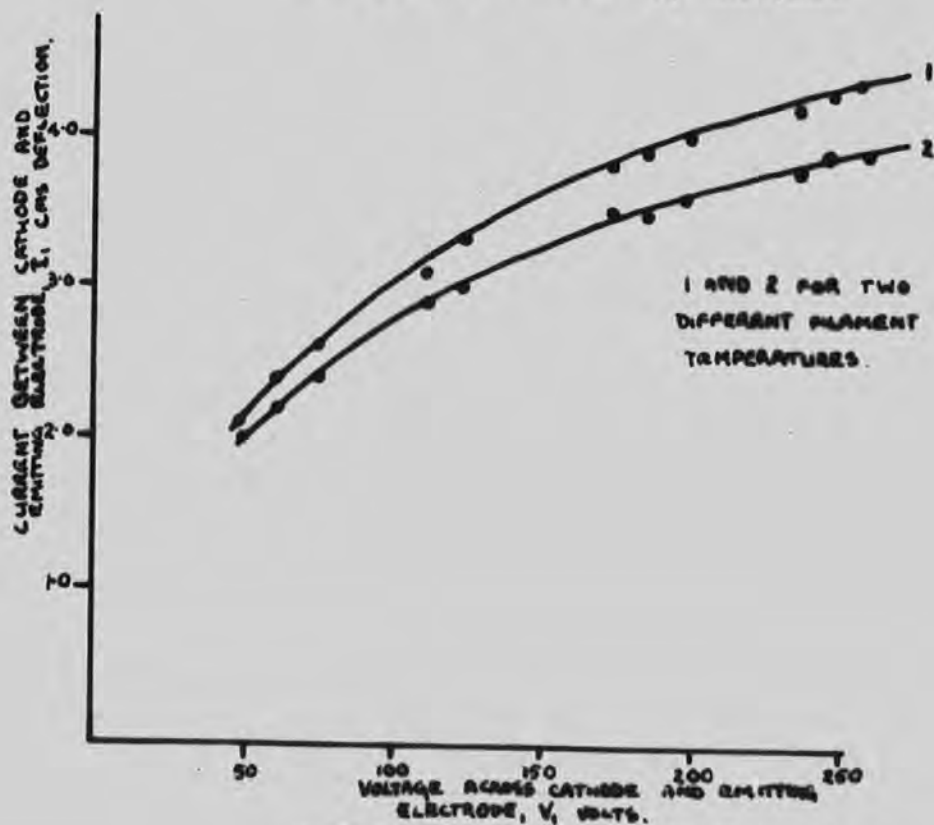


FIG. 6.3 VARIATION OF ELECTRON CURRENT TO THE EMITTING ELECTRODE WITH VOLTAGE ACROSS THE CATHODE AND THE ELECTRODE.

*between*

oxides of several alkali earth metals were investigated. The emission of the plain wire was small compared with that of the coated type, being approximately in the ratio of 1:500, for similar conditions. This indicated that an oxide coated cathode should be used, especially as the heating effect can be reduced further by winding the platinum wire in a very small tight coil, thus localising the heat to the emissive surface. The oxide coating was applied to clean platinum wire by painting it with a suspension of mixed Barium and Strontium carbonates subsequently converted to the oxides by heating in vacuo. With the arrangement of the cathode in a small coil, the emission takes place from a small area on the axis of the electrode system, a guard plate being attached behind the cathode so that most of the electrons move towards the inner surface of the electrode face, Fig. 2.1.

Tests were made of the dependence of the current between the cathode and surrounding electrode,  $I_1$ , and the current across the gap,  $I_2$ , on the voltage between the cathode and surrounding electrode,  $V_1$ , and the voltage across the gap,  $V_2$ , in hydrogen at a pressure lower than 0.1 mm. of Hg. with the circuit of Fig. 6.2. The relationship between  $I_1$  and  $V_1$  was similar to that of a simple diode provided that  $V_1$  was not too high. Typical curves are shown in Fig. 6.3.

There was practically no variation of  $I_2$  with  $V_2$  up to

300 volts indicating that the perforated electrode acted as a control grid and the far electrode as a collector.

Investigations were also made of the variation of  $I_2$  with  $V_1$  for constant  $V_2$ , Fig. 6.4. This shows that  $I_2$  increases linearly with  $V_1$  for high values,  $I_2$  being approximately one tenth of  $I_1$ .

The pressure was now increased to a few mms. of Hg. by admitting hydrogen to the system and a further investigation of  $I_2$  as a function of  $V_2$  was made. This showed that the value of  $I_2$  increased rapidly when the value of  $V_2$  exceeded 1500 volts which accorded with the assumption of gas amplification in the gap. However, there was now a dependence of  $I_1$  on  $V_2$ ,  $I_1$  increasing with  $V_2$ , but sufficient results could be taken to determine  $I_2$  as a function of  $V_2$  for two constant values of  $I_1$ , Fig. 6.5. These curves show the rapid increase in current associated with collision ionization.

This preliminary investigation resembles Townsend's experiments on collision ionization, and except for the use of unidirectional fields instead of the 100 Mc/sec. field, resembles the experiments to be undertaken in the main investigation.

Initially it was thought that the dependence of  $I_1$  on  $V_2$  was due to field penetration through the holes augmenting the value of  $V_1$ . This can be rejected on two accounts. Firstly, as stated earlier, it was shown that at low pressures (no

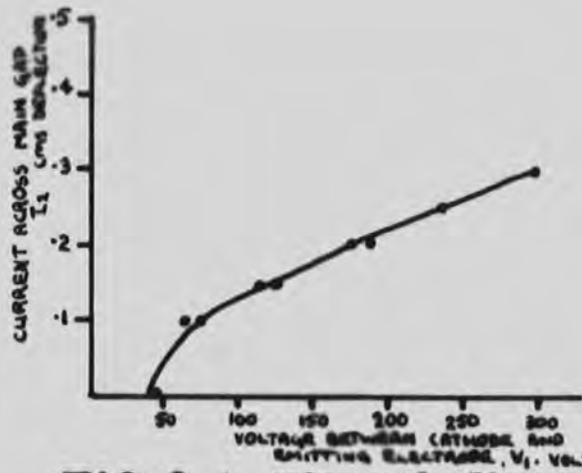


FIG. 6.4 VARIATION OF CURRENT ACROSS MAIN GAP WITH VOLTAGE ACROSS CATHODE AND EMITTING ELECTRODE.

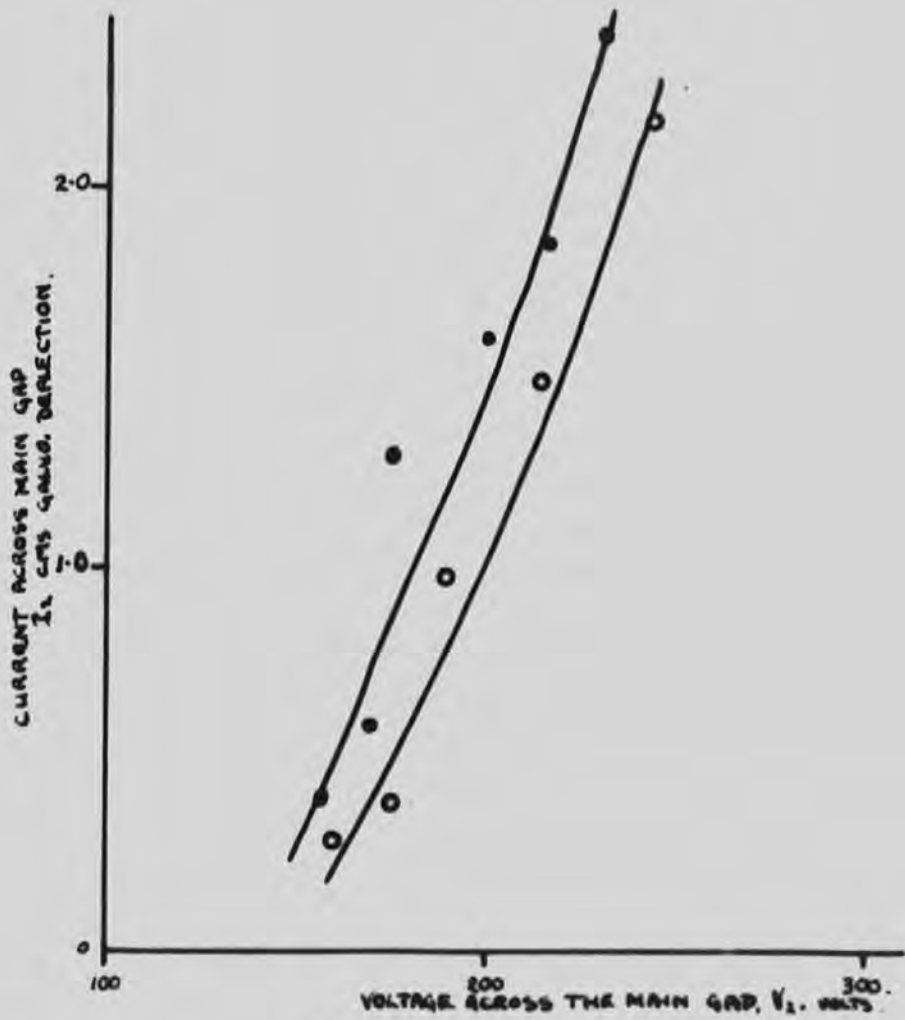


FIG. 6.5 VARIATION IN THE CURRENT ACROSS THE MAIN GAP WITH A VOLTAGE ACROSS IT. HYDROGEN AT A FEW MM. OF Hg. PRESSURE.

ionization)  $I_2$  does not change with  $V_2$  and secondly, an electrolytic tank study of a plate with more perforations per unit area than the electrode indicates that any penetration is slight and should not affect the field behind deep holes, Fig. 6.6.

It appears therefore, that the variation of  $I_1$  depends on the properties of the gas when ionized and is thought to express the action of positive ions reaching the filament and causing secondary emission. This is supported by the fact that at high values of  $I_2$  and  $V_2$ , before a self sustaining discharge had started, a visible discharge channel formed across the gap from one of the holes in the electrode surface, and whilst  $I_2$  increased steadily during the onset of the discharge,  $I_1$  increased abruptly.

This effect will be apparent in the final apparatus and must be reduced. Accordingly the number and size of the holes were reduced and arranged so that none of them came opposite to the oxide spot of the cathode. This markedly reduced the dependence of  $I_1$  on  $V_2$  indicating the positive ion mechanism.

Ideally the electrons should diffuse into the gap through the perforations and not be injected in under the influence of  $V_1$ . This is equivalent to saying that the electrons entering the gap should have low energies compared to that required to ionize the gas. Thus  $V_1$  must be as small as



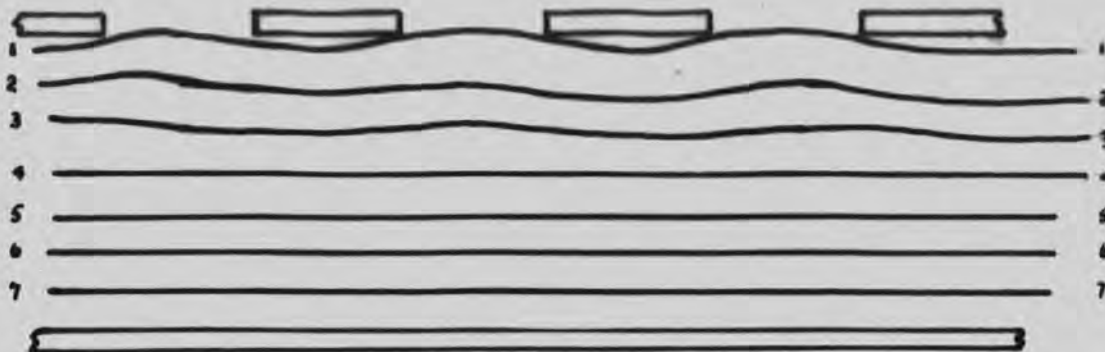


FIG. 6.6 EQUIPOTENTIAL LINES REPRESENTING EQUAL INCREMENTS OF POTENTIAL FOR BETWEEN A PERFORATED PLATE AND PLANE PLATE. NUMBERED FOR COMPARISON

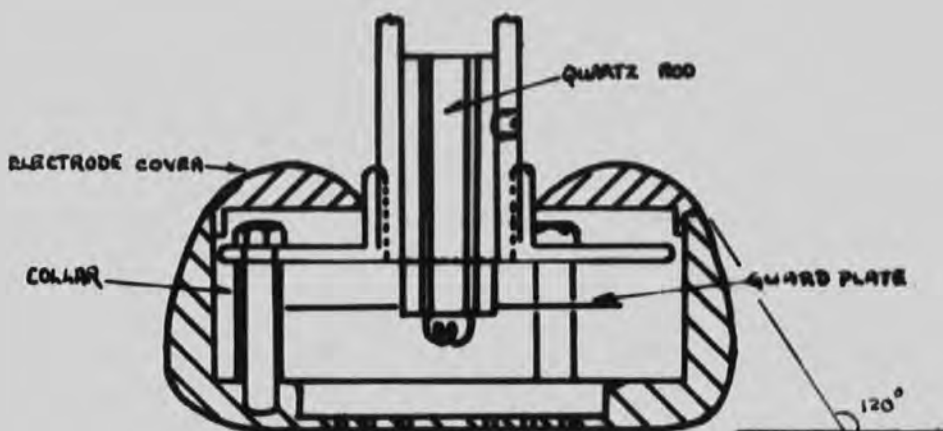


FIG. 6.7 THE ELECTRODE ASSEMBLY TWICE FULL SIZE.

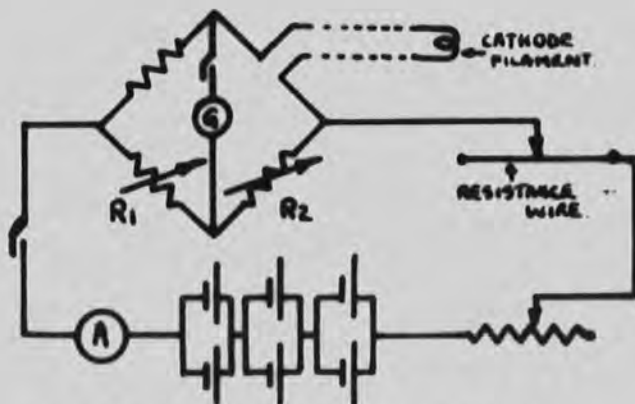


FIG. 6.8 CIRCUIT FOR STABILIZING THE FILAMENT TEMPERATURE.

possible whilst still maintaining a measurable current  $I_2$ . A slight increase in  $I_2$  with increase in  $V_2$  can be expected even before ionization, due to the reduced chance of the electrons diffusing out of the gap.

Following these preliminary investigations the final test electrodes were designed and constructed as described below.

#### The construction of the test electrodes.

The copper tubes which support the electrodes (electrode stems) were screwed into brass plates on which the electrode shells were mounted, Fig. 6.7. The hollow test electrode shell is bolted to this plate by means of three 8 BA studs and nuts with brass collars to separate the two. This design enables the electrodes to be adjusted so that their faces are parallel by replacing two of the collars in the collecting electrode by springs when any minor change in orientation can be made by adjusting the nut on the appropriate stud. The shape of the electrodes was based on the 120° Rogowski profile which involves a flat central portion joined to the stem by transition surfaces of increasing curvature. The term '120°' refers to the angle that the surface near the stem makes with the electrode face, Fig. 6.7.

An electrode blank and cover blank were cut on the lathe with the insides hollowed out and polished. The electrode blank was mounted on the back plate in the manner described,

the cover screwed on and the whole filed in the lathe until their projected shadow was exactly coincident with a master curve for the  $120^\circ$  profile plotted from the parameters published by Jones, 1956. The cover was now unscrewed to reveal the ends of the mounting studs and by unscrewing the retaining nuts the electrode was dismantled in order to fix the internal connections etc.

The thin electrode faces, which are 0.076 cm. thick, were drilled with 35 holes of diameter 0.038 cm. these being counter-sunk on the inside to a depth of 0.038 cm. The holes in the collecting electrode were subsequently enlarged to twice the diameter and their number increased by half in order that a measurable portion of the current collected by the electrode should pass through to the collecting plate. It was found that this proportion did not depend directly on the ratio of the plane portion of the electrode to the total area of the holes. This can be tentatively explained by the finite depth of the hole effectively reducing the area of the hole due to the diffusion of the electrons to the walls. As a precaution against positive ions causing secondary emission from the filament no holes were drilled in the centre of the face for an area of 0.6 cm. diameter. After the initial holes had been drilled the electrode faces were ground flat on a reference flat.

Both the filament in the emitting electrode and the plate in the collecting electrode are supported by a quartz rod secured in the electrode stem by a grub screw which mates in a slot ground in the quartz rod. This quartz rod has two holes running through it so that the two connections to the filament are insulated from one another and from the main transmission line. Although it is not necessary, two leads also pass through the quartz in the collecting electrode and both are connected to the collecting plate. Both the guard plate and the collecting plate are polished discs cut from thin brass sheet, Fig. 6.7.

#### Stabilisation of the filament temperature.

It is apparent that the temperature of the filament will depend on the pressure of the gas surrounding it due to the removal of heat by the gas and it became necessary to ensure that the filament temperature, and hence emission, should be constant during both an experiment at a fixed pressure and successive experiments at different pressures. In order to do this the filament was incorporated into a low resistance arm of a Wheatstone net, Fig. 6.8. This circuit enables the temperature of the filament to be kept at a particular value if the following procedure is adopted. Initially the current in the circuit is increased until the emission from the filament is satisfactory and then the net is balanced using  $R_1$  and  $R_2$ . This balance is obtained for one particular

value of filament resistance which depends on the temperature of the platinum, as in the platinum resistance thermometer or the Pirani gauge. This resistance can now be checked at regular intervals by checking the balance of the bridge and any deviation can be allowed for by altering the total current through the circuit.

In order to eliminate any current leakage to earth which might mask the ionization currents the Wheatstone net circuit was mounted on a polystyrene panel, the accumulators placed on a platform raised off the floor by polystyrene supports and all the leads were polythene covered E.H.T. cable.

## CHAPTER VII

### THE MEASUREMENT OF THE U.H.F. FIELD.

#### The Diode Voltmeter.

Preliminary measurements of the maximum voltage attainable across the ends of a tuned transmission line similar to that of the apparatus were made with a symmetrical valve voltmeter of the type used successfully by Gill and Von Engel, 1948, and Clark, 1957, Fig. 7.1. The reading of the electrostatic voltmeter is half the peak voltage across the electrodes,  $P_1$  and  $P_2$ , and can easily be converted to a value for the field strength between the electrodes by determining the electrode separation. The electrostatic voltmeter may be replaced by a micro-ammeter when the peak voltage is the product of the current flowing (in micro-emps) and  $2\pi$ . The upper frequency limit of the acorn diodes is 200 Mc/sec this being well above the working frequency of the apparatus.

It was found however, that in spite of the high resistances in the voltmeter circuit, the presence of the voltmeter across a tuned transmission line considerably affected the tuning, this possibly being due to the appreciable inter-electrode capacitances of the valves. This effect was reduced by inserting quarter wave chokes between the valves and all leads.

Although this voltmeter is useful for determining the voltage attainable it can not be used to make a direct

determination of the voltage across the electrodes in the actual apparatus because, due to the evacuation of the chamber etc. the voltmeter can not remain across the gap whilst the experiment is in progress. Furthermore, the voltmeter can not be attached to the electrodes before or after the experiment because the readings thus obtained would be false due to the de-tuning effect.

There was a possibility that this voltmeter could be attached to the line outside the chamber so that it is as near as possible to the high voltage end. The voltage readings would then be a certain high fraction of the actual voltage across the gap and would depend on the voltage distribution along the line. The value of this fraction would have to be checked and would involve the use of a step-over instrument. If the valve voltmeter were attached directly across the transmission line the ionization current across the gap as measured by the external galvanometer, would be masked by the constant current flow through the valve voltmeter. This consideration made it imperative to develop a step-over instrument so that the circuit for indicating the u.h.f. voltage across the gap could be loosely coupled to the line and not directly connected to it. This being the case, the indicating circuit would also take less power.

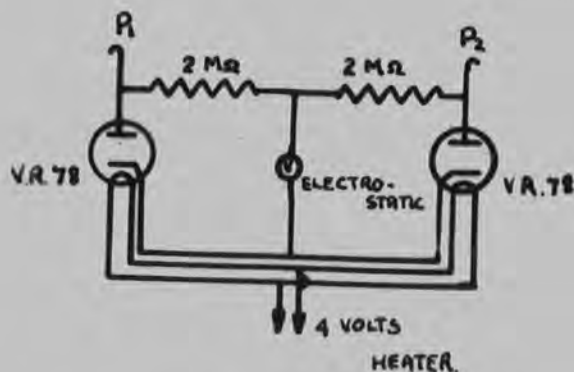


FIG. 7.1 VALVE VOLTMETER  
FROM GILL AND WOOD ENGEL, 1948.

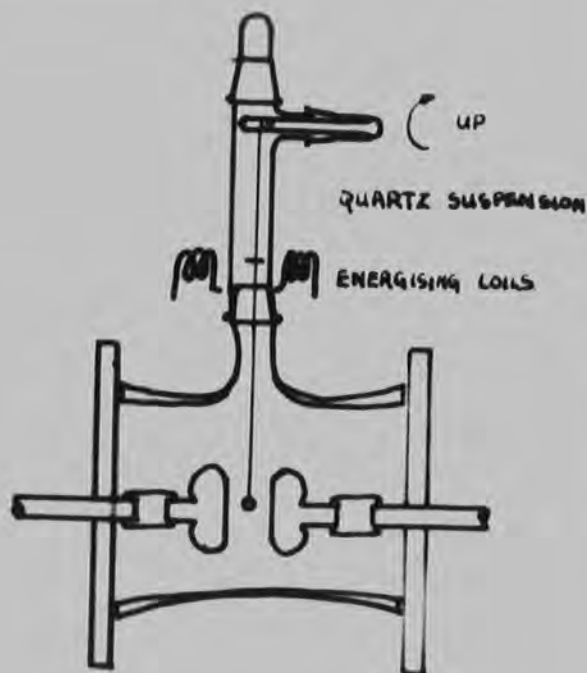


FIG. 7.2 DETAILS OF SUSPENSION  
OF OSCILLATING DISC

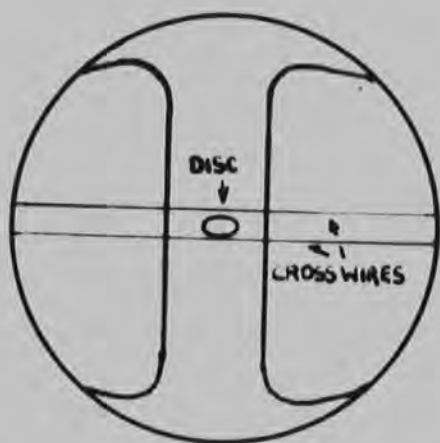


FIG. 7.3 VIEW THROUGH  
TELESCOPE EYEPiece.

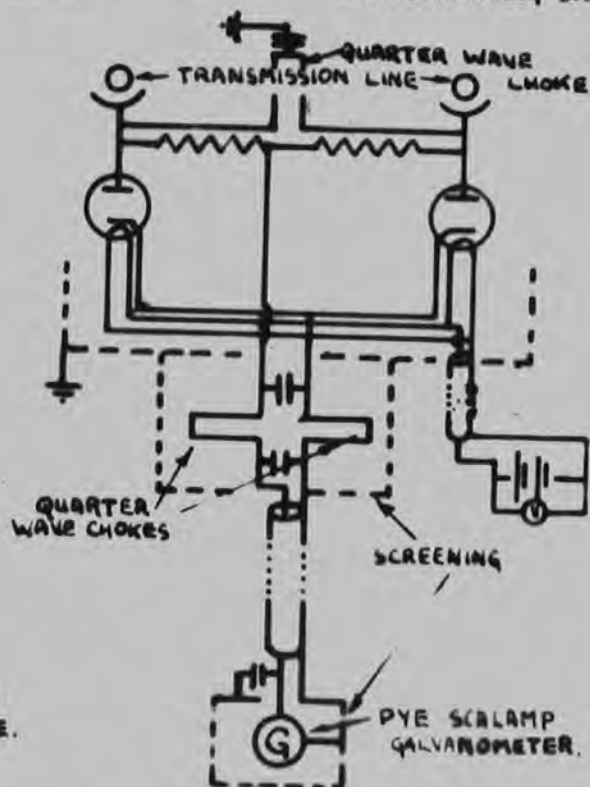


FIG. 7.4 U.H.F. FIELD INDICATING  
METER.



### Oscillation voltmeter.

It seemed necessary therefore, to develop some type of step-over instrument which could be calibrated at power frequencies or D.C., and then used to calibrate a u.h.f. indicating instrument. Such a step-over instrument has been developed from experiments by Thornton and Thompson, 1932, on the determination of high voltages to an accuracy of 0.1%. To do this they used an ellipsoid made of Duralumin, 3.9 cm. long and 0.59 cm. in diameter, suspended in a uniform field from a minor axis of the ellipsoid by an insulating torsionless suspension. The uniform field was produced by applying the unknown voltage to a large pair of circular electrodes so that a determination of the field would easily result in the value of the voltage. The ellipsoid was allowed to oscillate about its suspension, and from Maxwell, 1904, it can be shown that the value of the electric field,  $F$  is given by:

$$F^2 = K(n^2 - n_0^2) \dots\dots\dots 7.1.$$

where  $n$  is the frequency of oscillation of the ellipsoid in the applied field, and  $n_0$  the frequency of oscillation in the absence of the field, which is dependent on the constants of the suspension. The constant  $K$  depends only on the dimensions and the mass of the ellipsoid. Thornton used this ellipsoid to measure very high direct fields but as the relationship 7.1 is independent of the field direction the ellipsoid can be used to determine the value of alternating fields as shown by Bruce, 1947.

Owing to the relatively smaller size of electrodes and gap width in the apparatus under consideration, it is necessary to scale the ellipsoid and the type of suspension down so that the ellipsoid is small compared to the gap and the torsional effect of the suspension is small compared to the effect of the field, i.e.  $n_0 \ll n$  for the normal working conditions, and that the frequency is low enough to be measured from visual observation. As the instrument is to be used as a step-over instrument any inaccuracies as dealt with by Bruce, 1947, can be neglected, provided that the conditions for both stages of the calibration are the same.

The original large instrument could be used as an absolute voltmeter but the small size of the present apparatus precludes this. Nevertheless the instrument satisfies completely the requirement that a low-frequency or unidirectional field calibration should be applicable to u.h.f. measurements. It is not necessary for the body to be an ellipsoid provided that the body has a major and minor axis when it will behave in a manner described by equation 7.1 where  $K$  is replaced by another constant  $K'$  which depends on the size and the mass of the body and  $n_0$  by  $n'_0$  depending on the suspension.

Several shapes of body were investigated which had major axes of less than 3 mm. so that the field was not appreciably distorted. It was found that a disc suspended from its edge

was the most convenient shape and a method was perfected whereby a small Woodsmetal bead was heated between two microscope slides so that it flattened to form such a disc. Whilst the Woodsmetal was molten, a fine piece of wire was inserted into its centre across a diameter of the disc and the whole allowed to cool. The fine wire enabled the suspension to be attached to the disc by means of black wax in a manner advised by Braddick, 1954.

The suspension was initially made from unspun silk but this was too stiff and was replaced by a quartz fibre, drawn in the laboratory from a molten rod using an elastic crossbow and arrow. This method produced long fine fibres which were only visible with scattered light.

A preliminary investigation of the behaviour of the disc suspended by a quartz fibre between dummy electrodes showed that the relationship  $F^2 = K (n^2 - n_0^2)$  held for power frequency fields and for u.h.f. fields when the voltage across the electrodes was determined directly by means of the valve voltmeter. In view of this, the test chamber was designed to accommodate the instrument.

The disc is suspended from the top of a wide 'Pyrex' glass tube so that it hangs in the centre of the electrode gap, with the top of the suspension attached to a glass rod which can be rotated externally through a ground glass seal. This allows the disc to be drawn clear of the electrode gap for

ionization observations by rotating the rod, Fig. 7.2.

The ellipsoid and electrodes are viewed from underneath the chamber by a telescope and plane mirror system. Initially the ellipsoid is orientated with the major axis at right angles to the electrodes, i.e. parallel with the field, so that it is in a position of rest whether or not there is an electric field, Fig. 7.5. In order that the disc should make oscillations about this position of rest a very small piece of iron wire is fastened to the quartz fibre near its fixed end inside the supporting tube (Fig. 7.2) and two small coils are mounted outside the supporting tube as close as possible to it. On momentarily energising the coils the wire turns so that its length lies along the magnetic field and in turn transfers its motion to the disc. By energising the coil in phase with the natural oscillation of the disc a large amplitude can be built up so that in spite of the oscillations decaying, observations can be made over the time of 1 minute.

The frequency of the disc is measured using a stop-watch and an electro-mechanical counter operated by a Morse key. With this arrangement a maximum frequency of about two oscillations per second can be measured with an accuracy of 1%. This error could be reduced by using a method similar to that used by Bruce, 1947, where the counts and pulses every two seconds were recorded on a constantly moving tape.

It was found that the measured frequency depended both

on the amplitude of the oscillation and on the total time of the oscillations measured. This was presumably caused by the reaction of the electrodes on the disc, due to their nearness to the disc and to the finite size of both disc and electrodes. In order to ensure that every observation was made with the same initial amplitude two parallel crosswires were inserted into the eyepiece of the telescope so that the amplitude can be kept within these bounds, Fig. 7.3.

#### The u.h.f. indicating circuit.

It was thought that a valve voltmeter as already described could be incorporated into a circuit loosely coupled magnetically to the transmission line so that if the electrostatic voltmeter were replaced by a sensitive galvanometer the current through it would be an indication of the power level in the line. This was not feasible, as any magnetic coupling loop had to be placed near to the current maximum and consequently picked up power from the oscillator. In this case the galvanometer current was not only dependent on the power level in the line but also on the coupling between the line and the oscillator. This was over come by loosely coupling a similar circuit capacitatively to the high voltage end of the line, i.e. the electrode end, where the voltmeter circuit could be shielded from the oscillator.

Consequently the valve voltmeter is soldered to two strips of copper foil which are attached to the line as near

to the chamber as possible. The foil is insulated from the line by polythene tape. The position of the voltmeter is such that it comes between the electrodes and the compensating condenser and is well shielded by the shielding of the line itself, as described in Chapter IV. The leads to the galvanometer are led out through the shielding and through a filter circuit, Fig. 7.4, so that no standing waves are developed in the coaxial leads or apparatus external to the shielded line. Furthermore, a quarter wave choke is connected across the input to the valve voltmeter (Fig. 7.4) and earthed through a condenser at its closed end. This eliminates pick-up from the modulation oscillator being displayed on the galvanometer, as any such pick-up is short circuited to earth whilst the quarter wave choke presents a high impedance at frequencies of about 100 Mc/sec. Absence of pick-up from the u.h.f. oscillator was established by determining the field in the gap with the oscillating disc. The deflection of the galvanometer in the indicating circuit was kept constant for varying degrees of coupling between the line and the oscillator, when it was found that the field remained constant.

The presence of the ellipsoid in the gap has no apparent affect on the tuning of the line at gap widths greater than 0.6 cm.

### The experimental results and calibration.

It is likely that the u.h.f. indicating instrument measures some fraction of the u.h.f. voltage across the electrodes and that this fraction is not constant for different gap widths owing to the position of the voltmeter varying with respect to the standing wave pattern on the line. It is therefore necessary to calibrate for all gap widths, or rather to calibrate for several gap widths and infer the calibration of the others.

The calibration of the oscillating disc is carried out with a direct field which is developed between the electrodes by applying the output from a 1000 volt variable D.C. supply across the electrodes, the voltage being measured with an Ayrton Mather Electrostatic Voltmeter with a full scale reading of 600 volts and an accuracy of 1.0% in the middle of the range, (calibration by Clark, 1957.) The full range from 0 to 1000 volts <sup>was</sup> being covered by using a scaling circuit.

The calibration of the disc for four gap widths is shown in Fig. 7.5 where the linearity of the relationship of equation 7.1 is shown to hold. It must be emphasized that the initial calibration using a direct field is more desirable than using an alternating one, in that the A.C. reading will be affected by the waveform, and the measuring instrument has eventually to be referred back to a D.C. standard. Initially an alternating voltage was used for the calibration and irregularities were apparent in the measurements which were

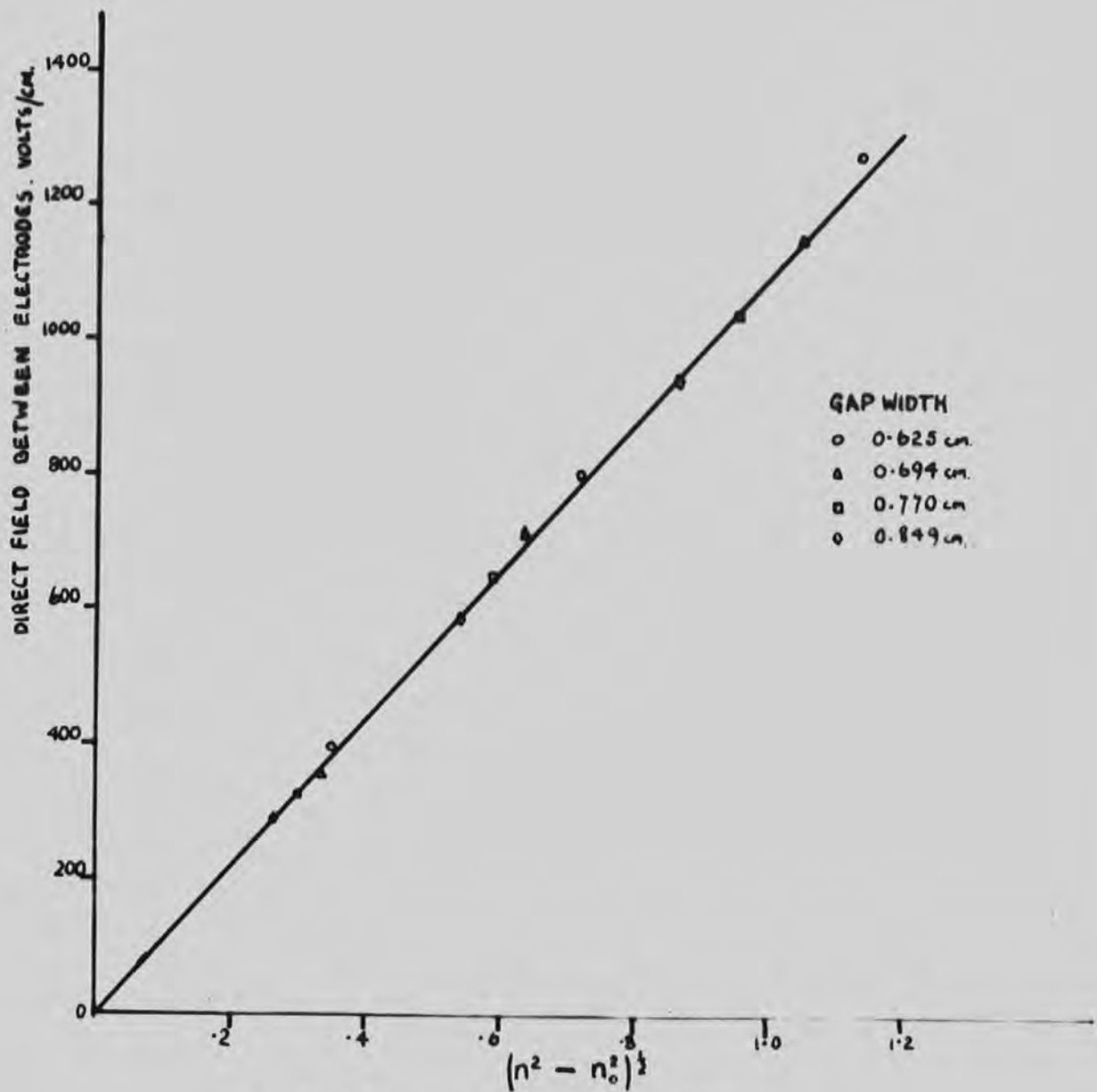


FIG. 7.5 DIRECT FIELD CALIBRATION OF OSCILLATING DISC FOR FOUR GAP WIDTHS.



attributed to variations in waveform.

As the disc measures the field between the electrodes, and the valve voltmeter measurement is dependent on the u.h.f. Voltage across the end of the line, the calibration of the valve voltmeter in terms of field will result in a set of particular curves for the separate gap widths. This is seen in Fig. 7.6 for five gap widths and Table 7.1 indicates a typical set of results for one of these.

From Fig. 7.6 it is seen that the calibration curves are of the form described by the equation:

$\theta + c = m.E_u$ , where  $c$  is the intercept,  $\theta$  the deflection as displayed on the galvanometer and  $m$  is a function of the gap width  $d$ . This function is shown to be linear in Fig. 7.7 where  $m$  is plotted against  $d$ .

The method of determining the field corresponding to a particular deflection  $\theta_1$  and gap width  $d_1$  is to find the value of  $m_1$  from Fig. 7.7 and calculate the field from  $E_u = \frac{\theta_1 + c}{m_1}$  volts/cm.

If the u.h.f. field across the electrodes is plotted as a function of the gap width ( $E_u \cdot d$  versus  $d$ ) for a particular valve voltmeter deflection (Fig. 7.8) it can be seen that the voltage measured at small gap widths is larger than that at large gap widths. This can be shown to be due to the position of the valve voltmeter circuit with respect to the electrodes and compensating condenser. When the electrode gap width

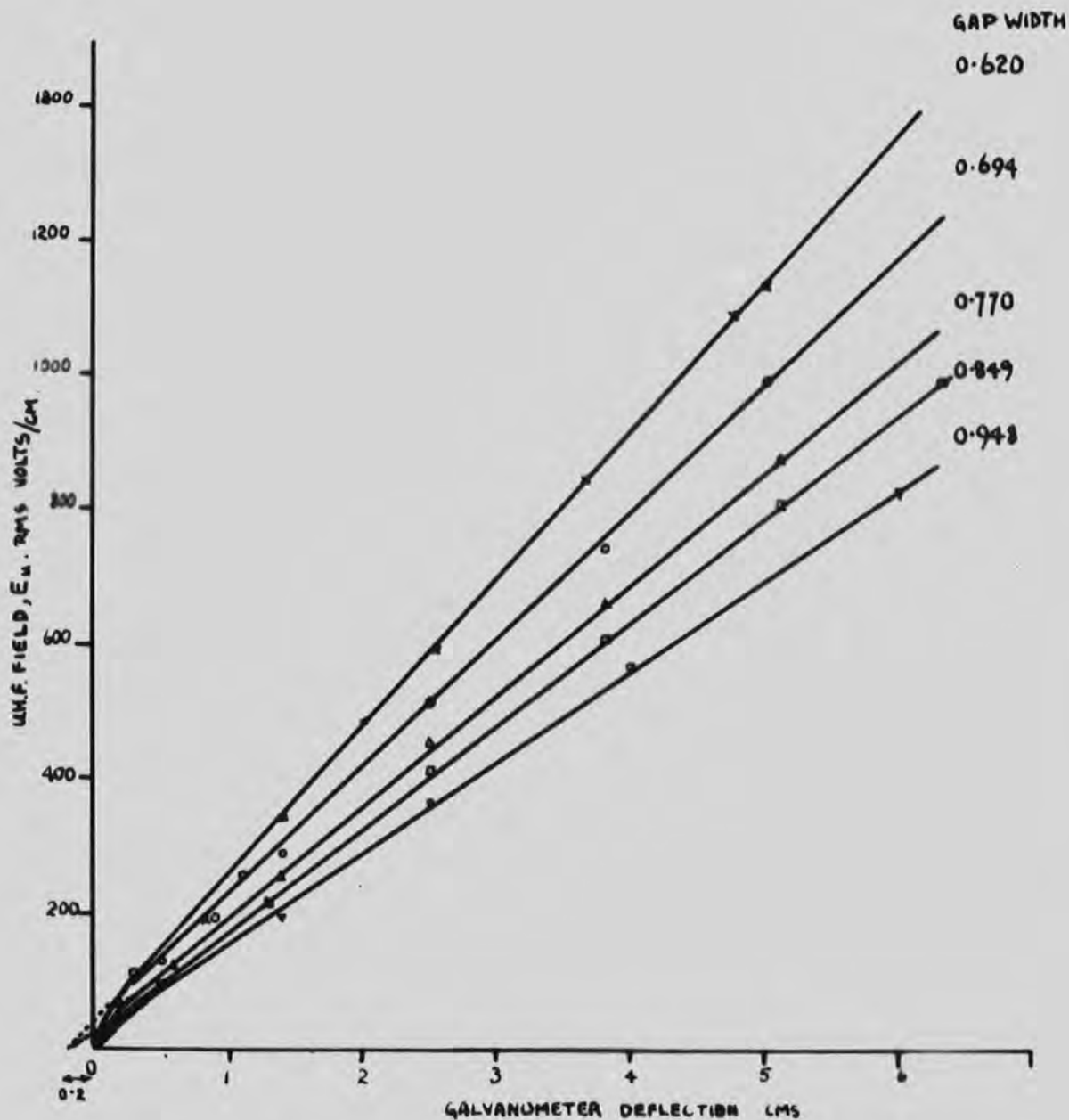


FIG. 7.6

CALIBRATION OF THE VALVE VOLTMETER  
IN TERMS OF UHF FIELD AT THE  
ELECTRODES FOR FIVE GAP WIDTHS.

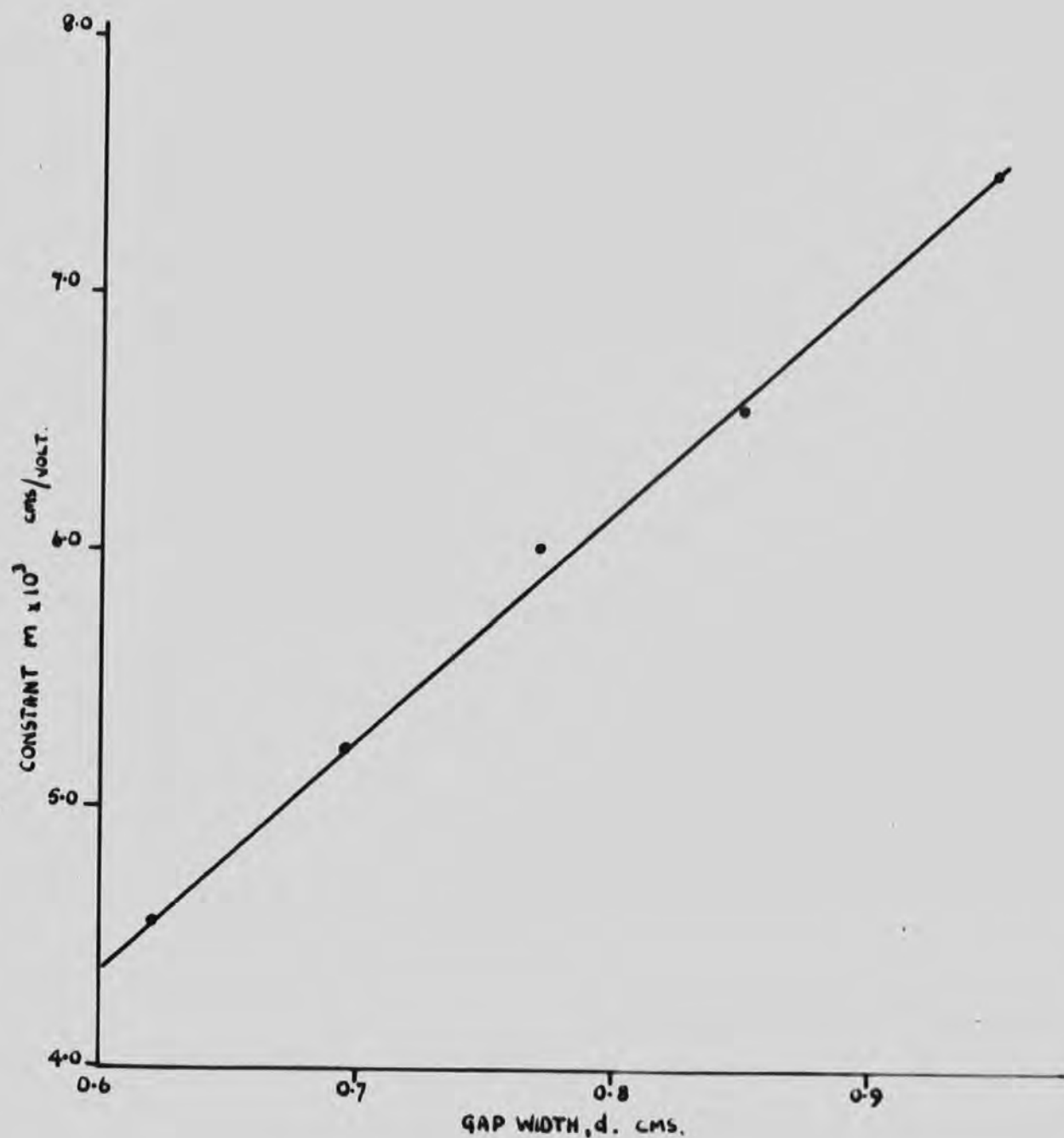


FIG. 7.7 CONSTANT  $m$ , ( $\frac{\theta \cdot C}{E_m}$ ) AS A FUNCTION OF THE GAP WIDTH

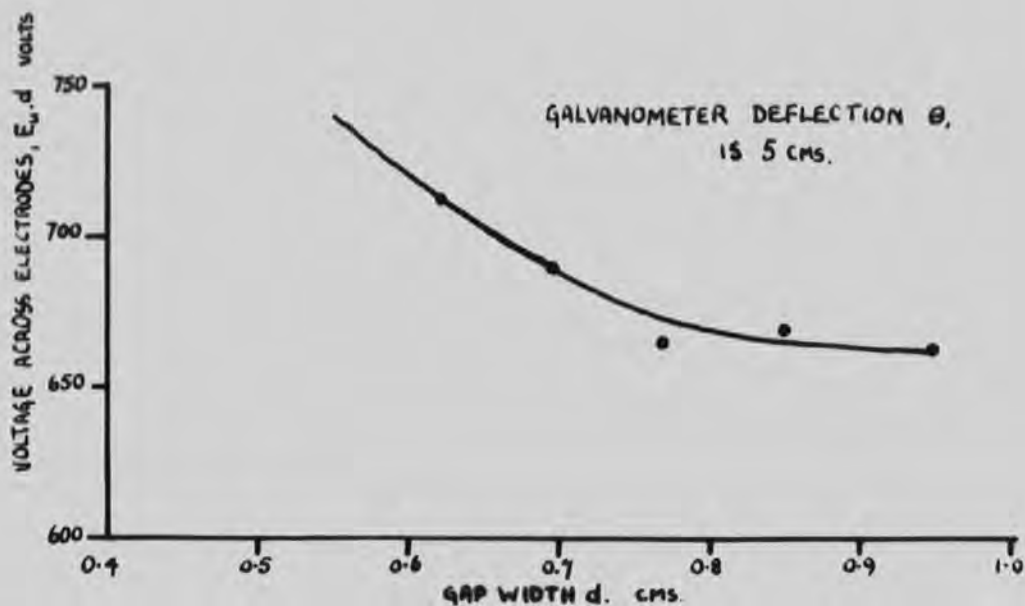


FIG. 7.8 VOLTAGE ACROSS THE ELECTRODES AS A FUNCTION OF GAP WIDTH FOR A CONSTANT VALVE VOLTMETER READING.

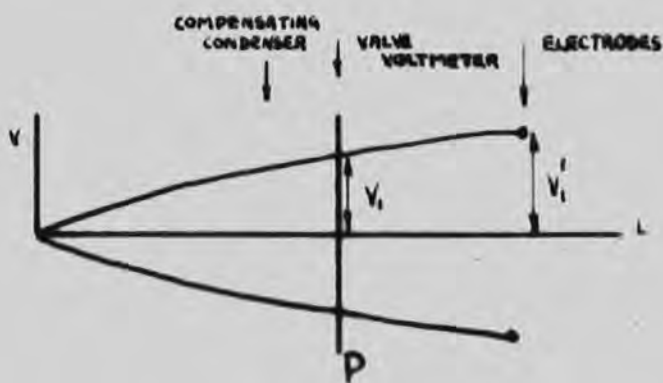


FIG. 7.9, (a) SMALL GAP WIDTH.

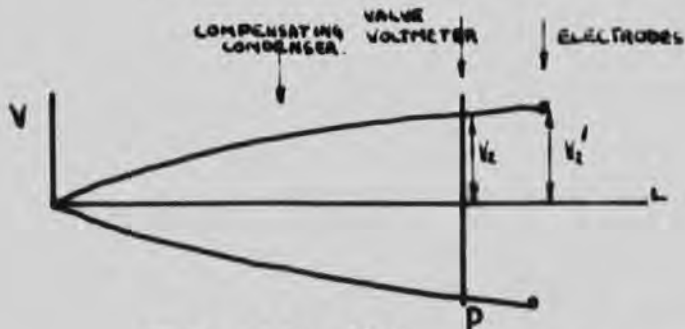


FIG. 7.9, (b) LARGE GAP WIDTH.

is small and the compensating gap width correspondingly large, the position of the meter with respect to the standing wave pattern will be as in Fig. 7.9a and when the electrode gap width is large as in Fig. 7.9b.

Let the deflection of the voltmeter galvanometer be proportional to the voltage at point P as indicated in the Figures 7.9a and 7.9b, then the deflection for the small electrode gap width is given by:

$$D_1 = f.V_1$$

where f is the proportionality constant and

$$D_2 = f.V_2 \text{ for the large gap width.}$$

Thus, when  $D_1 = D_2$  i.e. the deflection is constant, Fig. 7.9c,

$$V_1 = V_2$$

Due to the different positions of the meter with respect to the standing wave pattern,  $V_1$  is related to  $V_1^1$  by the equation;  $V_1 = k_1.V_1^1$  and  $V_2$  to  $V_2^1$  by;  $V_2 = k_2.V_2^1$ , where  $k_1$  and  $k_2$  are the respective proportionality constants. From these  $k_1/k_2 = V_2^1/V_1^1$  and as  $k_1$  is smaller than  $k_2$  (Figures 7.9a and b), so that  $V_2^1$  is smaller than  $V_1^1$  indicating that the voltage measured at the larger gap width is smaller than that at the small gap width.

Also, the value of k will only depend on the electrode gap width and consequently is unaffected when the line is tuned by devices to the left of the voltmeter. This was found to be the case experimentally.

It can be seen in Fig. 7.5 that the calibration curves are not linear for very small deflections of the galvanometer. It has been shown that this is not due to the galvanometer but is thought to be due to the characteristics of the diode valves.

The error in the measurement of the field in this manner is considered to be  $\pm 1\%$  for fields above 100 volts/cm. r.m.s.

TABLE 7.1.

Gap width 0.849 cm.  $n_0^2 = 0.360$ . Gradient of D.C. calibration = 1.106  $\frac{\text{volts/cm.}}{\text{cm. defln.}}$

Galvo.defl.	$n^2$	$n^2 - n_0^2$	$\sqrt{n^2 - n_0^2}$	Field from
cms.	/sec <sup>2</sup>	/sec <sup>2</sup>		D.C.calib.Volts/cm.
6.3	1.135	.775	.880	998
5.1	.896	.536	.732	810
3.8	.664	.304	.551	610
2.5	.501	.141	.375	415
1.3	.399	.039	.198	219
0.5	.368	.008	.089	99

## CHAPTER VIII

### THE DETERMINATION OF THE TRANSIT TIME.

The modulating potential is applied to the electrodes as in Fig. 8.1 which is purely a diagrammatical representation of the circuit. The actual circuit is essentially different in that the D.C. measuring circuits are prevented from short circuiting the modulating potential by using a system of air core chokes. All the leads to the electrodes are led in at the loop end of the transmission line so that they have little effect on its operation. It can be seen that both the electrodes are at the same potential which can be considered to be earth potential for the frequencies considered, by virtue of the  $0.1 \mu F$  condensers. This ensures that the modulating potential causes no additional field between the electrodes. A valve voltmeter is connected across the capacitance of the tank circuit so that the potential across the electrodes can be determined.

The intention is that the field between the cathode, K, and the emitting electrode,  $P_1$ , shall determine whether the electrons emerge from  $P_1$  also whether they are carried through the collecting electrode,  $P_2$ , to the collector, C. Emergence will occur when  $P_1$  is positive with respect to K and collection at C when C is positive with respect to  $P_2$ . Hence a maximum in the collector current may be expected when the transit time

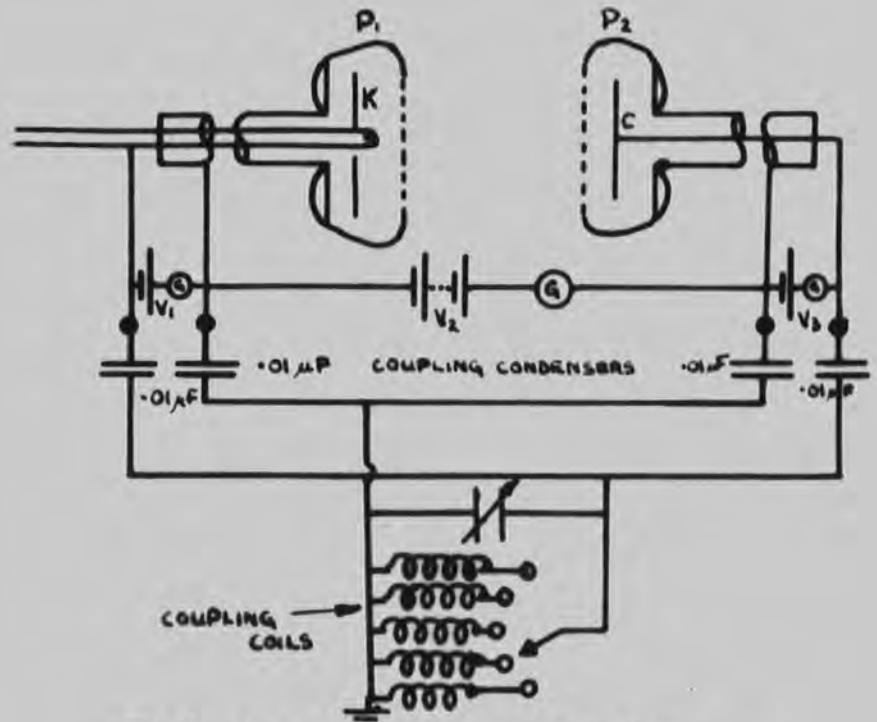


FIG. 8.1 APPLICATION OF THE MODULATING POTENTIAL TO THE ELECTRODES ETC.

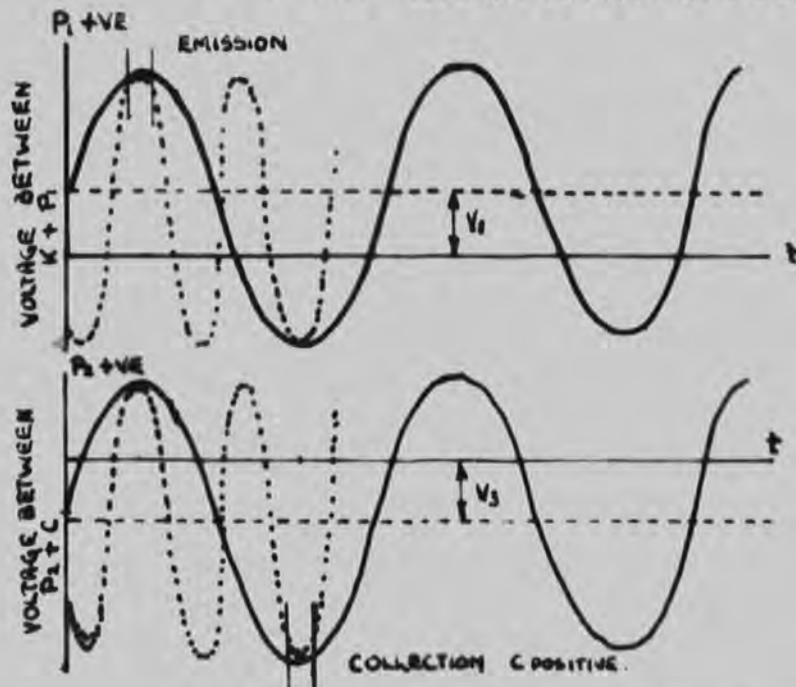


FIG. 8.2 CONDITIONS OF EMISSION AND COLLECTION FOR THE RESPECTIVE ELECTRODES.



of the electrons is that of an odd number of half cycles of the applied oscillations.

Consider Fig. 8.2. Let  $T$  be the transit time of the electrons,  $t$  the periodic time of the field and  $\omega$  the angular frequency of the field.

$$t = \frac{2\pi}{\omega}; t/2 = \frac{\pi}{\omega}.$$

The condition is that:  $T = (2n + 1) \pi/\omega$

$$\text{or } \omega/\pi = (2n + 1)/T$$

for successive maxima,  $\omega_1 = (2n_1 + 1)\pi/T$   
 $\omega_2 = (2n_2 + 1)\pi/T$  }  $\omega_2 - \omega_1 = (2\pi/T)(n_2 - n_1)$

i.e.  $\omega = 2\pi/T$  at adjacent maxima.

Thus by varying the frequency of the modulating potential so that a succession of maxima are obtained in the collector the actual transit time may be determined. Also, should there be any zero error in this value for the transit time the use of measurements with various gap widths at the same pressure and the same drift field  $E_d$ , will enable it to be eliminated.

It has been seen in Chapter II that this transit time  $T$  may be expected to vary from  $0.5 \mu\text{secs}$  to  $1.9 \mu\text{secs}$  corresponding to a range of oscillator frequency of  $250 \text{ Kc/sec.}$  to  $7 \text{ Mc/sec.}$  This range will accommodate at least two current maxima for the smaller transit time.

#### The modulation oscillator.

An oscillator has been built to operate from  $250 \text{ Kc/sec.}$

to 7 Mc/sec. using five separate coils for overlapping ranges. The circuit diagram is shown in Fig. 8.3. The oscillator is of the simple tuned anode, tuned grid type employing a PT15 pentode and the output can be varied by varying the D.C. input, using a Variac in the A.C. power supply to the 1000 volt D.C. power pack.

It was originally intended that the potential on the electrodes would be developed across a heavily damped coil so that there would be a similar response for a particular coil over the whole of its frequency range. These coils were to be coupled to the respective anode coils of the oscillator so that the frequency of the modulation could be varied smoothly through any particular range during the experiment. It was estimated that a maximum of 100 volts peak to peak would be required across the electrodes but with this system it was not possible on the two highest ranges and it was decided to use a range of tuned circuits coupled to the oscillator as in Fig. 8.1.

The maximum potential developed across the tuned circuits is far in excess of the estimated requirements which may be of advantage at some later stage.

### Results.

Although the apparatus has been developed as described no measurements of transit time have been made. It has been

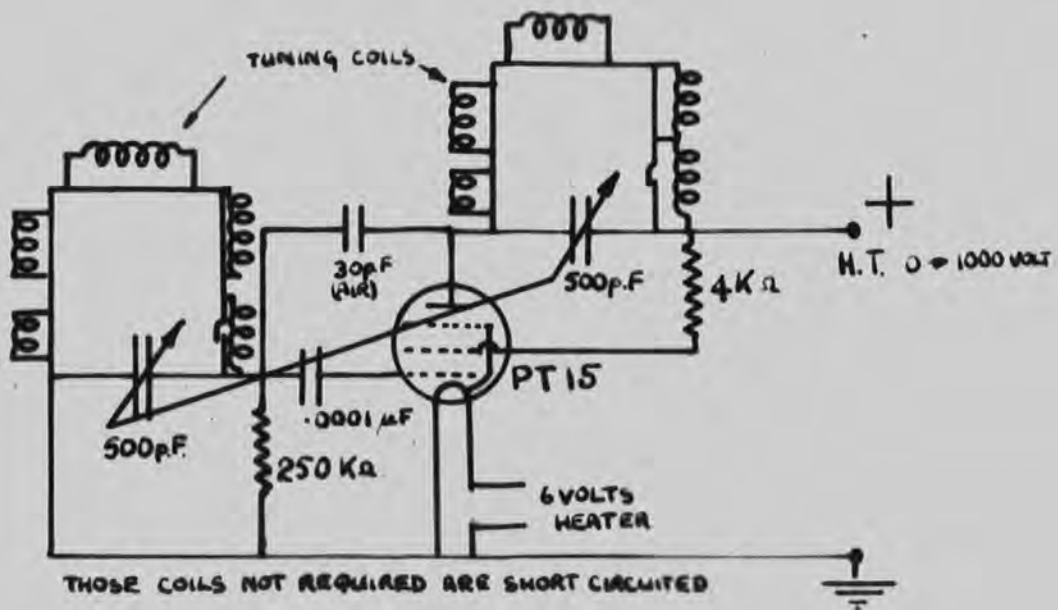


FIG. 8.3 THE MODULATION OSCILLATOR

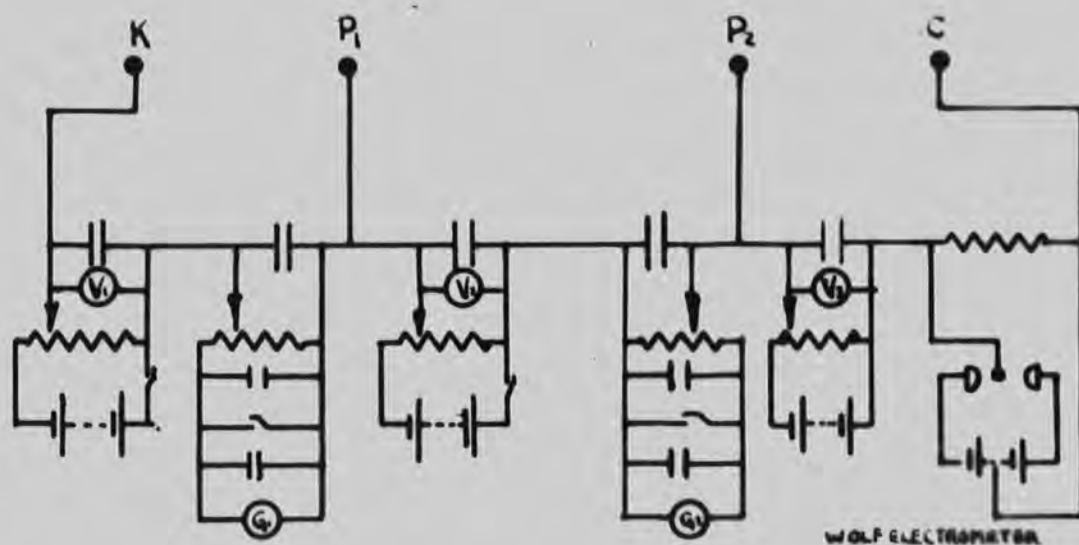


FIG. 9.1 THE DIRECT CURRENT MEASURING CIRCUIT

shown though, that when the modulating potential is superimposed on a small direct potential which is causing electrons to emerge into the gap, the electron current is increased. Such a current will no doubt be modulated at the applied frequency. It has been shown therefore that the modulating potential affects the initial current entering the gap but it has not yet been possible to observe the affect of the modulating potential on the distribution of the current leaving the gap between  $P_2$  and the collector.

## CHAPTER IX

### THE DIRECT CURRENT MEASURING SYSTEM

It is necessary to measure the current flowing to all the electrodes, i.e. from K to  $P_1$ , to  $P_2$  and to C, and suitable potentials have to be applied in order that the electrons move in the required direction. These potentials are applied across the relevant gaps by potentiometer circuits as in Fig. 9.1. There are no high resistances in these circuits so that when small currents ( $\sim 10^{-7}$  amp) are flowing the potentials as realised at the terminals of the potentiometers appear across the gap.

The current flowing between K and  $P_1$  when  $P_1$  is made positive with respect to K is measured with a Tinsley galvanometer  $G_1$ , which has a scaling circuit incorporated in the damping resistor so that there are four ranges of sensitivity as indicated in Appendix I. The current across the gap  $P_1$  to  $P_2$  is measured by a sensitive Cambridge Ballistic Galvanometer  $G_2$ , which also has four sensitivity scales, A.I. In the investigations dealt with in this thesis the minimum current measured by  $G_2$  was  $1 \times 10^{-9}$  amp. ( $i_0$ ), and the maximum stable current before breakdown under the u.h.f. field was  $6 \times 10^{-8}$  amp. (1). It is assumed that these currents are small enough for there to be no appreciable space charge effects. This was substantiated when it was

observed that the u.h.f. field amplification in the gap was unaffected by the value of the initial current  $i_0$ , more fully described in Chapter XI.

The determination of the current flowing to C is a more difficult proposition and it was thought advisable to measure it when a direct potential is applied across  $P_2$  and C before any measurement was attempted under the modulated conditions, when the current will be smaller. However, any attempts have only been successful when amplified or breakdown currents are flowing to  $P_2$ .

The two methods that have been used to measure the current both involve a Wolf String Electrometer, an instrument with a very small capacitance, a very high leak resistance and a sensitivity of one volt when used heterostatically.

One of the methods has been to use this electrometer to determine the rate of charge or discharge of a small capacitance by currents flowing to C, Figures 9.2 a and b. This method is not capable of a continuous determination of the current and in order to overcome this another method has been used involving the measurement of the potential drop across a very high resistor produced by the current flowing through it from the collector, Fig. 9.3. In this case the electrometer may be replaced by an electrometer valve.

It appears that one of the difficulties in measuring the smaller currents flowing to the collector is not due to the

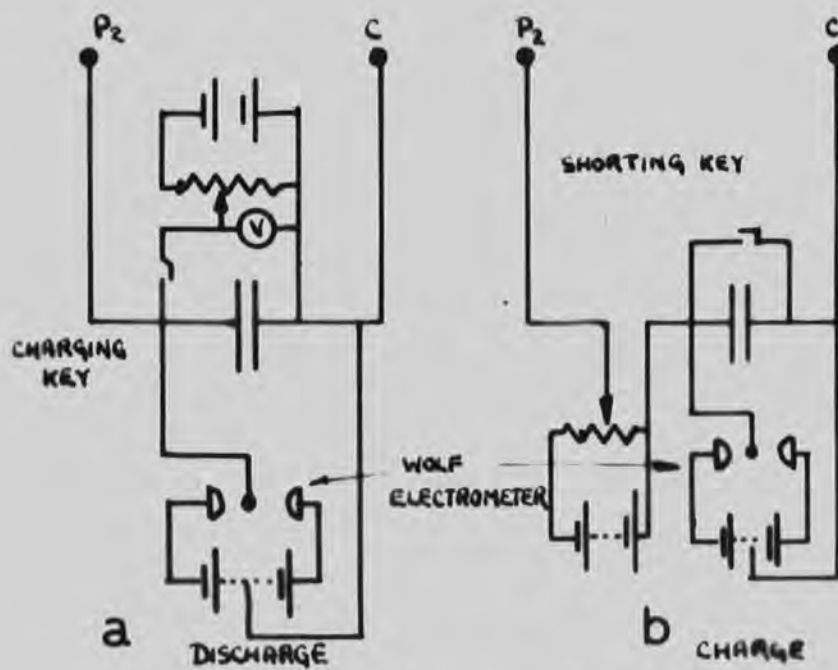


FIG. 9.2 TWO CIRCUITS FOR MEASURING THE CURRENT TO THE COLLECTOR.

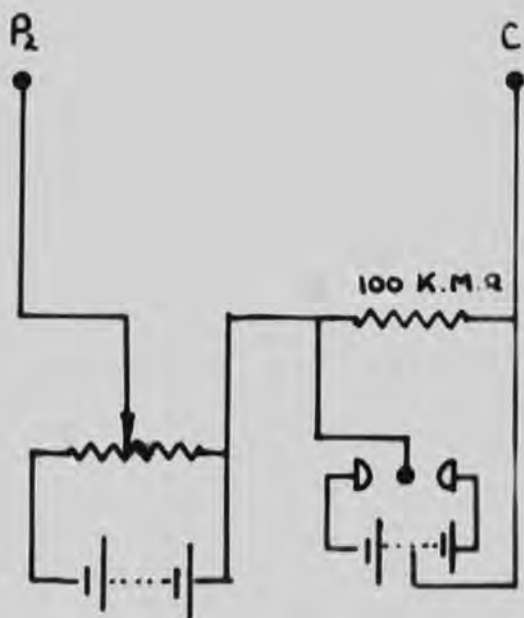


FIG. 9.3 CIRCUIT FOR CONTINUOUS DETERMINATION OF THE CURRENT TO THE COLLECTOR.

insensitivity of the measuring apparatus but arises from the masking effects of larger currents leaking through poor insulation in some part of the circuit. The major contribution to this leak is through the condensers coupling the line to the modulation potential tank circuit, which have a leak resistance of about  $10^{11}$  ohms. They are of the ceramic type and until they were used it was thought unlikely that the modulation field could be applied in this manner because of the very much lower leak resistance of other types of condenser.

In order to reduce these leak currents to a minimum all the leads are covered in polythene and the components (batteries, resistances etc.) are mounted on polystyrene sheets and the leakages are now too small to be registered on either of the galvanometers,  $G_1$  and  $G_2$ .

As the leak current in the collector circuit could not be reduced below that flowing through the coupling condensers, the proportion of the current passing through the collecting electrode to the collector was increased by increasing the number and size of the holes in the electrode face. It may now be possible to detect the current under the initial conditions of the experiment, i.e. no u.h.f. field amplification.

It was found that when the modulation oscillator was operating small deflections of the galvanometers,  $G_1$  and  $G_2$  were observed. These were found to be caused by non-linear



circuit elements in the circuits and condensers were connected across all such possible elements so that any alternating currents are by-passed, Fig. 9.1. Even so, it is preferable for any such currents to be prevented from flowing through the measuring circuits as the leads are long and difficult to screen. From Fig. 8.1 it can be seen that two of the measuring circuits, the one in the cathode circuit and the other in the collector circuit, will short circuit the modulation potentials applied across K and  $P_1$  and C and  $P_2$  unless these circuits present a high impedance to the modulation oscillations. If this condition is satisfied the high frequency current through these circuits will be reduced, thus reducing the possible effects of the non-linear elements as described above.

This is achieved by connecting air core, high frequency chokes between the leads to the measuring circuits and the points where the high frequency potential is led to the respective electrode. All these chokes and the coupling condensers are mounted on a polystyrene sheet and enclosed in a metal box to reduce pick-up. The circuit diagram of this filter system is as in Fig. 9.4. The chokes in the heater leads had to be specially wound as they not only had to present a high impedance to high frequency currents but also to take the filament heating current.

Owing to the many problems encountered it has not yet been



possible to measure the transit time of the electrons in the gap but this has not seriously affected the scope and interpretation of the preliminary results obtained.

## CHAPTER X

### THE EVACUATING AND GAS CONTROL SYSTEM.

The vacuum system is essentially the same as that used by J. Clark, 1957, who designed it so that different pure gases could be admitted to the test chamber at particular pressures, whilst being absolutely free from mercury contamination. The vacuum line is constructed from wide bore 'Pyrex' glass tubing and stopcocks with 1 cm. plug bores to ensure a high pumping speed. Two pumps are used to evacuate the system, a backing pump and an oil diffusion pump. The backing pump is a 'Speedivac' rotary oil pump and the diffusion pump, a 'Metrovac' single stage oil pump which gives an ultimate vacuum of  $10^{-5}$  mm. of Hg. Permanent ground glass joints are sealed with black Apiezon wax and the stopcocks etc. treated with Apiezon grease N.

A gas circulator (Fig. 10.1) connected to the chamber ensures continuous circulation of the gas through it during an experiment. The entire system takes considerable time to out-gas, it being advisable to pump out for a least a day before any test gas is admitted. Provision is made for small amounts of different gases to be admitted to the evacuated system by means of a pipetting arrangement from spectrally pure gas supplies provided by the British Oxygen Company in 1 litre containers. A separate supply of Hydrogen is

provided by passing impure laboratory hydrogen over a hot Palladium tube, when the pure hydrogen diffuses through the walls into the vacuum system.

#### Pressure measurement.

Three gauges are used as follows:

a) Atmospheric pressure to 5 mm. of Hg.

Pressures in this range are to be measured by a differential bellows gauge which can be calibrated against a mercury column for differences in pressure on the two sides. This method avoids any mercury contamination of the test gas and consequent falsification of the results by the easily produced mercury ions (Penning, 1927). This gauge was constructed by Monk, 1959, and used successfully but has not yet been calibrated when connected to this vacuum line.

b) 30 mm. of Hg. to 1 mm. of Hg.

Pressures in this range have been measured by a direct reading Edwards Dial Gauge but it is intended that finally all pressures will be measured by the differential gauge.

c) 1 mm. of Hg. to  $10^{-5}$  mm. of Hg.

Pressures in this range are measured by an Edwards Pirani Gauge. This instrument does not need to be particularly accurate as it is only used to indicate whether the system has been out-gassed. It is also used as a leak detector when a fine hydrogen jet is played onto the suspected leaky area.

Fig. 10.2 shows a diagram of the complete system.

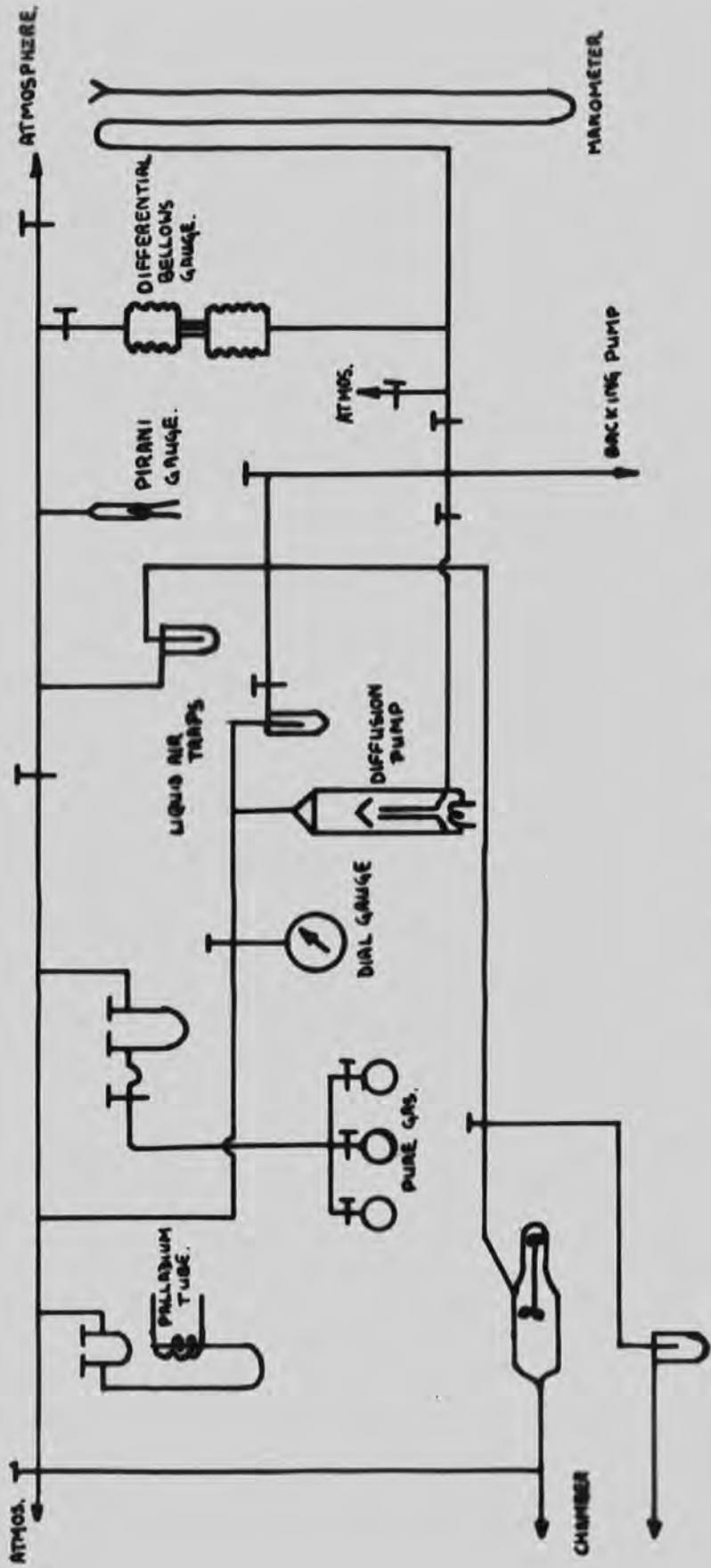


FIG.10.2 THE EVACUATION AND GAS CONTROL SYSTEM

As the results described in this thesis are of a preliminary nature all the pressures were recorded on the Edwards Dial Gauge.

## CHAPTER XI

### MEASUREMENTS OF THE PRE-BREAKDOWN IONIZATION IN HYDROGEN

#### Experimental Procedure.

The test side of the vacuum system is evacuated for about a day when the pressure as determined by the Pirani gauge is less than  $10^{-5}$  mm. of Hg. with liquid air in the cold traps. Small samples of Hydrogen are now pipetted into the line and allowed to circulate before being flushed out by the pumps. Finally the test side of the system is isolated and a pure sample of Hydrogen is admitted at the required pressure. The circulating fan can now be started and the apparatus is ready for investigations to be made on Hydrogen at the particular pressure and gap width.

A voltage of 30 volts is applied between the cathode and the emitting electrode, a direct voltage between the electrodes  $P_1$  and  $P_2$  corresponding to the lowest direct field required,  $E_d$ , and the filament current is increased until the electron current flowing to the collecting electrode is large enough to deflect the indicating spot of the measuring galvanometer ( $G_2$ , Fig. 9.1) about 1 cm. at a distance of 1 metre when on its most sensitive range.

The u.h.f. field across the gap is now increased from zero in steps and the current as measured by  $G_2$  is recorded for the particular values of the u.h.f. field as recorded by



the valve voltmeter. No attempt has been made to measure the transit time of the electrons in these experiments and the results recorded below are only preliminary results in order to see whether the apparatus functions as expected.

### Experimental Results.

Figures 11.1, 11.2, 11.3 and 11.4 show four sets of pre-breakdown ionization curves where the current amplification,  $i/i_0$ , is plotted against the u.h.f. ionizing field for four separate pressures and different direct fields. The asymptotic limit of the u.h.f. field for a particular direct field and pressure is the value of the u.h.f. breakdown stress. A typical set of results are indicated in Table 11.1 for a pressure of 8 mm. of Hg. Fig. 11.5 shows a graph of the u.h.f. breakdown stress plotted against the drift field for constant pressures. These are seen to be linear for small values of drift field.

The variation of the u.h.f. breakdown stress with pressure for zero drift field is shown in Fig. 11.6. As these results are taken for conditions for which the diffusion theory is valid these points should fall on the unique curve obtained by Clark, 1957 for  $E_b \cdot \Lambda$  plotted against  $p \cdot \Lambda$ , where  $\Lambda$  should be the diffusion length of the gap and is equal to 0.19 cm. for the case in point. This is seen to be the case from Fig. 11.7 where Clark's results and the present measurements, which come at the end of

HYDROGEN

$p = 3.5$  mm. of Hg.  
GAP WIDTH,  $d = 0.635$  cm.

$E_d = 7.9, 15.8, 23.5, 31.5, 39.5, 47.3$   
VOLTS/cm.

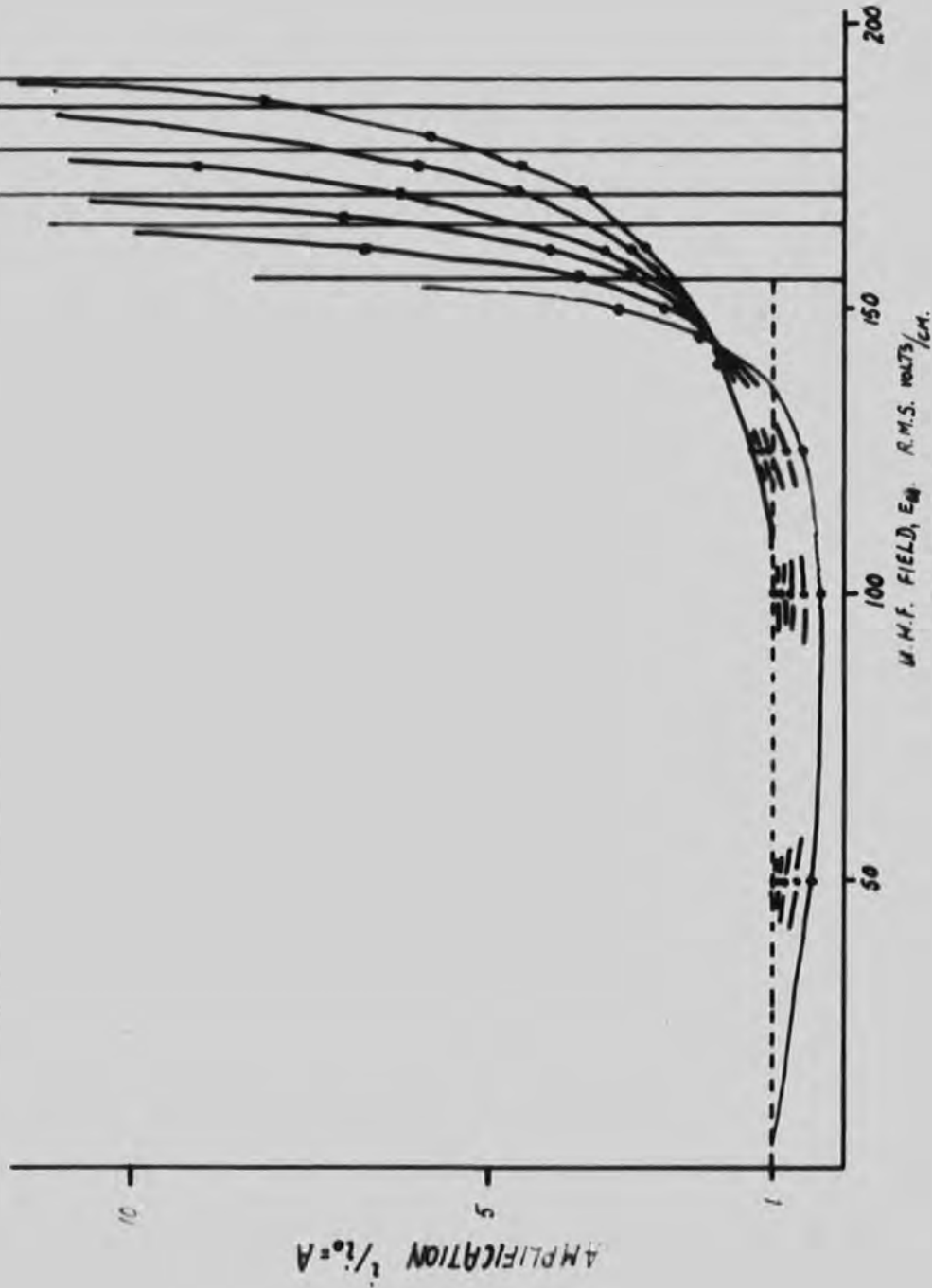


FIG.11.1

# HYDROGEN

$p = 6 \text{ mm. of Hg.}$   
 $\text{gap width, } d = 0.635 \text{ cm.}$

$E_d =$   
VOLTS/  
CM.

47.3

31.5

15.8

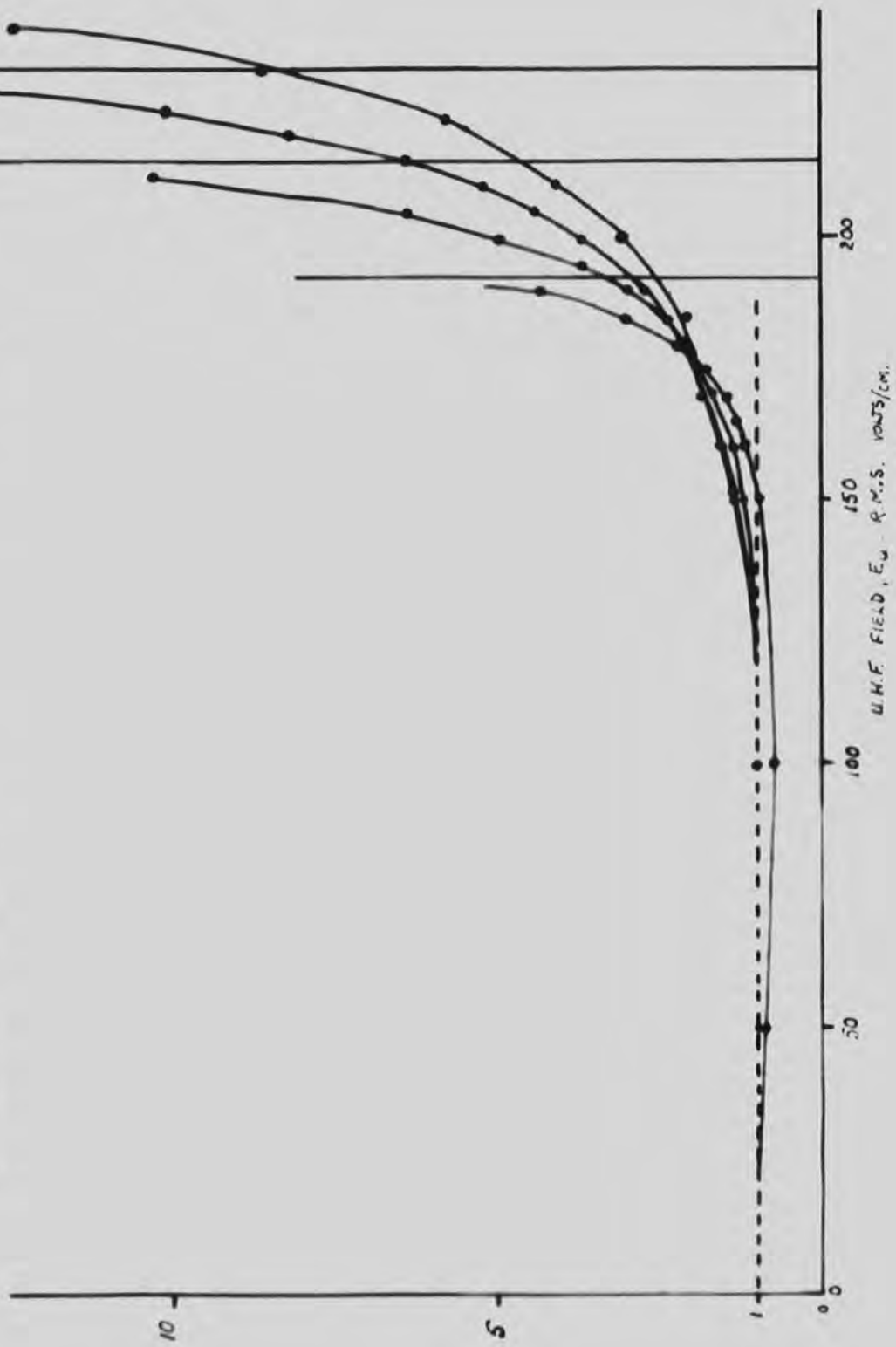


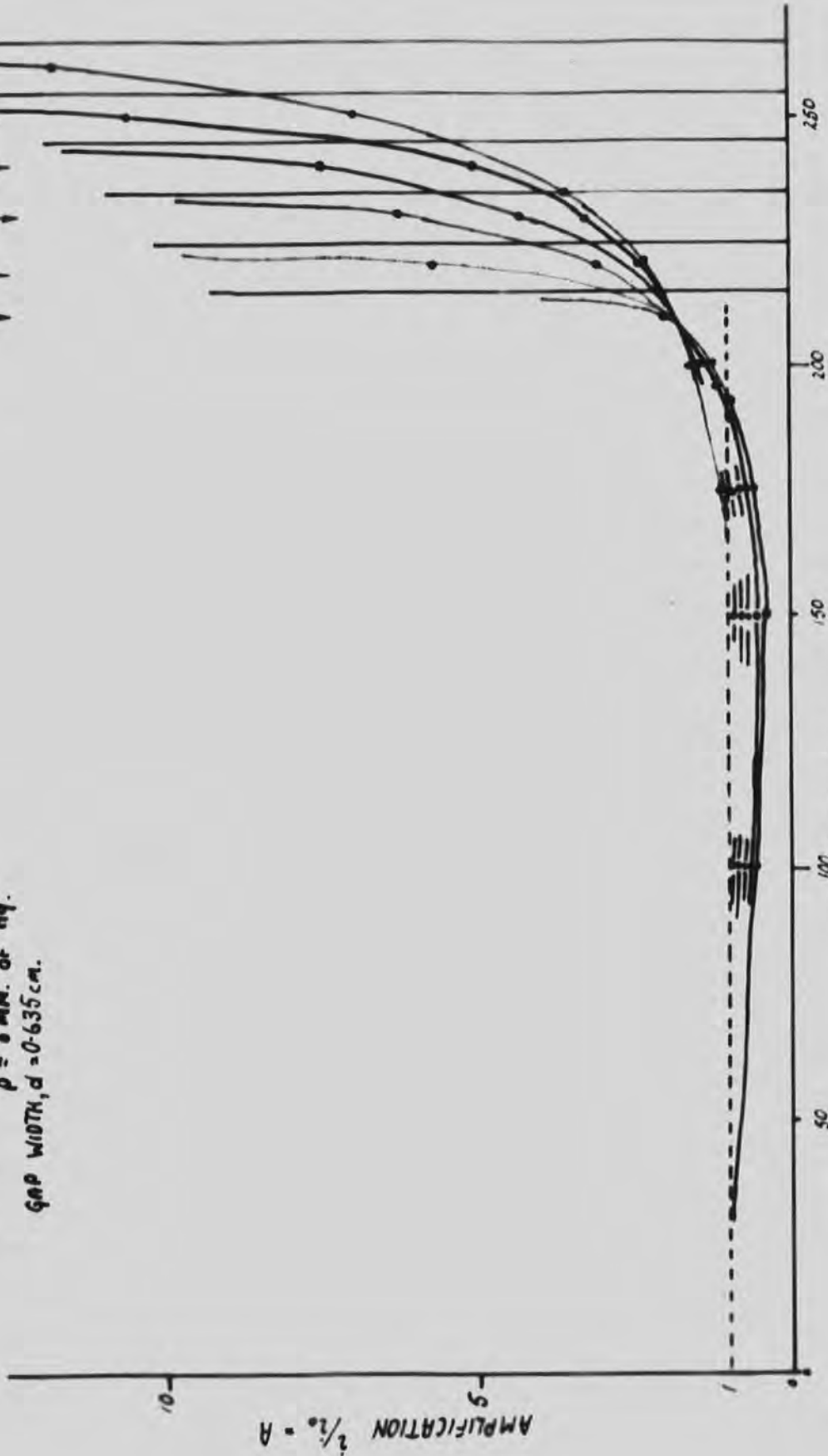
FIG.11.2

U.M.F. FIELD,  $E_0$  - R.M.S. VOLTS/CM.

HYDROGEN

$p = 8$  mm. of Hg.  
 GAP WIDTH,  $d = 0.635$  cm.

$E_d = 9.45, 15.8, 23.5, 31.5, 39.5, 47.3$   
 VOLTS/CM.



U.H.F. FIELD  $E_u$ . R.M.S. VOLTS/CM.

FIG. 11.3

HYDROGEN

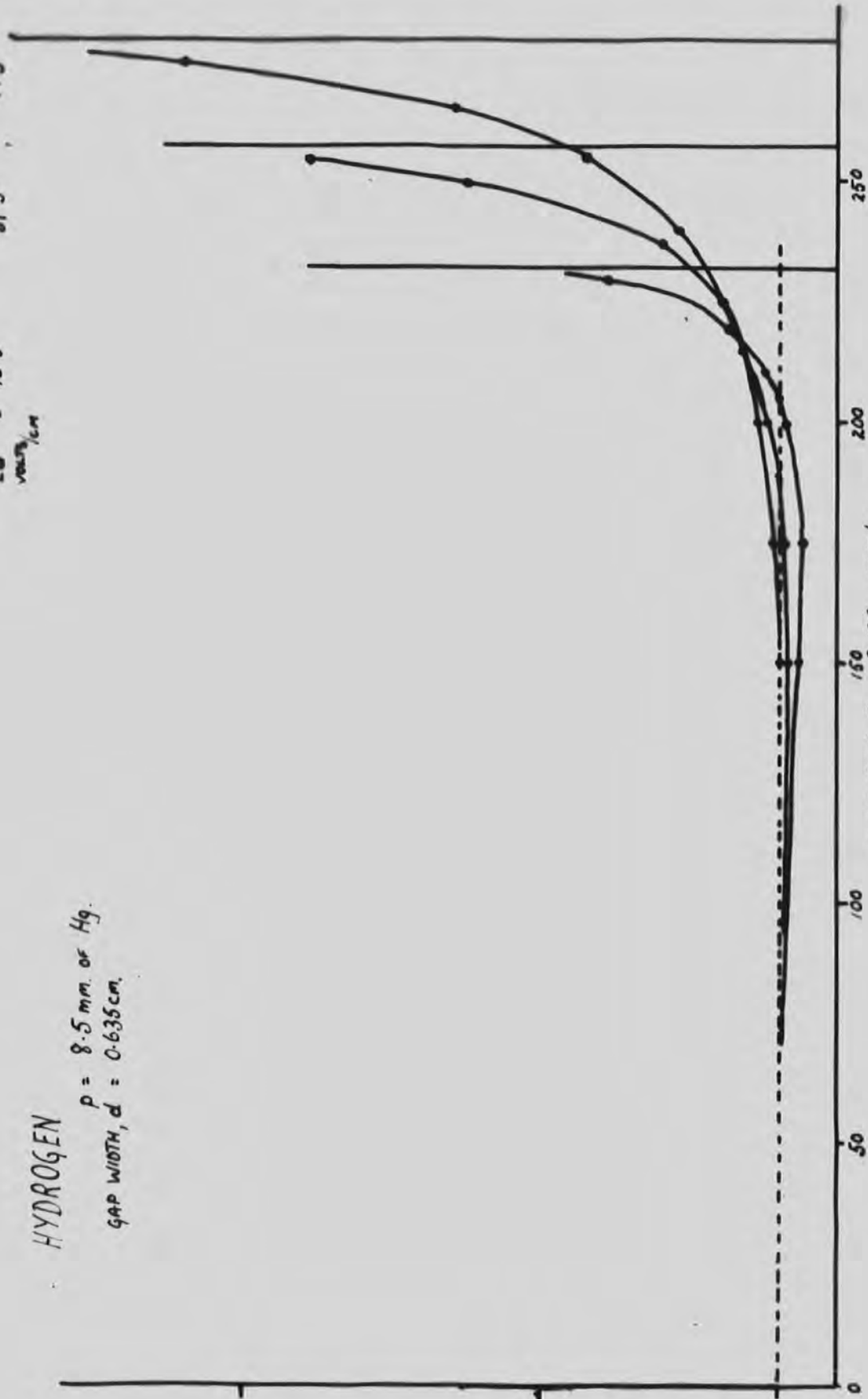
$p = 8.5 \text{ mm. of Hg.}$

$\text{GAP WIDTH, } d = 0.635 \text{ cm.}$

$E_d = 15.8$   
VOLTS/CM

31.5

47.3



U.H.F. FIELD,  $E_u$ , R.M.S. VOLTS/CM.

FIG. 11.4

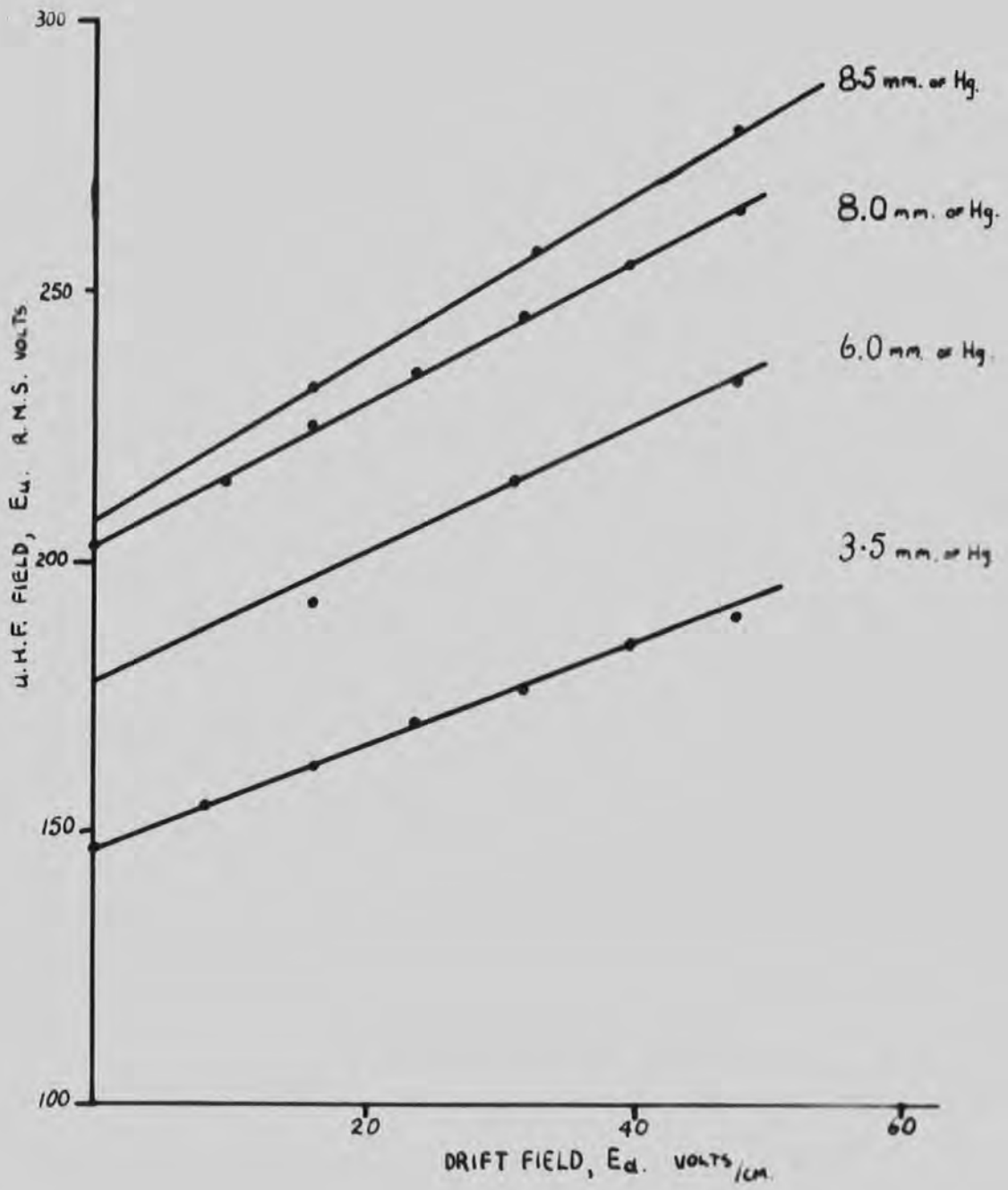


FIG.11.5

BREAKDOWN VALUES OF  
U.H.F. FIELD AS A FUNCTION  
OF DRIFT FIELD

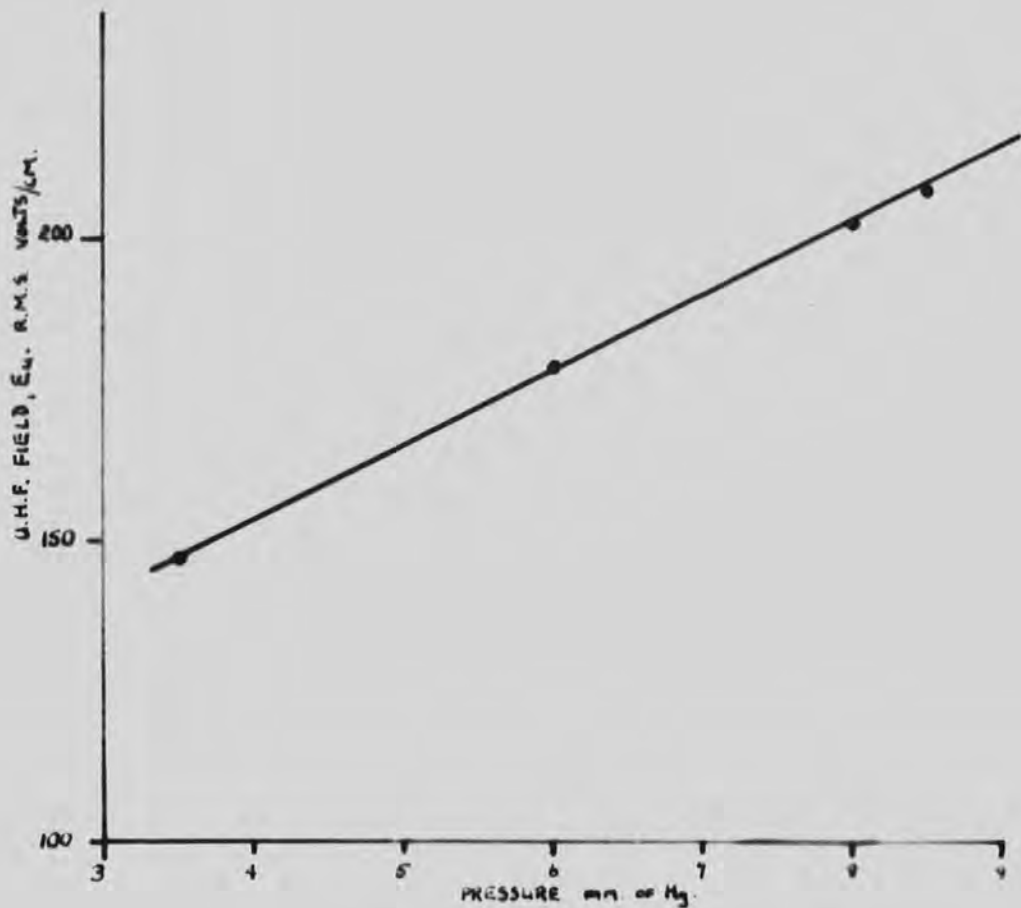
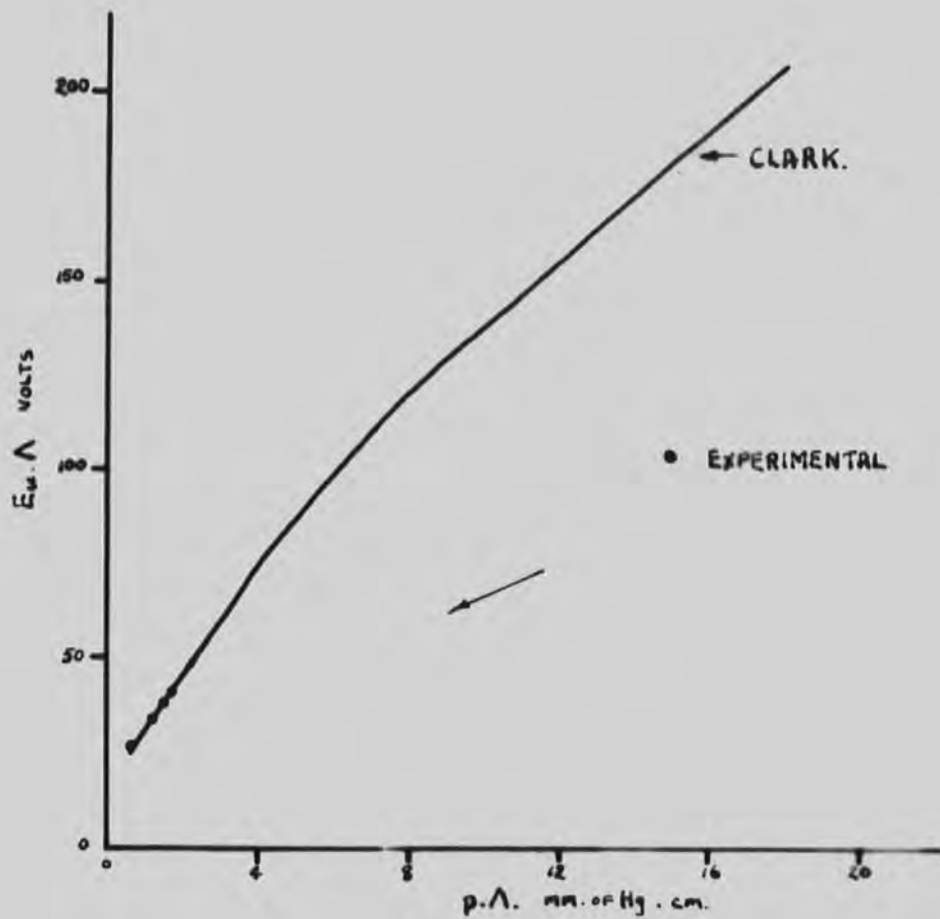


FIG.11.6 U.H.F. BREAKDOWN FIELD  
IN THE ABSENCE OF A DRIFT FIELD



**FIG. 11.7**  $E_{u,\Lambda}$  AS A FUNCTION OF  $p_{\Lambda}$  AT BREAKDOWN, FROM EXPERIMENTAL RESULTS AND FROM CLARK, 1957



TABLE 11.1

Hydrogen.

$p = 8$  mm. of Hg.

Gap width = 0.635 cm.

$E_d$  (drift field) = 9.45 volts/cm.

U.h.f. field.	Current to coll. elec., $P_2$	$i/i_0 =$
$E_u$ r.m.s. volts/cm.	(1)	amplification.
	Deflec.	A

0	2.1 = $i_0$	1.0
55	1.7	.81
81	1.5	.71
105	1.3	.57
137	1.0	.48
145	1.0	.48
168	1.3	.62
184	2.0	.95
200	4.2	2.0
	breakdown	

$E_d$  (drift field) = 15.8 volts/cm.

0	2.6 = $i_0$	1.0
60	2.2	.85
95	1.8	.69
122	1.5	.58
145	1.5	.58
168	1.9	.73
180	2.5	.96
185	3.0	1.15
190	3.4	1.31
200	5.3	2.05
210	14.9	5.7
	breakdown	

Clark's range are compared.

It was considered from Llewellyn Jones's work that there would be no space charge effect in the gap and in order to show that this is the case a subsidiary experiment was done. This involved obtaining the amplification curves for varying initial currents ( $i_0$ ) but constant field conditions in the gap. The initial current  $i_0$  can be varied either by varying the emission of the cathode or by varying the voltage between the cathode and the emitting electrode.

The current has been varied by both of these methods and the drift field kept at 15.8 volts/cm. whilst the u.h.f. field is varied from zero to the breakdown value at a pressure of 4.3 mm. of Hg. The results are shown in Fig. 11.3 and Table 11.3 indicates the conditions represented by the points. It is seen that the points fall on a unique curve which indicates that not only is any space charge effect negligible but that the voltage between the cathode and the emitting electrode does not affect the behaviour of the electrons.

At one stage during the experiments, after the chamber had been open to the atmosphere for several days it was found that the u.h.f. breakdown stress was initially that observed on previous occasions for these particular conditions but subsequent breakdown stresses were lower for the same conditions of drift field and pressure. None of these lower

HYDROGEN.

$p = 4.3$  mm. of Hg.

DRIFT FIELD,  $E_d = 15.8$  volts/cm.

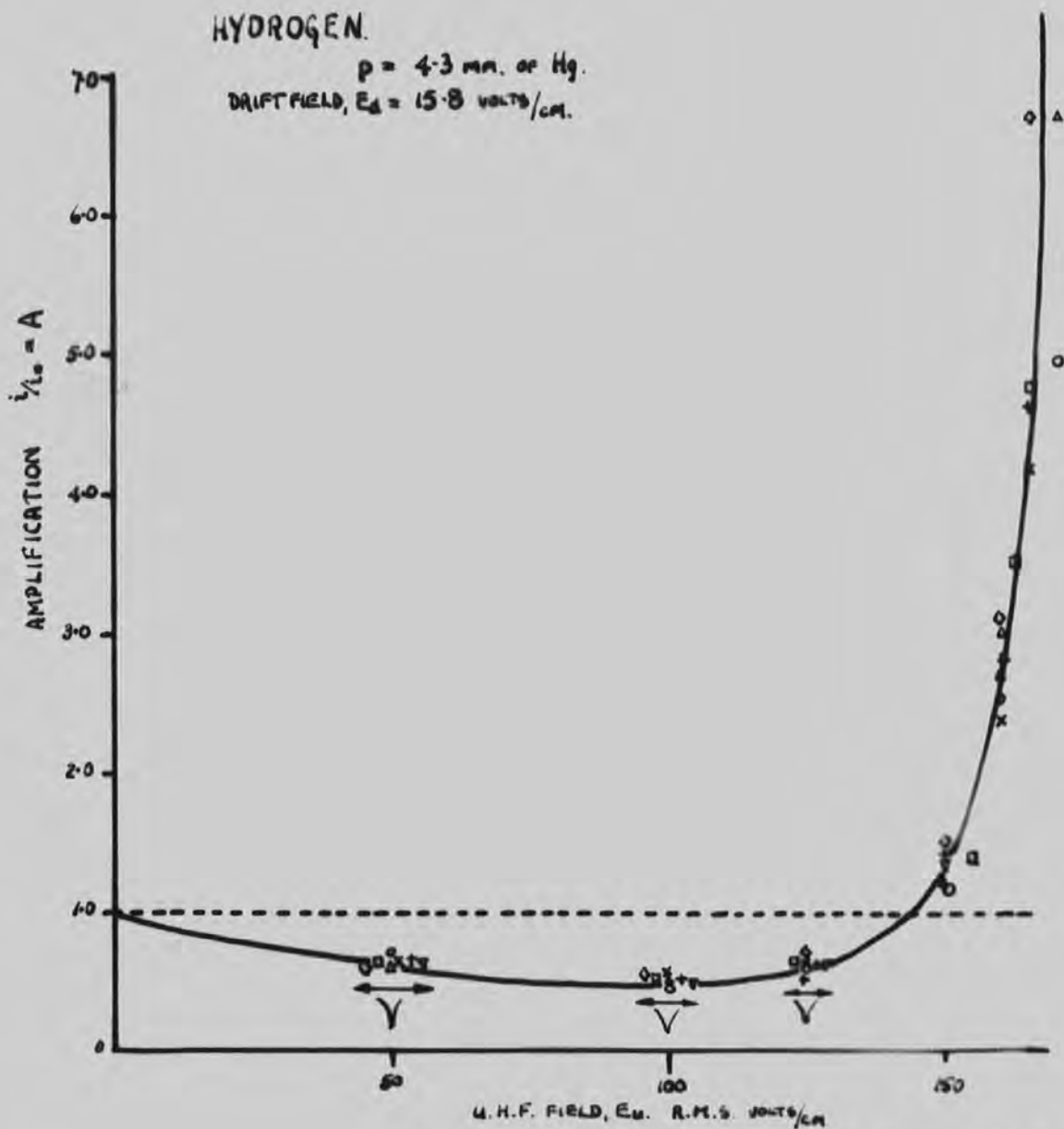


FIG.11.8

AMPLIFICATION UNDER A U.H.F. FIELD FOR DIFFERENT CONDITIONS OF ELECTRON EMERGENCE FROM THE EMITTING ELECTRODE.

TABLE 112.

Hydrogen.

$p = 4.3$  mm. of Hg.

$E_d$  (drift field) = 15.8 volts/cm.

Gap width = 0.635 cms.

Voltage between K and $P_1$ , volts.	Current to the emit. elec., $P_1$ Cms.deflec. of $G_1$ range 2.	Initial current, $i_0$ , to the coll. elec., $P_2$ , Cms.defl. $G_2$ range 4.
20	3.5	$\Delta$ .2 )
20	11.5	$\circ$ .85 )
20	16.0	$\times$ 1.2 )
20	22.5	$\square$ 1.6 )
24	5.8	$+$ .5 )
28	14.0	$\diamond$ 1.1 )
32	24.5	$\nabla$ 1.9 )

Variation of  
current to the  
emit. by varying  
temp.

Variation by  
varying the voltage  
between K and  $P_1$ .

breakdown stresses were lower than that obtained when there was no drift field and were attributed to a layer of charge remaining on the electrode surfaces long after a discharge had been extinguished.

#### Qualitative interpretation.

It can be seen that the amplification initially decreases and then begins to increase as the u.h.f. field increases, Figures 11.1 to 11.4. This increase is due to ionization in the gap by the u.h.f. field.

If the drift field is small compared to the u.h.f. field and the ionizing lifetime of the electrons can be determined it should be possible to find  $\psi$  the rate of ionization from the values of amplification for a particular u.h.f. field at different values of drift field. e.g. the statements  $i^1 / i^1_0 = e^{\psi T_1}$  and  $i^2 / i^2_0 = e^{\psi T_2}$  etc. where  $\psi$  depends solely on the u.h.f. field, enable  $\psi$  to be found. It should be possible to find the ionizing lifetime of the electrons if it is controlled solely by the drift motion from one electrode to the other either by an experimental method (modulation) or by calculation. However, several factors have arisen which show that the ionizing lifetime of the electrons is controlled not only by the drift motion but by diffusion also, when it becomes difficult to determine the significance of the amplification  $i/i_0$ . This is dealt with more fully in the following chapters.

In Figures 11.1 to 11.4 the current measured by the galvanometer  $G_2$  (1) initially decreases as the u.h.f. field increases so that it is difficult to say what is the true amplification for any particular value of u.h.f. field because the current that would be flowing to the collecting electrode in the absence of ionization but at the same u.h.f. field, cannot be precisely determined from the experiment. However, it seems possible that the theoretical value of this current can be determined and then the true amplification found.

This reduction in the current may be caused by one or both of two processes as follows:

a) On emerging from the emitting electrode the electrons may be swept back to the electrode under the action of the u.h.f. field, when it might be expected that a greater number of electrons would be lost with high fields than with low fields.

b) As the field is increased the electrons acquire energy which increases their diffusion rate but decreases their mobility under an electric field. This will tend to reduce the rate of arrival of the electrons at the collecting electrode and hence reduce the current through the galvanometer  $G_2$ .

The following chapter deals theoretically with (a) and (b) above and shows that it is most likely that the true value of the current in the absence of ionization at high values of u.h.f. field (true  $i_0$ ) is expressed by the minima of Figures 11.1 to 11.4.

## CHAPTER XII

### A DISCUSSION OF THE POSSIBLE CAUSES OF THE REDUCTION OF THE ELECTRON CURRENT TO THE COLLECTING ELECTRODE

It has been seen in the previous chapter that as the u.h.f. field is increased the electron current to the collecting electrode decreases until there is collision ionization when it begins to increase. Hence the true value of the amplification cannot be determined from the value of the electron current with no u.h.f. field.

Attempts have been made to ascertain theoretically the cause of this reduction and hence to find the current that would be expected to flow to the collecting electrode with a large u.h.f. field, but no collision ionization. This chapter describes the two approaches that have been considered and discusses their relative merits.

#### 1) The sweeping of the electrons to the emitting electrode by the u.h.f. field.

As the electrons emerge from the emitting electrode they will tend to execute oscillations under the u.h.f. field and drift across the gap under the direct field. If the u.h.f. field is larger than the direct field, electrons entering the gap at certain times will experience a field tending to return them to the electrode, when they will be lost. Even at other times, when they will tend to move out into the gap the reversal of the u.h.f. field may still cause them to be swept

back to the electrode and lost. Consequently, as the u.h.f. field is increased fewer electrons<sup>n</sup> will be free to traverse the gap and hence the rate of arrival, i.e. the current, at the collecting electrode will be reduced. The magnitude of this reduction can be calculated from theoretical considerations as below.

The drift velocity of the electrons under the influence of the u.h.f. field may be written

$$w_u = \frac{e}{j \omega m + m \nu_c} E_{u.o.} e^{j\omega t}$$

where  $e$  is the electronic charge,  $m$  the electronic mass,  $E_{u.o.}$  the peak value of the u.h.f. field,  $\omega$  the angular frequency of the field and  $\nu_c$  the frequency of collision between electrons and gas molecules. This expression is taken from Brown, 1956.

Thus the A.C. mobility takes the form

$$= \frac{e}{j \omega m + m \nu_c}$$

In the present experiment a typical value of  $\nu_c/\omega$  is about 500, so that  $\nu_c \gg \omega$ , the mobility will be real, of value  $e/m\nu_c$  and the velocity of the electrons will be in phase with the field.

In this experiment the u.h.f. field is modified by a small direct field,  $E_d$ . The real component of the combined field is

$$E = E_d + E_{u.o.} \cos. \omega t.$$



As the A.C. mobility is real and most of the electron travel occurs near the peak value of  $E_u$ , it will have the same value as the mobility under a direct field corresponding to this peak. Therefore:  $W = \mu E$  where  $\mu$  is the mobility and  $W$  the drift velocity under the combined fields.

$$\text{Hence } W = \mu (E_d + E_{u.o} \cos. wt)$$

If  $x$  is the distance travelled after time  $t$ , then

$$W = \frac{dx}{dt}$$

$$\text{and } dx = \mu (E_d \cdot dt + E_{u.o} \cdot \cos. wt \cdot dt)$$

i.e.  $x = \mu (E_d \cdot t + E_{u.o} \cdot \frac{\sin wt}{w} + C)$  where  $C$  is the integration constant.

The extreme conditions for the emergence of the electrons are indicated in Fig. 12.1 by  $t_1$  and  $t_2$ . Electrons entering the gap before  $t_1$  are acted on by a reverse field tending to return them to the holes or the electrode surface. Electrons entering the gap after  $t_2$  will be swept out into the gap during the rest of the half cycle but will be swept back to the electrodes during the succeeding half cycle. The criterion for the electrons to just get out (the value of  $t_2$ ) is given by equating the two shaded areas in Fig. 12.1 which is equivalent to finding the value of  $t$  from the expression for  $x$  above when the distance travelled from the electrode is just equal to that towards the electrode when the field is reversed.

Therefore the value for  $t_1$  is given by the condition that

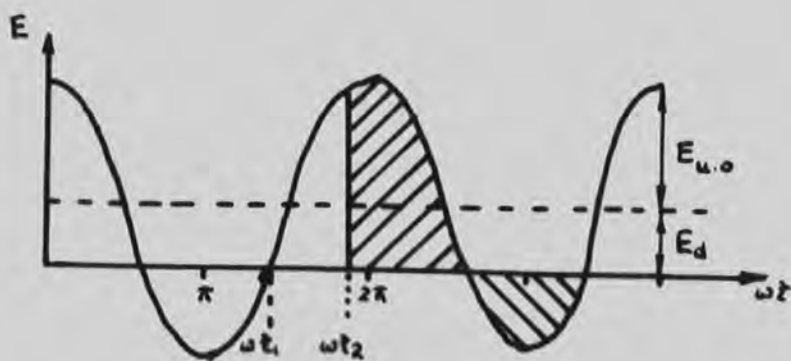


FIG.12.1 THE FIELD VARIATION IN THE GAP DUE TO THE U.H.F FIELD AND DIRECT FIELD.

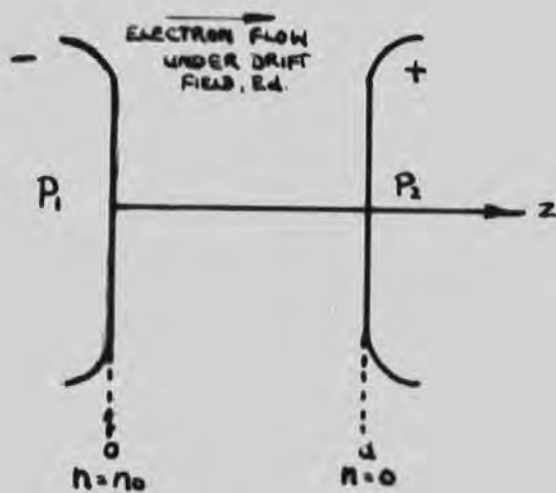


FIG.12.2 BOUNDARY CONDITIONS APPLIED TO THE ELECTRODE GAP.

$E = 0$  and the value for  $t_2$  by the following expression:

$$\left| \begin{array}{l} t_1 \\ t_2 \end{array} \right. E_d \frac{\omega t}{\omega} + \left| \begin{array}{l} t_1 \\ t_2 \end{array} \right. E_{u.o} \frac{\sin \omega t}{\omega} = \frac{2\pi}{\omega} E_d$$

As  $E_{u.o} > E_d$  the interval  $t_1$  to  $t_2$  will be small compared to the time period. If the number of electrons entering the gap per second under purely D.C. conditions is  $n$ , then the rate of entrance under the combination of the two fields is:

$\frac{(t_2 - t_1) \cdot n}{2\pi/\omega}$  and the current to the collecting electrode may be expected to decrease by such an amount,

$$\frac{(t_1 - t_2) \cdot n}{2\pi/\omega}$$

Consider the experimental conditions of the amplification curves of Fig. 11.3. Taking the curve where  $E_d = 9.45$  volts/cm. the u.h.f. field  $E_u$  corresponding to the minimum is 150 volts/cm.

Thus the rate of entrance into the gap under the influence of the two fields is:

$$\frac{0.8 \cdot n}{2} = 0.13 \cdot n.$$

This fraction, 0.13, is much lower than that determined experimentally, 0.5 and in view of this discrepancy it is likely that the loss of electrons by sweeping to the emitting electrode is not an operative mechanism. It is possible that there is a space charge effect at the electrode forming a

type of virtual cathode when the entrance of the electrons into the gap is controlled by diffusion and the effect of the u.h.f. field is to increase their energy and hence their rate of diffusion. This is dealt with in the next section.

2) Loss of electrons by diffusive processes.

In view of the above arguments it was decided to treat the problem as if the u.h.f. field only increases the energy of the electrons and does not affect their entrance into the gap.

If this is the case then not only are the electrons free to diffuse radially out of the gap but also to diffuse back to the emitting electrode. Some indication of the size of these respective mechanisms can be obtained by considering the expression given by Herlin and Brown, 1948, for the characteristic diffusion length,  $\Lambda$ , when applied to the gap in question.

i.e.  $\frac{1}{\Lambda^2} = \left(\frac{\pi}{d}\right)^2 + \left(\frac{2.405}{r}\right)^2$  where the first term involving the gap width  $d$ , represents diffusion to the electrodes, and the second, involving the radius of the plane portion of the electrodes  $r$ , represents the diffusion radially.

Substituting the experimental values of  $d$  and  $r$ :

$$\frac{1}{\Lambda^2} = \left(\frac{\pi}{0.635}\right)^2 + \left(\frac{2.405}{1.257}\right)^2$$

It can be seen that in this case the contribution to the diffusion length of the term involving the electrode separation, is much greater than that involving the electrode

radius, indicating that to a first approximation it is justifiable to treat the electron flow as a problem in one dimension (along the electrode axis) of diffusion with a superimposed direct field. The effect of the u.h.f. field is to alter the diffusion coefficient and the mobility of the electrons.

In order to apply this it is necessary to make two assumptions concerning the boundary conditions. These are that:

a) the electron concentration at the collecting electrode would be zero a distance of one mean free path behind the electrode surface. As the mean free path is small compared to the electrode separation the concentration at the electrode surface is sensibly zero

b) the electron concentration at the emitting electrode is kept constant at a value of  $n_0$  electrons per unit area. This implies that there is a space charge effect in operation either in the holes or near to the surface of the electrode such that however many electrons are removed from this region they are always replaced by electrons from the cathode so producing a virtual cathode. These conditions are summarised in Fig. 12.2.

Let  $\Gamma$  be the electron current density in electrons per second per unit area, then this flow of electrons is given by:

$$\Gamma = n \cdot \mu \cdot E_d - D \frac{\partial n}{\partial x} \text{ where } n \text{ is the number of electrons per}$$

unit area at a distance  $z$  from the emitting electrode. The first term of the expression for  $\Gamma$ , is the contribution due to the electron mobility  $\mu$  and the second term, the contribution due to the concentration gradient where  $D$  is the diffusion coefficient.

There is also the condition that there are no electrons generated between the electrodes, i.e. no ionization, or that none are lost by diffusing radially out of the gap.

In this case  $\frac{\partial \Gamma}{\partial z} = 0$

therefore

$$\Gamma = C, \text{ where } C \text{ is a constant.}$$

Solving the differential equation,

$$n \cdot \mu \cdot E_d - D \frac{\partial n}{\partial z} = C = \text{ or}$$

$$\mu \frac{E_d}{D} - \frac{\partial n}{\partial z} = A, \text{ where } A = C/D,$$

$$n = \frac{B e^{\mu E_d z/D} + A}{E_d/D}, \text{ where } B \text{ is an}$$

integration constant. Inserting the boundary conditions:

$$z = 0, n = n_0; \quad z = d, n = 0.$$

$$B = \frac{\mu E_d \cdot n_0 / D}{1 - e^{\mu E_d \cdot d/D}} \quad \text{and}$$

$$A = \frac{-(\mu E_d \cdot n_0 / D) e^{\mu E_d \cdot d/D}}{1 - e^{\mu E_d \cdot d/D}}$$

so that

$$n = n_0 \frac{(e^{\mu E_d \cdot z/D} - e^{\mu E_d \cdot d/D})}{1 - e^{\mu E_d \cdot d/D}}$$

When  $E_d$  approaches zero the expression for  $n$  must be

the same as that for a case of pure diffusion. This is shown to be the case by expanding the exponentials:

$$n = n_0 \frac{(\mu E_d(z-d)/D + \mu^2 E_d^2 (z^2-d^2)/D^2 \cdot 2! + \dots)}{1 - (1 + \mu E_d \cdot d/D + \mu^2 E_d^2 \cdot d^2/D^2 \cdot 2! + \dots)}$$

$$n = n_0 \frac{((z-d) + \mu^2 E_d^2 (z^2-d^2)/D^2 \cdot 2! + \dots)}{(-d - \mu E_d \cdot d^2/D \cdot 2! + \dots)}$$

when  $E_d \rightarrow 0$

$n = n_0(1 - z/d)$ , which is the function for diffusion with no direct field.

The electron flow across a boundary is given by:

$$\begin{aligned} &= \mu E_d \cdot n - D \frac{dn}{dz} \\ &= \mu \frac{E_d \cdot n_0 \cdot e^{\mu E_d \cdot d/D}}{e^{\mu E_d \cdot d/D} - 1} \\ &= \mu \frac{E_d \cdot n_0}{1 - e^{-\mu E_d \cdot d/D}} \end{aligned}$$

This again will reduce to an expression for  $\Gamma$  when  $E_d \rightarrow 0$

$$\text{i.e. } \Gamma = D \cdot n_0 / d.$$

If  $\Gamma$  is the electron flow across the gas to electrode boundary it must be equal to the current measured by the galvanometer  $G_2$ , i.e.  $i$ , and assuming  $n_0$  to be constant, an increase in the u.h.f. field will alter the values of  $D$  and so that the expected variation of current can be evaluated. It has been shown by Varnerin and Brown, 1950, that the energy of electrons under the influence of combined direct and

alternating fields corresponds to that of an effective field  $E_0$ , where  $E_0^2 = E_d^2 + E_u^2$ .

Table 12.1 shows the respective values of  $D$  and  $\mu$  from Crompton and Sutton, 1950, for different values of  $E_0$ . It can be seen from the values for  $\mu/D$  that the value of  $e^{-\mu E_d \cdot d/D}$  is negligible for the conditions of the experiment, viz.  $e^{-22}$  to  $e^{-5}$ , thus the current is proportional to the mobility.

Hence if  $\Gamma_0$  is the current to the collecting electrode when the u.h.f. field is zero, i.e. the previous  $i_0$ , and  $\Gamma_u$ , the current collected when there is a u.h.f. field  $E_u$  with no amplification, then  $i/i_0$  is given by:

$$\frac{i}{i_0} = \frac{\Gamma_u}{\Gamma_0} = \frac{n_0 \cdot \mu_u \cdot E_d}{n_0 \cdot \mu_0 \cdot E_d} = \frac{\mu_u}{\mu_0} = A.$$

A theoretical curve can therefore be drawn relating  $i/i_0$  to the u.h.f. field and compared with that obtained experimentally. These theoretical results (Tables 12.2 and 12.3) and the experimental ones from Chapter XI are plotted together for two values of direct field at a pressure of 8 mm. of Hg. in Fig. 12.3.

It is seen that although the shapes of the curves do not agree in detail the general trend is similar, in that the experimental curve approaches the theoretical at high values of u.h.f. field. It is thought that the experimental curve represents two effects, one associated with the change in mobility and the other with the behavior of the electrons as



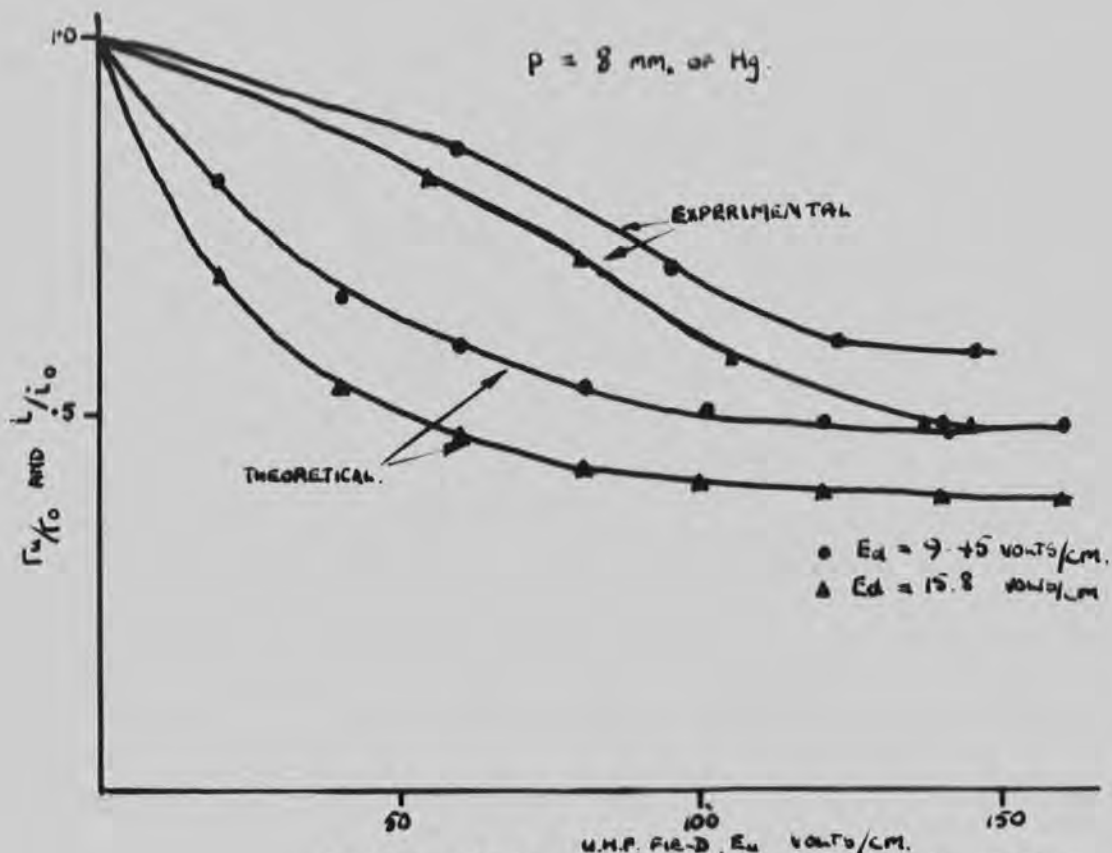


**FIG. 12.3**

U.M.P. FIELD,  $E_u$  VOLTS/CM.  
 THEORETICAL AND EXPERIMENTAL VARIATION  
 OF THE CURRENT TO THE COLLECTING ELECTRODE  
 WITH U.M.P. FIELD

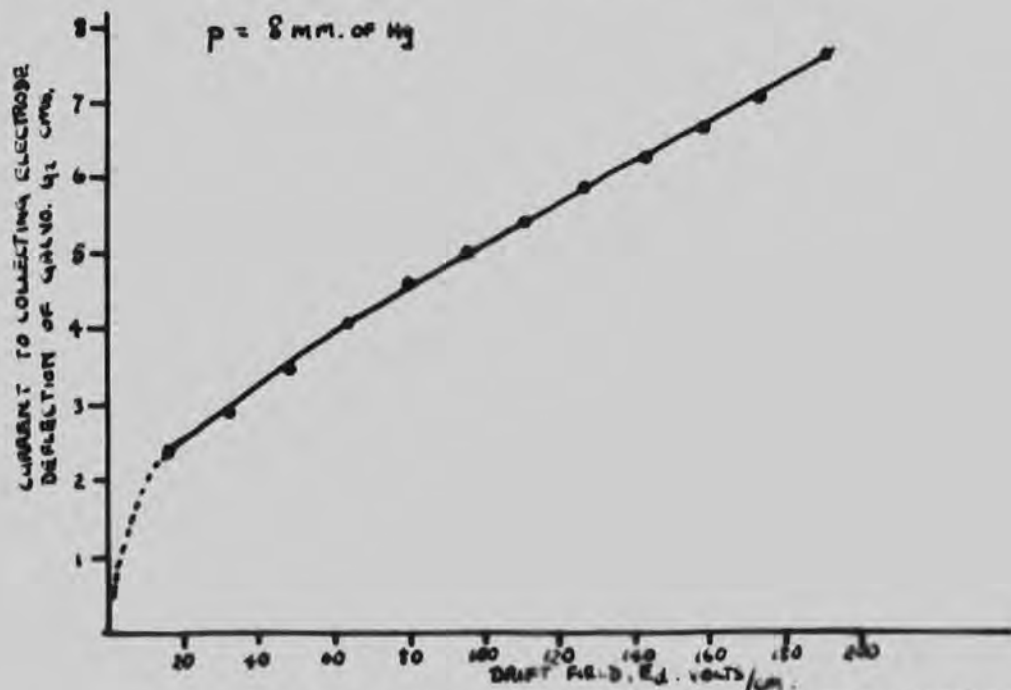


**FIG. 12.4**

VARIATION OF CURRENT TO COLLECTING  
 ELECTRODE WITH DRIFT FIELD ONLY.

TABLE 12.1.

Hydrogen

$p = 8$  mm. of Hg. Drift field,  $E_d = 9.45$  volts/cm.

Gap width,  $d, = 0.635$  cm.

U.h.f field $E_u$ , F.m.s. volts/cm.	Effective field, $E_0$ F.m.s. volts/cm.	$E_0/p$ F.m.s. V. cm.mm.Hg.	Mobility $\mu \times 10^{-4}$ cm./sec.v.	$\mu/D$ , where D is diffusion coef. cm.-1volt-1.
0	9.45	1.18	3.4	11.3
20	22.3	2.8	4.5	7.7
40	41.1	5.1	5.5	6.0
60	61.0	7.6	6.3	5.3
80	81.0	10.1	7.2	4.8
100	101.0	12.6	7.9	4.5
120	121.0	15.1	8.6	4.4
140	141.0	17.6	9.2	4.35
160	161.0	20.1	9.7	4.3

3.6  
↓  
.5

From Crompton and Sutton, 1950.

TABLE 12.2.

Hydrogen

$p = 8$  mm. of Hg. Drift field,  $E_d = 9.45$  volts/cm.

$d = 0.635$  cm.

U.h.f. field  
 $E_u$ , F.m.s.volts/cm.

Calcul. ratio of  
current to cell.elect.  
at  $E_u$  to initial current,  
 $\Gamma_u/\Gamma_0$

0	1
20	.68
40	.55
60	.47
80	.425
100	.40
120	.39
140	.385
160	.38

they emerge into the gap.

It was considered that the second effect might have been caused by the electrons that enter the gap, having high energies, acquired in moving from the cathode, K, to the perforations in the emitting electrode, P<sub>1</sub>. However, variations in the field between K and P<sub>1</sub> do not affect the conditions of current flow across the gap, or amplification and breakdown in the gap, (Chapter XI, experiments to observe the effect of varying the initial current across the gap). This indicates that the energy of the electrons entering the gap is small.

From the results described in Chapter XI it is possible to determine the dependence of the current to the collecting electrode on the direct field in the absence of the u.h.f. field, Fig. 12.4. There is no appreciable current to the collecting electrode ( $i \ll 1$  mm. deflection.) when the direct field is zero, indicated by the broken line.

A curve can also be plotted from the theoretical considerations as discussed above. The ratio of the current expected at a particular direct field,  $\Gamma^1$ , to the current expected with no direct field,  $\Gamma^1_0$ , is plotted against the drift field,  $E_d$ , in Fig. 12.5. When  $E_d = 0$  then  $\Gamma^1_0 = D \cdot n_0 / d$  and when  $E_d > 10$  volts/cm.  $\Gamma^1 \approx .E_d \cdot n_0 \cdot \mu$ , and the values of  $\Gamma^1 / \Gamma^1_0$  are shown in Table 12.4.

The experimental and the theoretical curves are not

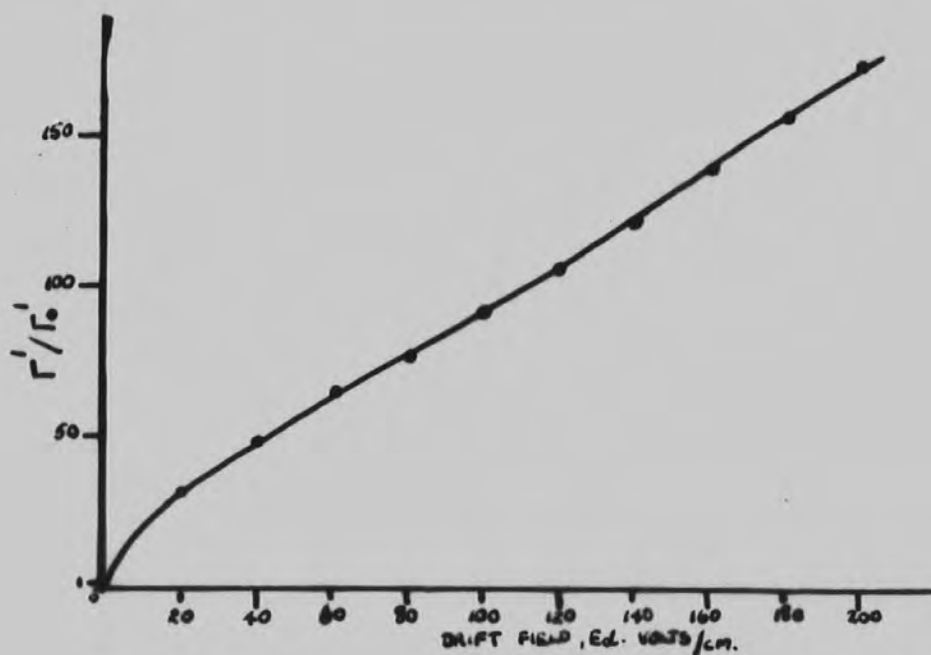


FIG.12.5 THEORETICAL RATIO OF THE CURRENT TO THE COLLECTING ELECTRODE WITH A DRIFT FIELD TO THAT WITHOUT A FIELD AS A FUNCTION OF THE FIELD.

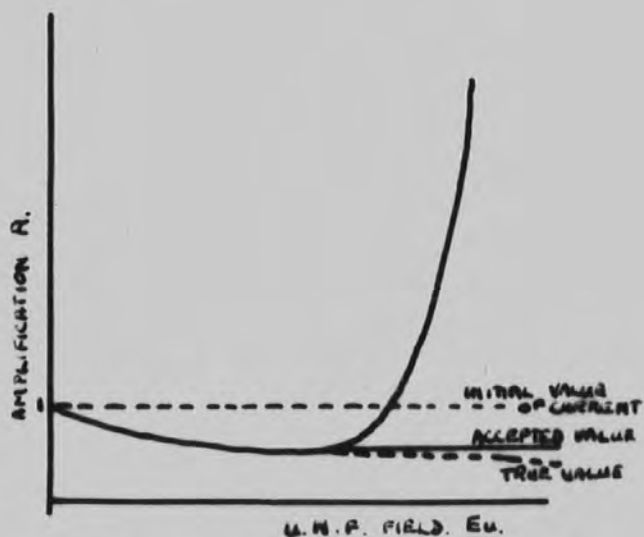


FIG.12.6 SHOWING POSSIBLE VARIATION OF INITIAL CURRENT,  $I_0$  IN THE ABSENCE OF DISTORTION.

TABLE 12.3

## Hydrogen

$p = 8$  mm. of Hg. Drift field,  $E_d = 15.8$  volts/cm.

Gap width,  $d, = 0.635$ .

U.h.f. field  
 $E_u$ , r.m.s. volts/cm.      Calcul. ratio of current  
 to collec. elect.,  $P_0$ , at  $E_u$ ,  
 to initial current,  $\Gamma_u/\Gamma_0$

0	1
20	.81
40	.655
60	.59
80	.53
100	.50
120	.49
140	.485
160	.480

TABLE 12.4

## Hydrogen

$p = 8$  mm. of Hg.  $E_d = 0$

Gap width,  $d, = 0.635$  cm.

Initial current across the gap with NO field,  
 $\Gamma_0 = 5 \times 10^4 \times n_0$  electrons/sec., where  $n_0$  is the  
 electron concentration  
 at the emitting electrode.

Drift field,  
 $E_d$ , volts/cm.      Calcul. current to the  
 collec. elect.  $\Gamma^1 \times \frac{10^{-5}}{n_0}$       Ratio of  $\Gamma^1$  to  
 $\Gamma_0$

0	.5 = $\Gamma_0^1$	1
20	16.0	32
40	34.0	48
60	52.4	64.8
80	68.4	76.8
100	86.0	92.0
120	102.8	105.6
140	121.6	123.2
160	140.4	140.0
180	159.0	158.0
200	178.0	176.0

similar near the origin and indicate that the current arriving at the collecting electrode is not entirely accounted for by the previous argument. The reasons for this discrepancy may be:

a) that the initial assumption that the electron concentration at the emitting electrode is constant at a value of  $n_0$  electrons per unit area is incorrect and that in fact there is not an inexhaustible supply of electrons.

b) that the electrons may be lost out of the gap by radial diffusion.

These two processes might be separated experimentally by measuring the current to the collecting electrode for constant conditions of  $E_d$  and pressure,  $p$ , and different gap widths. If the process is as described in (a) the current can be expected to be the same for all gap widths, if (b), the current can be expected to decrease for larger gap widths.

However, it seems likely that the initial decrease in the ionization curves can be interpreted on the basis of the above argument, namely that it is caused by the change in the electron mobility as the u.h.f. field increases.

From Fig. 12.3 it appears that both the experimental and the theoretical curve level out at high values of  $E_d/p$  so that the true value of the initial current without amplification at high values of u.h.f. field is more nearly the value of the current at the minimum, Fig. 12.6. This justifies a

HYDROGEN

GAP WIDTH,  $d = 0.635$  cm.

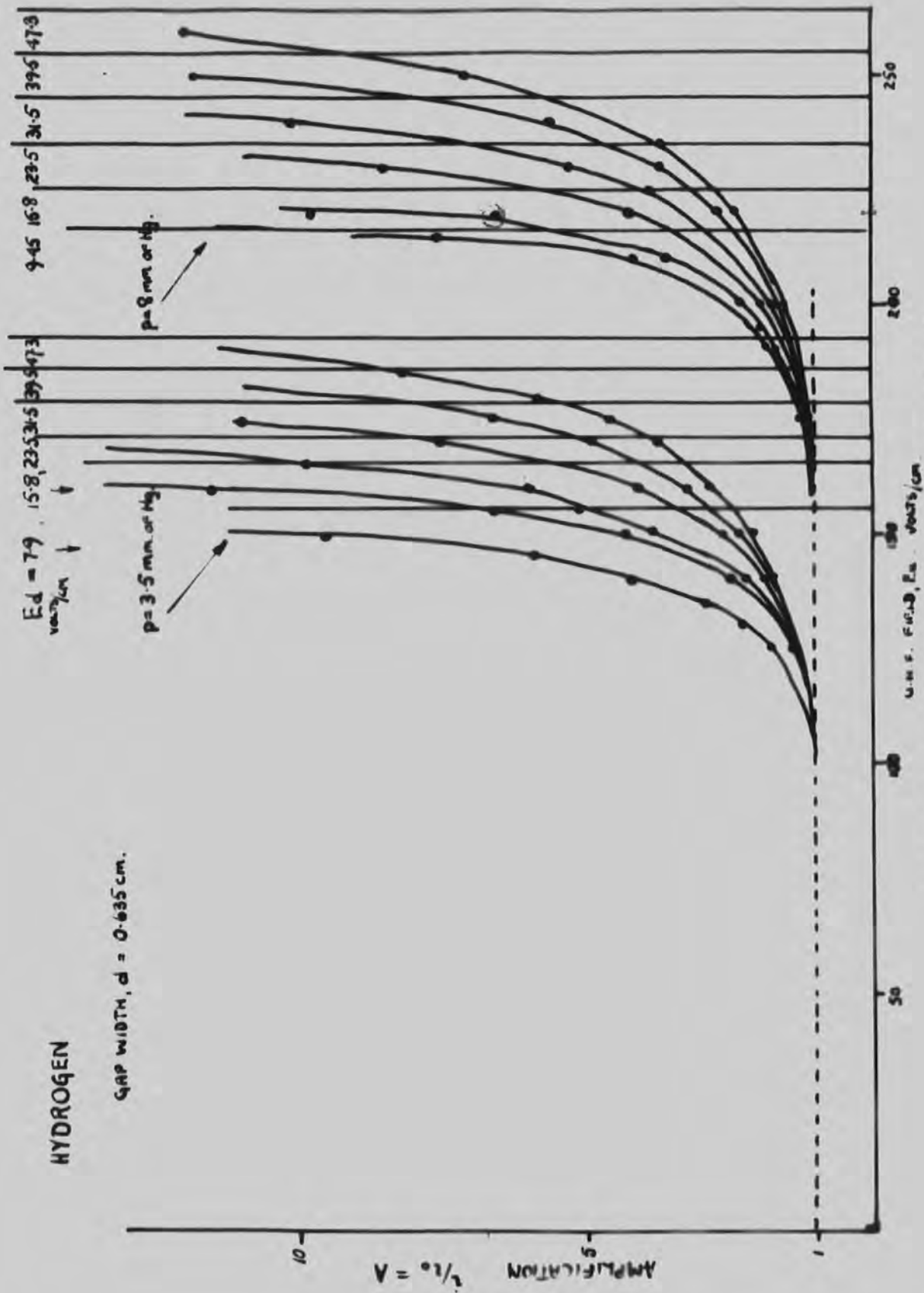


FIG. 12.7  
 CURRENT AMPLIFICATION CURVES FOR TWO  
 VALUES OF PRESSURE, TAKING  $I_0$  TO BE THAT  
 AT THE MINIMA OF FIGURES 11.1 AND 11.3.

recalculation of the amplification on the basis of  $i_0$  being the value at the minimum. The new ionization curves resulting from this are shown in Fig. 12.7 where it is seen that the curves are more uniform than those of Fig. 11.1 and 11.5, at the value of u.h.f. field where collision ionization is deemed to begin.



### CHAPTER XIII

#### DETERMINATION OF THE AVERAGE LIFETIME OF AN ELECTRON IN THE ELECTRODE GAP.

In the absence of attachment or recombination the mechanism of u.h.f. breakdown in Hydrogen has been shown to be that of diffusion by Clark and Prowse 1958. More specifically the breakdown stress depends on the lifetime of the electrons in the gap as controlled by diffusion, i.e. the rate of production of the electrons must balance the rate of loss of electrons from the high field region by diffusion. The lifetime can be calculated from the dimensions of the gap and the diffusion coefficient corresponding to the applied field. With the lifetime and the corresponding data of the breakdown conditions values of  $\eta$ , the ionizing efficiency can be determined (Clark and Prowse, 1958), these agreeing fairly closely with those determined by Llewellyn Jones and others.

In the experiments described in this thesis, not only are the electrons lost from the gap by diffusion but also by the application of a small unidirectional field. Consequently, for any particular pressure, the u.h.f. breakdown stress will be greater with the direct field than without it so that the processes of production of electrons and loss, balance.

The main difficulty of the experiment has been the determination of the average lifetime of the electron under

these conditions and an attempt has been made to identify it with the transit time of the electron as it crosses the gap. These transit times can be calculated from Townsend's equation relating drift velocity to the electron energy and the direct field for any particular value of the u.h.f. field, which contributes to the electron energy. According to these calculations the transit time of the electrons are in the region of a microsecond, (Table 13.3).

This method has two objections:

a) the method involves straight forward calculation of the times without any means of direct experimental verification until of course the modulating oscillator etc. is operating.

b) with no applied direct field the average lifetime of the electron as controlled by diffusion is smaller than that calculated from drift considerations with a small direct field applied (Table 13.3). However the u.h.f. breakdown stress with no direct field is less than with the field applied, indicating that the lifetime should be shorter under the latter conditions if the diffusion theory is valid.

Clark and Prowse, 1958, have shown that the diffusion theory is valid for a plane parallel plate gap in Hydrogen stressed by a u.h.f. field and observations described in Chapter XI show that for breakdown conditions in this experiment without a direct field, the variation of  $E_{p,\Delta}$  with  $p,\Delta$  is incomplete agreement with their results (Fig. 11.7), indicating that

breakdown is essentially diffusion controlled.

From work by Varnerin and Brown, 1950, it is apparent that the identification of the transit time of the average electron with its ionizing lifetime is erroneous and that the true ionizing lifetime is the result of a balance between the drift and diffusion processes.

Resulting from the above considerations two other methods, one based on the observations of breakdown conditions and the other on the work of Brown and Varnerin, for determining the ionizing lifetime of the electrons have been studied as described below.

1) The experimental method of determining the lifetime.

It has been found for Hydrogen that the u.h.f. breakdown field,  $E_{u1}$ , varies linearly with the direct field  $E_d$ , for constant pressures (Fig. 11.5 and Fig. 13.1). Furthermore, the relationship is colinear when the ratio of the breakdown stress at a particular value of  $E_d$ , to that when  $E_d$  is zero, is plotted against  $E_d$  (Fig. 13.2 and Fig. 13.3). This relationship can be used as a tool for finding not only the average lifetime of the electrons under breakdown conditions but also under non-breakdown conditions, i.e. conditions when there is current amplification. The calculation of these times involves the following argument:

If each electron in the gap can be considered to give rise

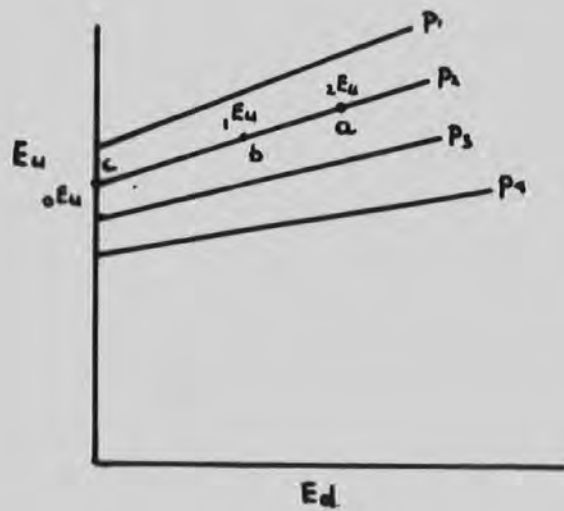


FIG.13.1 U.H.F. BREAKDOWN FIELD AS A FUNCTION OF DRIFT FIELD FOR DIFFERENT PRESSURES

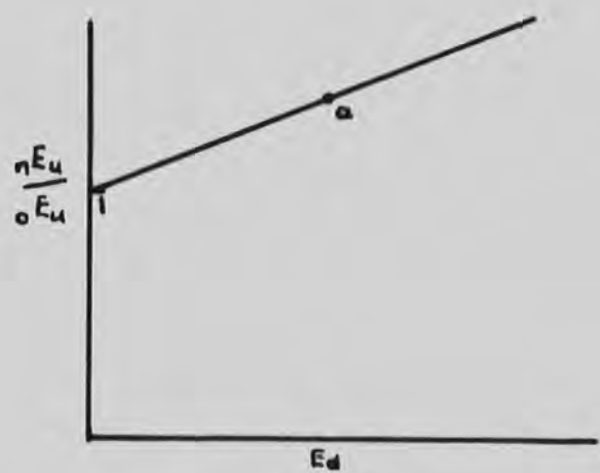


FIG.13.2 RATIO OF BREAKDOWN FIELD AT A PARTICULAR VALUE OF DRIFT FIELD TO THAT WITH NO DRIFT FIELD AS A FUNCTION OF THE DRIFT FIELD

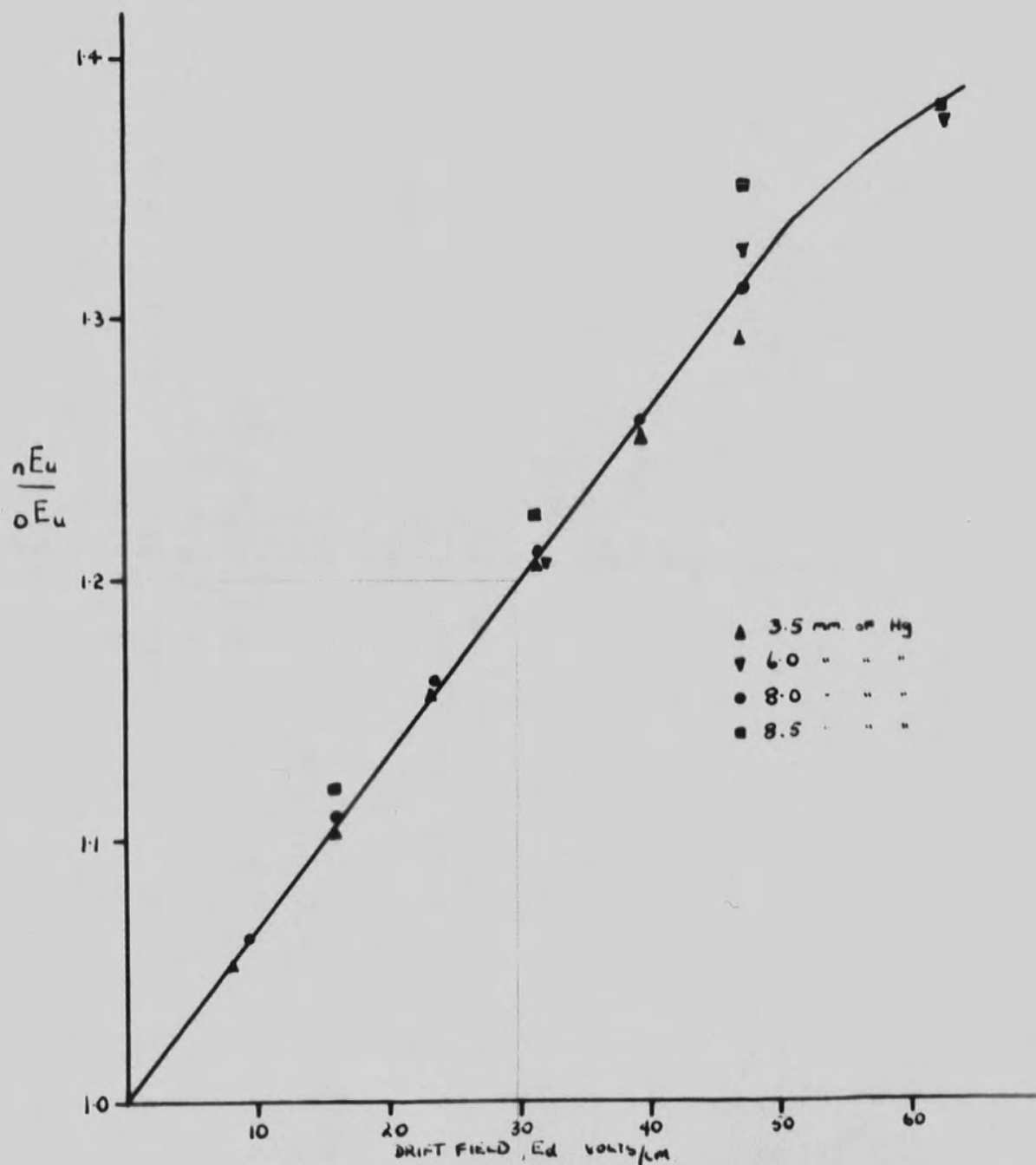


FIG.13.3

RATIO OF UHF BREAKDOWN FIELD AT A PARTICULAR VALUE OF DRIFT FIELD TO THAT WITH NO FIELD AS A FUNCTION OF THE DRIFT FIELD.

to  $\psi$  ion pairs in unit time, in time  $t$  one electron initially present in the gap gives rise to a total number  $e^{\psi t}$ , and is related to Townsend's coefficient  $\alpha$  by the expression:

$\psi = \alpha \cdot W$ . where  $W$  is the drift velocity of the electron.

The condition for the onset of breakdown in a sustained field is that  $\alpha \cdot W \cdot t_d = 1$ , where  $t_d$  is the average lifetime of the electron. This equation satisfies the condition that an electron shall produce one more electron in the gap during its lifetime in order that it is replaced, and will hold irrespective of the conditions governing  $t_d$ . If  $\eta$  is the ionizing efficiency, i.e. the number of ionizations per volt,

then 
$$\eta = \frac{\alpha}{E}$$

and 
$$\eta \cdot E \cdot W \cdot t_d = 1$$

The drift velocity when the electron is moving with the field is determined by  $(E_u^2 + E_d^2)^{\frac{1}{2}}$  and against the field by  $(E_u^2 - E_d^2)^{\frac{1}{2}}$  where  $E_u$  is the u.h.f. field and  $E_d$  the drift field. From these the mean velocity is determined by  $E_u(1 + E_d^4/4E_u^4 + \dots)$  which if  $E_d$  is small compared with  $E_u$  is sensibly  $E_u$ . This is the case in the experiment when  $E_u/E_d > 5$ .

In the ranges considered for Hydrogen the drift velocity is nearly proportional to the  $E$  the applied field and may be expressed as:  $W = \mu \cdot E$  where  $\mu$  is the mobility and is constant. Thus  $E \cdot W \propto E^2$ , of which the mean value is  $E_u^2$  exactly.

Therefore 
$$\eta \cdot E \cdot W \cdot t_d = \eta \cdot \mu \cdot E_u^2 \cdot t_d = 1.$$

Consider two conditions of  $E_d$ ,  ${}_1E_d$  and  ${}_2E_d$  such that there are two different values of breakdown stress,  ${}_1E_u$  and  ${}_2E_u$ , then there will be two different values of  $\eta$  and  $t_d$  corresponding to the two points on Fig. 13.1, a and b, such that:

$$1 = \eta_1 \cdot \mu \cdot {}_1E_u^2 \cdot {}_1t_d$$

$$\text{and } 1 = \eta_2 \cdot \mu \cdot {}_2E_u^2 \cdot {}_2t_d$$

from which:

$$\frac{{}_1t_d}{{}_2t_d} = \frac{\eta_2 \cdot {}_2E_u^2}{\eta_1 \cdot {}_1E_u^2}$$

Thus if  ${}_1t_d$  is known  ${}_2t_d$  can be found from the published values of  $\eta_1$  and  $\eta_2$  for  ${}_1E_u/p$  and  ${}_2E_u/p$ , or preferably from a separate experiment carried out with the apparatus as outlined later.

When  $E_d = 0$  ( point (c), Fig.13.1) only diffusion conditions exist and  $t_d = \frac{\Lambda^2}{D}$  and is equivalent to  ${}_0t_d$  in the above expression.  $D$  is the diffusion coefficient for  ${}_0E_u/p$  (the value of  $E/p$  for breakdown with no direct field) and  $\Lambda$  is the diffusion length of the gap.

Because the ratio  ${}_2E_u/{}_1E_u$  is independent of pressure (Fig. 13.2 and 13.3) it follows that the above relationship:

$$\frac{{}_1t_d}{{}_2t_d} = \frac{\eta_2 \cdot {}_2E_u^2}{\eta_1 \cdot {}_1E_u^2}$$

will hold for any conditions of pressure including breakdown values.

For example, consider the measurement of the amplification before breakdown at a pressure  $p_1$ , a u.h.f. field of  ${}_2E_u$  and a direct field of  ${}_2E_d$ .

Now consider reducing the pressure to the value  $p_2$  at which breakdown can just occur, when the loss of electrons will be equal to the gain and due to this change in pressure  $\eta$  and  $t_d$  will be changed. The gas is now breaking down at  $p_2$  under similar electrical conditions to those in the experiment and from Fig. 13.1 points (a) and (c), the u.h.f. breakdown stress,  ${}_0E_u$ , corresponding to a pressure  $p_2$  with no direct field can be determined. This can be obtained more directly from Fig. 13.2 point (a), which gives the ratio of  ${}_2E_u/{}_0E_u$  for the value of  ${}_2t_d$ .

Consequently, from the data available the ratio of  ${}_0t_d$  to  ${}_2t_d$  corresponding to the pressure  $p_2$  can be calculated.

$$\text{i.e. } \frac{{}_0t_d}{{}_2t_d} = \frac{\eta_2 {}_2E_u^2}{\eta_0 {}_0E_u^2} \quad \text{where } \eta_0 \text{ and } \eta_2 \text{ are}$$

determined from the values  ${}_0E_u/p_2$  and  ${}_2E_u/p_1$ .

Under the conditions of the experiment at a pressure  $p_1$  there will be a similar relationship between new times  ${}_0t_d$  and  ${}_2t_d$  and new values  $\eta'_0$  and  $\eta'_2$ , corresponding to the same field values  ${}_0E_u$  and  ${}_2E_u$  for breakdown conditions, when:

$$\frac{{}_0t_d}{{}_2t_d} = \frac{\eta'_2 {}_2E_u^2}{\eta'_0 {}_0E_u^2} \quad \text{where } {}_2t_d \text{ is the average lifetime}$$

of the electrons under the experimental conditions of  ${}_2E_u, {}_2E_d$  and  $p_1$ , and  $\eta'_0$  and  $\eta'_2$  are now determined from the values of  ${}_0E_u/p_1$  and  ${}_2E_u/p_1$ . Here  ${}_0t_d$  is the lifetime of the electrons calculated from diffusion considerations, i.e.



for conditions  ${}_0E_u, E_d = 0$  and  $p_1$ , when  ${}_1t_d = \frac{\Lambda^2}{D}$ ,  $D$  being determined by the value of  ${}_0E_u/p_1$ .

From a separate experiment with no direct field a unique curve can be plotted relating  $E_u \cdot \Lambda$  to  $p \cdot \Lambda$  as in Fig. 11.7.

As this curve represents breakdown conditions  $\alpha W \cdot t_d = 1$  where  $t_d = \frac{\Lambda^2}{D}$ . Clark and Prowse, 1956, have shown from Townsend, 1947, that  $D = \frac{W \cdot k}{40.3 \cdot E_u}$  where  $k$  is the ratio of the energy of

the random movement of the average electron to the energy of the random movement of the average molecule and combining the two:

$$\frac{40.3}{p} E_u (p \cdot \Lambda)^2 = \frac{k}{\alpha/p}$$

and the ionizing efficiency is given by:

$$\eta = \frac{\alpha/p}{E_u/p} = \frac{k}{40.3 \cdot E_u^2} \Lambda^2.$$

The value of  $k$  has been determined by Townsend for a large range of values of  $E/p$  and by Crompton and Sutton, 1952, for values of  $E/p$  up to 20 volts/cm.mm.Hg. The agreement between the two sets of results is good and in the calculations following the values of  $D$ ,  $\mu/D$  etc. are recalculated from Townsend's values for  $k$  using the method of Crompton and Sutton which takes fully into account the velocity distribution of the electrons.

Fig. 13.4 shows the relationship between  $\eta$  and  $E_u/p$  as determined from the experimental points of Fig. 11.7 using the expression given above. It is necessary to include the results obtained by Clark and Prowse as the range of the

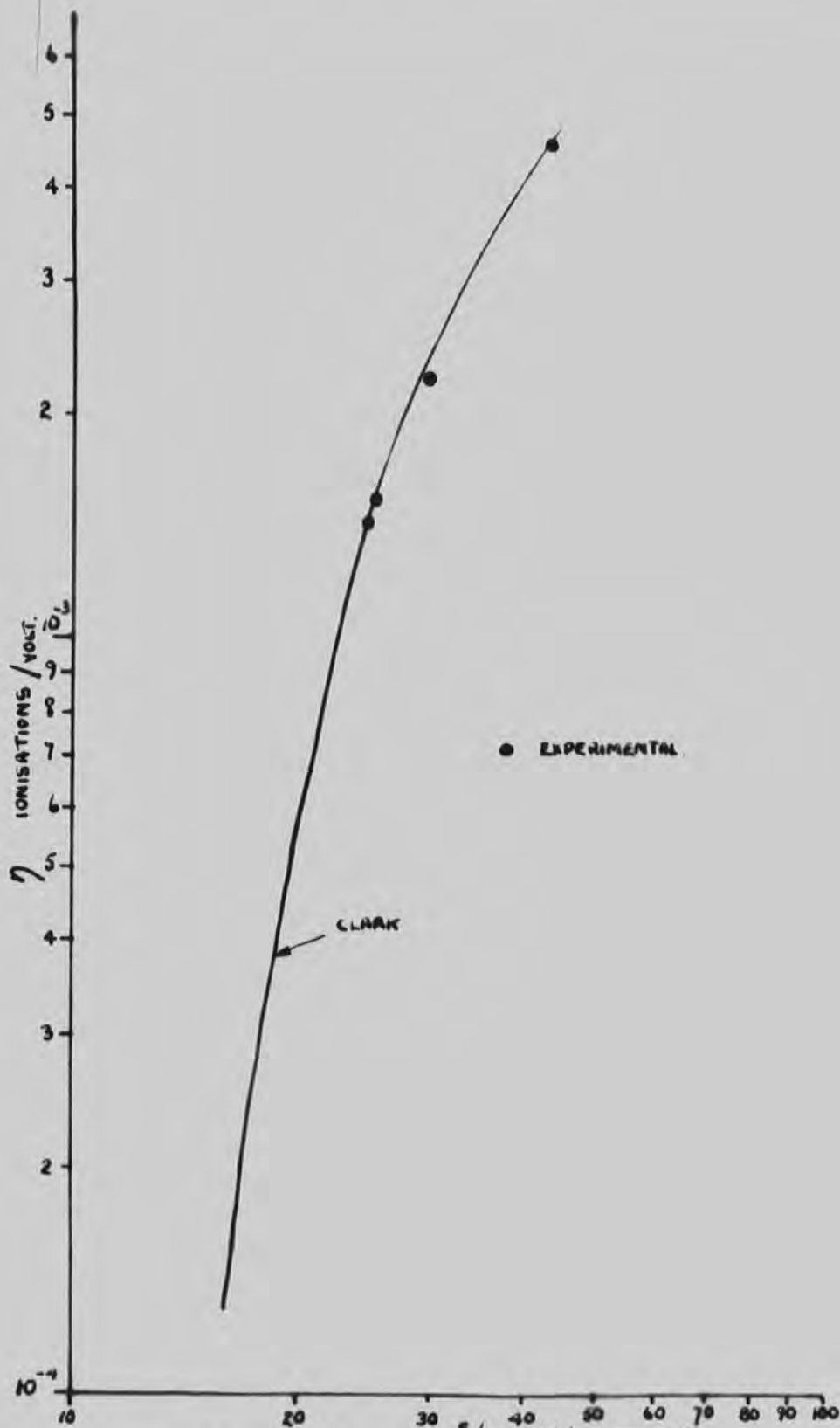


FIG.13.4

IONISING EFFICIENCY AS A FUNCTION OF  $E/p$  FROM EXPERIMENT AND CLARK, 1957.

present experiment was not wide enough to make it possible to determine all values of  $t_d$ .

Following the above argument it is necessary to perform an actual calculation of the lifetime of an electron under the experimental conditions in order that the process may be fully understood.

Example:

Let the pressure be 8 mm. of Hg., the value of the u.h.f. field be 220 volts/cm. and the value of the drift field,  $E_d$ , be 31.5 volts/cm.

From Fig. 13.3 the value of  ${}_2E_u/{}_0E_u$  is 1.21 for  $E_d = 31.5$  v/cm so that  ${}_0E_u$ ,  $(= {}_2E_u \cdot {}_0E_u / {}_2E_u) = 220/1.21$ , i.e. 182 volts/cm.

The lifetime of the electron as controlled by diffusion only,  $({}_0t_d)$  can now be determined for  ${}_0E_u/p = 182/8 = 22.8$  volts/cm.mm.Hg.

Also  $1/\Lambda^2 = 28.1 \text{ cms}^{-2}$  and  $D = 8.9 \times 10^{+4} \text{ cms}^2/\text{sec.}$   
 therefore  ${}_0t_d = \frac{\Lambda^2}{D} = 0.400 \text{ secs.}$

The values of  $\eta_0$  and  $\eta_2$  can be determined from Fig. 13.4. for  ${}_0E_u/p = 22.8$  v/c.m.Hg. and  ${}_2E_u/p = 27.5$  v/c.m.Hg.

$\eta_0 = 1.04 \times 10^{-5}$  ion./volt and  $\eta_2 = 1.85 \times 10^{-5}$  ion./volt.

$$\begin{aligned} \text{Hence } {}_2t_d &= {}_0t_d \cdot \frac{\eta_0 \cdot {}_0E_u^2}{\eta_2 \cdot {}_2E_u^2} \\ &= \frac{0.40 \times 1.04 \times 10^{-5}}{1.85 \times 1.21^2} \\ &= 0.15 \mu\text{secs.} \end{aligned}$$

The lifetime for different values of drift field and the same value of u.h.f. field are tabulated in Table 13.1. Determination of the lifetime using the method of Brown and Varnerin.

Brown and Varnerin, 1950, give an expression for the modified diffusion length of a gap when a small direct field is applied across the gap. This expression for the new length,  $\Lambda_d$  is:

$$\frac{1}{\Lambda_d^2} = \frac{1}{\Lambda^2} + \left( \frac{E_d}{2 \cdot D/\mu} \right)^2$$
 where D is the diffusion coefficient of the electrons at the particular u.h.f. field and  $\mu$  the mobility.  $\Lambda$  is the true diffusion length depending on the dimensions of the gap only.

This expression for  $\Lambda_d$  is obtained for an electron concentration in the gap associated with breakdown with no initial source of electrons other than casual, and may not apply for conditions before ionisation takes place when the distribution of the electron concentration is different (Fig. 13.5). The diagrams in Fig. 13.5 are drawn for the variation in electron concentration along the axis of the electrode system. At breakdown (c) the distribution is a sine function which is distorted by the direct field. The distribution before ionization (a) is derived from Chapter XII, where the concentration  $n_0$  is found to be

$$n = n_0 \left( \frac{e^{\mu E_d \cdot z/D} - e^{\mu E_d \cdot d/D}}{1 - e^{\mu E_d \cdot d/D}} \right).$$

TABLE 13.1

Hydrogen.

$p = 8 \text{ mm. of Hg. } \frac{1}{\Lambda^2} = 28.1 \text{ cm.}^{-2}$ , where  $\Lambda$  is the diffusion length.

Gap width,  $d$ , = 0.635 cm. U.h.f. field,  $E_u = 220 \text{ volts/cm.}$

$\frac{E_u}{p} = 27.5 \text{ volts/cm.mm.Hg.}$  and  $\eta_2 = 1.85 \times 10^{-5} \text{ ion/volt.}$

Drift field $E_d, \text{v/c.}$	$\frac{E_u}{E_d}$	$\frac{E_u}{p}$ v/c.m.Hg.	$D \times 10^{-4}$ c./sec.	$\frac{t}{d}$ $\mu\text{sec.}$	$\eta_1 \times 10^5$ ions/volt.	$\frac{t}{d}$ $\mu\text{sec.}$
0	1	27.5	10.5	.340	1.85	.340
9.45	1.05	26.1	10.0	.356	1.62	.283
15.6	1.11	25.0	9.5	.375	1.45	.239
23.5	1.15	23.9	9.2	.388	1.25	.198
31.5	1.21	22.8	8.9	.400	1.04	.154
39.5	1.25	22.0	8.6	.415	.90	.130
47.3	1.31	21.0	8.3	.430	.74	.105

Values of  $D$ , the diffusion coefficient from Townsend, 1947, and Crompton and Sutton, 1952.

Values of the electron lifetime from the experimental method.

The intermediate condition, where there is ionization but not enough to cause breakdown, is most likely to be as illustrated in (b) in which case the expression for  $\Lambda_d$  may be considered to be valid provided that  $n_0$  is small compared to the maximum value of  $n$ .

A calculation of the lifetimes of the electrons using this modified diffusion length and the expression  $t_d = \frac{\Lambda_d^2}{D}$  for the same conditions as these in the previous calculation result in Table 13.2 and the values for the lifetimes from the two methods and the times expected on the basis of the transit time are compared in Table 13.3.

From Table 13.3 it is seen that the lifetimes are in reasonable agreement over all the range although it could be expected that there would be better agreement over the longer times (greater ionization) than the shorter ones.

It has been shown how the electron lifetime can be determined from the conditions of the experiment itself provided that an ancillary breakdown experiment is performed to find the values of  $\eta$  at particular values of  $E/p$ . However, if the final object of the experiment is to measure the rate of ionization,  $\psi$ , it might be argued that the experimental method of determining the lifetime is not valid in that it involves determining the value of  $\eta$ , the ionizing efficiency which is itself related to  $\psi$  and that this lifetime will only be useful in finding how a stressed gap proceeds to

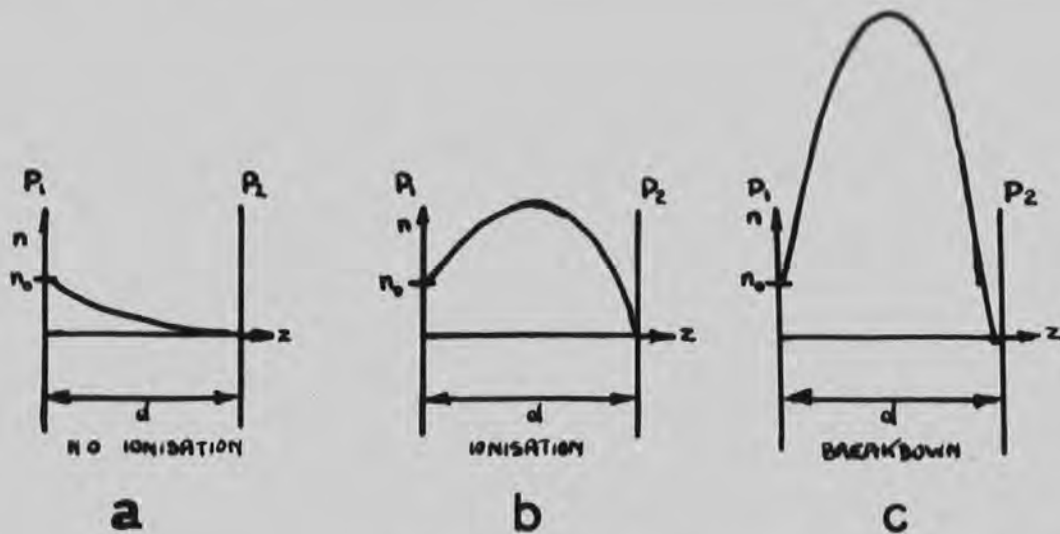


FIG.13.5

THE CHANGE IN ELECTRON DISTRIBUTION IN THE GAP AS THE U.M.F. FIELD IS INCREASED UP TO THE BREAKDOWN VALUE

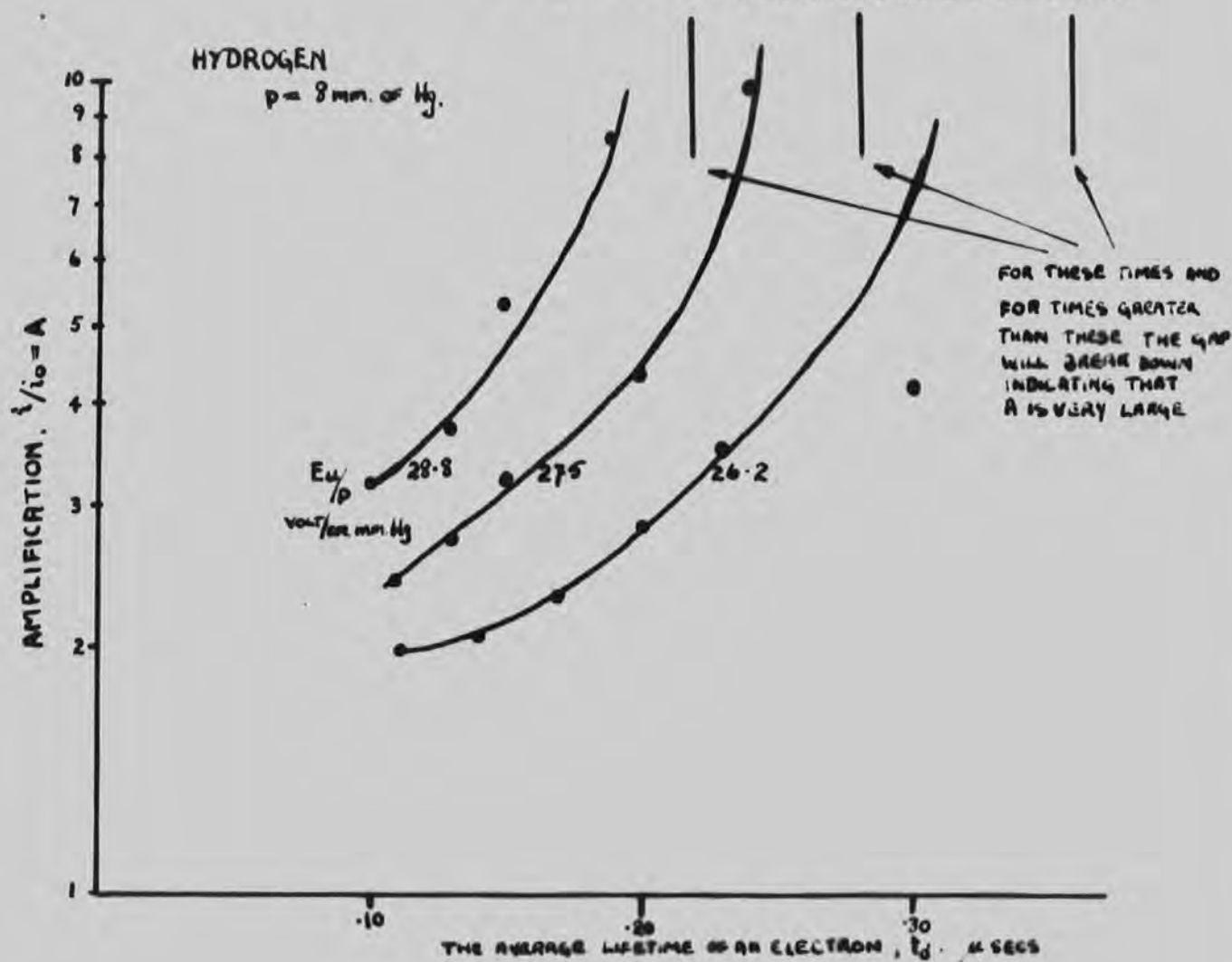


FIG.14.1

A GRAPH OF THE LOG OF THE AMPLIFICATION VERSUS THE ELECTRON LIFETIME.

TABLE 13.2

Hydrogen.

$p = 8 \text{ mm. of Hg. } E = 220 \text{ volts/cm. } E/p = 27.5 \text{ v/c.m.Hg.}$

$\frac{1}{\Lambda^2} = 28.1 \text{ cm.}^{-2} \text{ and } D = 10.5 \times 10^4 \text{ cm.}^2/\text{sec.}$

$E_d, \text{ drift field, v/c.}$	$\left(\frac{E_d}{2.D/\mu}\right)^2$ cm. <sup>-2</sup>	$\frac{1}{\Lambda_d^2}$ cm. <sup>-2</sup>	$t_d$ $\mu\text{sec.}$
0	0	28.1	.340
9.45	3.3	31.4	.300
15.8	9.2	37.3	.255
23.5	20.5	48.6	.200
31.5	37.7	65.8	.138
39.5	68.0	86.1	.110
47.5	66.0	94.1	.100

Values of  $D/\mu$  from Townsend, 1947., and Crompton and Sutton, 1952.

Values of the electron lifetime from the method of Brown and Varnerin.



TABLE 13.3

Hydrogen.

$p = 8$  mm. of Hg. Gap width,  $d = 0.635$  cm.

Drift field $E_d$	$t_d$ Experi.	$t_d$ Brn. and Varn.	$T$ Expected transit time.
volts/cm.	$\mu$ sec.	$\mu$ sec.	$\mu$ sec.
0	.34	.34	---
9.45	.28	.30	1.56
15.8	.24	.25	.93
23.5	.20	.20	.63
31.5	.15	.14	.47
39.5	.13	.11	.37
47.3	.11	.10	.31

Comparison of the values of the lifetime of the electrons from the two methods and also the expected transit time.

breakdown. But as the agreement between the results of the two methods for obtaining the lifetime is good, although they involve different arguments, it is thought that it is legitimate to use the experimental values of the lifetime to obtain more accurate values of  $\psi$  .

## CHAPTER XIV

### RESULTS AND DISCUSSION

Ideally, if the ionizing lifetime of the electrons were controlled by the drift motion from the emitting electrode to the collecting electrode under the direct field, they would have a definite lifetime such that if an electron leaves the emitting electrode at time  $t = 0$ , then both that electron, and the electrons produced by it due to collision ionization under the influence of the u.h.f. field, will arrive at the collecting electrode at time  $t = T$ , where  $T$  is the time for the initial electron to traverse the gap. Then if the rate of ionization is  $\psi$  ion pairs per second, one initial electron would produce  $e^{\psi T}$  electrons at the collecting electrode, and  $n_0$  initial electrons  $n_0 \cdot e^{\psi T}$ . Hence the amplification that would be expected is  $A = i/i_0 = e^{\psi T}$  and  $\text{Log}_e A = \psi T$ . If the conditions of the experiment are chosen so that the rate of ionization is constant, i.e. u.h.f. field constant, and  $T$  is varied by varying the drift field, then a graph of  $\text{Log}_e A$  against  $T$  should result in a straight line with gradient  $\psi$ .

However it has been shown from diffusion theory considerations that the lifetime of the electron is controlled not only by the drift motion but by a diffusive motion also (Chapter XIII). On replacing the transit time  $T$  by the lifetime as controlled by both processes ( $t_d$ ), and plotting

the graph of  $\log_e A$  versus  $t_d$  (Fig. 14.1 and 14.2) it can be seen that there is not a linear relationship. Furthermore, the condition for breakdown is that one electron leaving the gap has produced on an average one more during its lifetime to take its place, when  $\psi t_d = 1$  and the amplification should be equal to the value  $e$  indicating that the curves in Figures 14.1 and 14.2 should approach the value of  $2.7 (e^1)$  for conditions of breakdown. This is not the case.

Because the lifetime depends on diffusion as well as drift, its value as calculated is only an average time so that there is a finite possibility that electrons caused by one electron leaving the emitting electrode at a time  $t = 0$  remain in the gap considerably longer than time  $t = t_d$ . Also, because of diffusion, the electrons resulting from one initial electron can after a very short time be at any position in the gap so that the new electrons have as long a total lifetime as the initial one, and an equal probability of causing the same amount of ionization.

This necessarily alters the interpretation of the amplification as measured by the apparatus.

Consider one electron in the gap under conditions of transition to breakdown, when it produces one electron in its lifetime denoted by  $t_D$  and  $\psi t_D = 1$ . Now consider the condition that  $\psi$  is constant but the electron remains in the

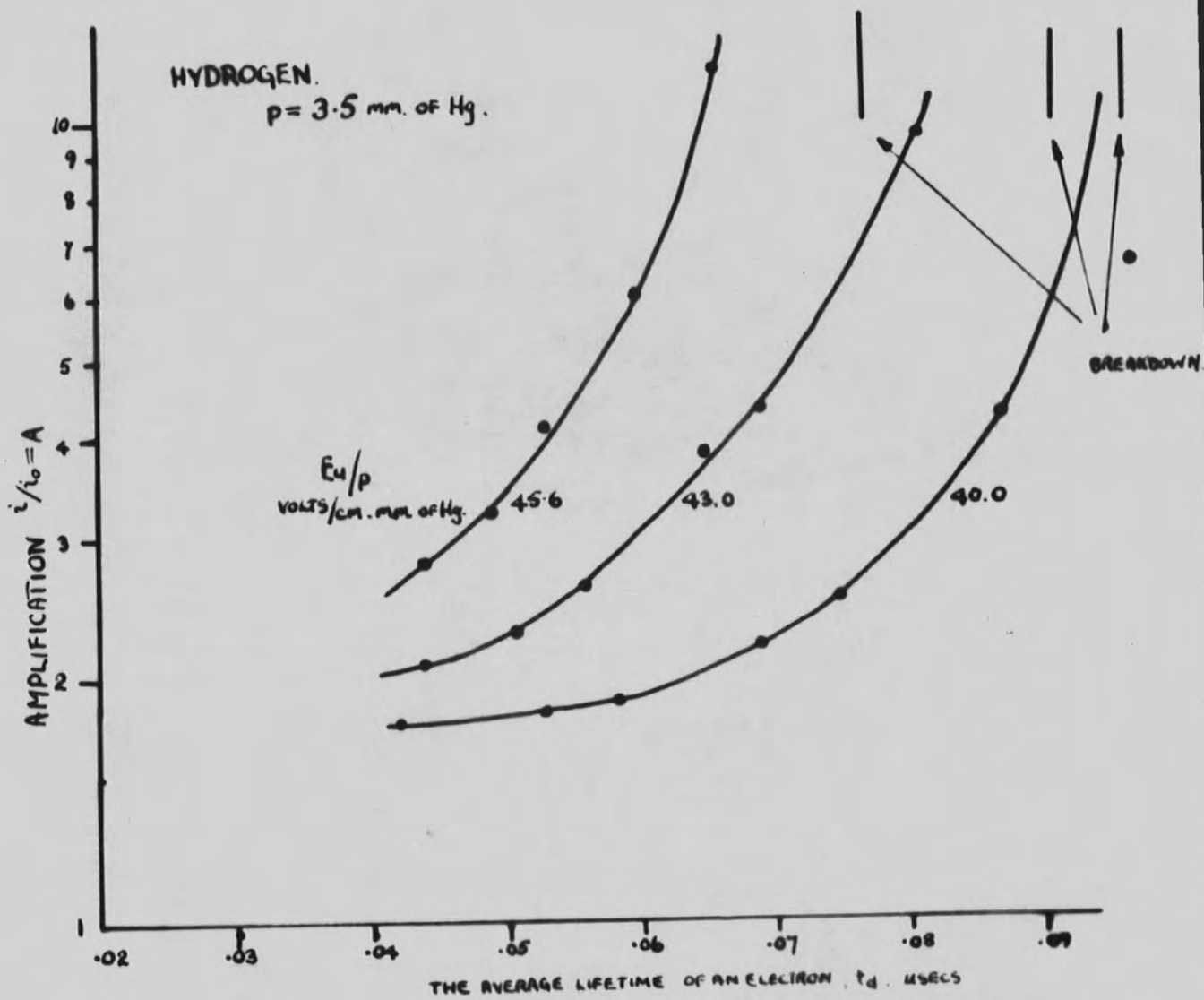


FIG.14.2

A GRAPH OF THE LOG. OF THE AMPLIFICATION VERSUS THE ELECTRON LIFETIME.

gap for a time  $t_d$ , shorter than  $t_p$  so that the breakdown condition is not achieved. An electron entering the gap at time  $t = 0$  will on the average leave the gap at time  $t = t_d$  and providing that the probability of ionization is constant will produce  $t_d/t_p$  new electrons, which will have an expectation of a life  $t_d$ . At time  $t = 2t_d$  on the average these electrons ( $t_d/t_p$ ) will have left the gap leaving behind  $(t_d/t_p)^2$  electrons.

Thus after time  $t = nt_d$  there will be left in the gap  $(t_d/t_p)^n$  electrons due to the initial electron at  $t = 0$ . Now consider the condition of electrons entering the gap continuously, such that one electron enters after each interval of time  $t_d$ , i.e. at  $t = 0, t = t_d, t = 2t_d$  etc., then after time  $t = nt_d$  there will be left in the gap  $1 + (t_d/t_p) + \dots + (t_d/t_p)^{n-1} + (t_d/t_p)^n$  electrons which will all leave in the next interval of time  $t_d$ , leaving behind the results of their collisions during their lifetime and the one new electron that enters the gap from the emitting electrode.

Thus after a long time a steady state will be reached where there are always  $1 + t_d/t_p + \dots$  (summed to infinity) electrons in the gap, and as there is no charge accumulation in the gap these electrons must be leaving after every interval of time  $t_d$ . Therefore if there are  $n_0$  electrons entering the gap per interval of time  $t_d$  there will be  $n$  electrons leaving, where  $n$  is given by the following

expression:

$$\begin{aligned}
 n &= n_0 \left( 1 + t_d/t_b + (t_d/t_b)^2 + \dots \right) \\
 &= n_0 \frac{1}{1 - t_d/t_b} \\
 &= n_0 \frac{t_b}{t_b - t_d}
 \end{aligned}$$

Now provided that all the electrons are swept to the collecting electrode by the unidirectional field the amplification as measured in the experiment will be:

$$A = i/i_0 = n/n_0 = \frac{t_b}{t_b - t_d}$$

But  $t_b = 1/\psi$  and therefore

$$A = \frac{1}{1 - \psi t_d}$$

and  $\psi t_d = \frac{A-1}{A}$  of which the quantities  $t_d$  and  $A$  are known. Figures 14.3 and 14.4 show graphs of  $t_d$  against  $\frac{A-1}{A}$  for two pressures.

It would be expected that when  $t_d = 0$  the amplification would be 1 when the lines should go through the origin. This is seen to be the case in Fig. 14.3 for a pressure of 5.5 mm. of Hg. but not for 8 mm. of Hg. (Fig. 14.4). However, both these graphs seem to be linear save for low values of  $t_d$  (Fig. 14.3) when the drift field is high. This may be expected, as the relationship  $\psi t_d = \frac{A-1}{A}$  depends on diffusion being predominant, i.e. high  $E_d/p$  and low  $E_u/p$ ; the gradient of these lines should be  $\psi$  and as  $\psi = W.\alpha$ , where  $W$  is the

HYDROGEN  
 $p = 3.5 \text{ mm. of Hg.}$

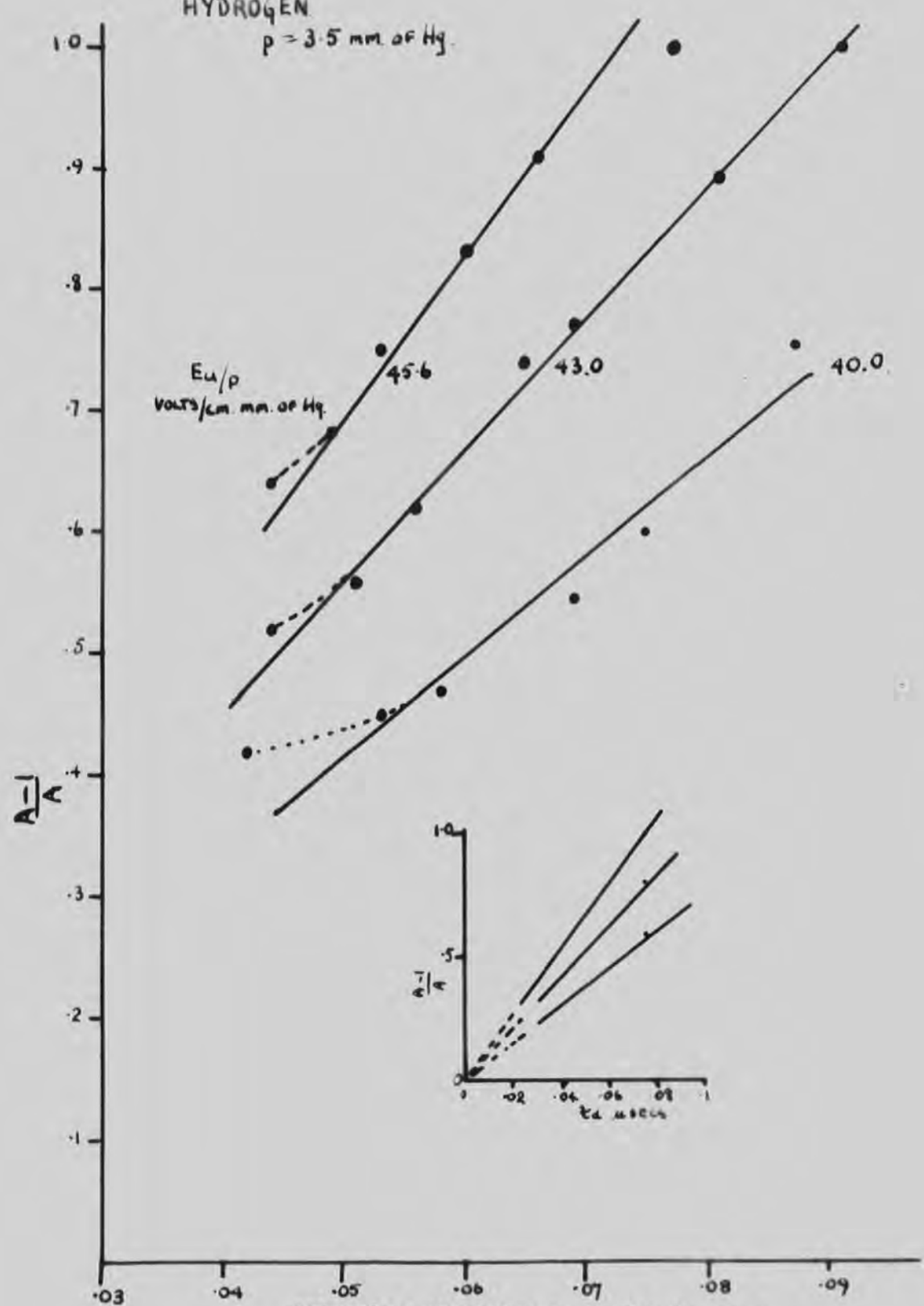


FIG.14.3 A GRAPH OF  $(A-1)/A$  VERSUS THE ELECTRON LIFETIME.



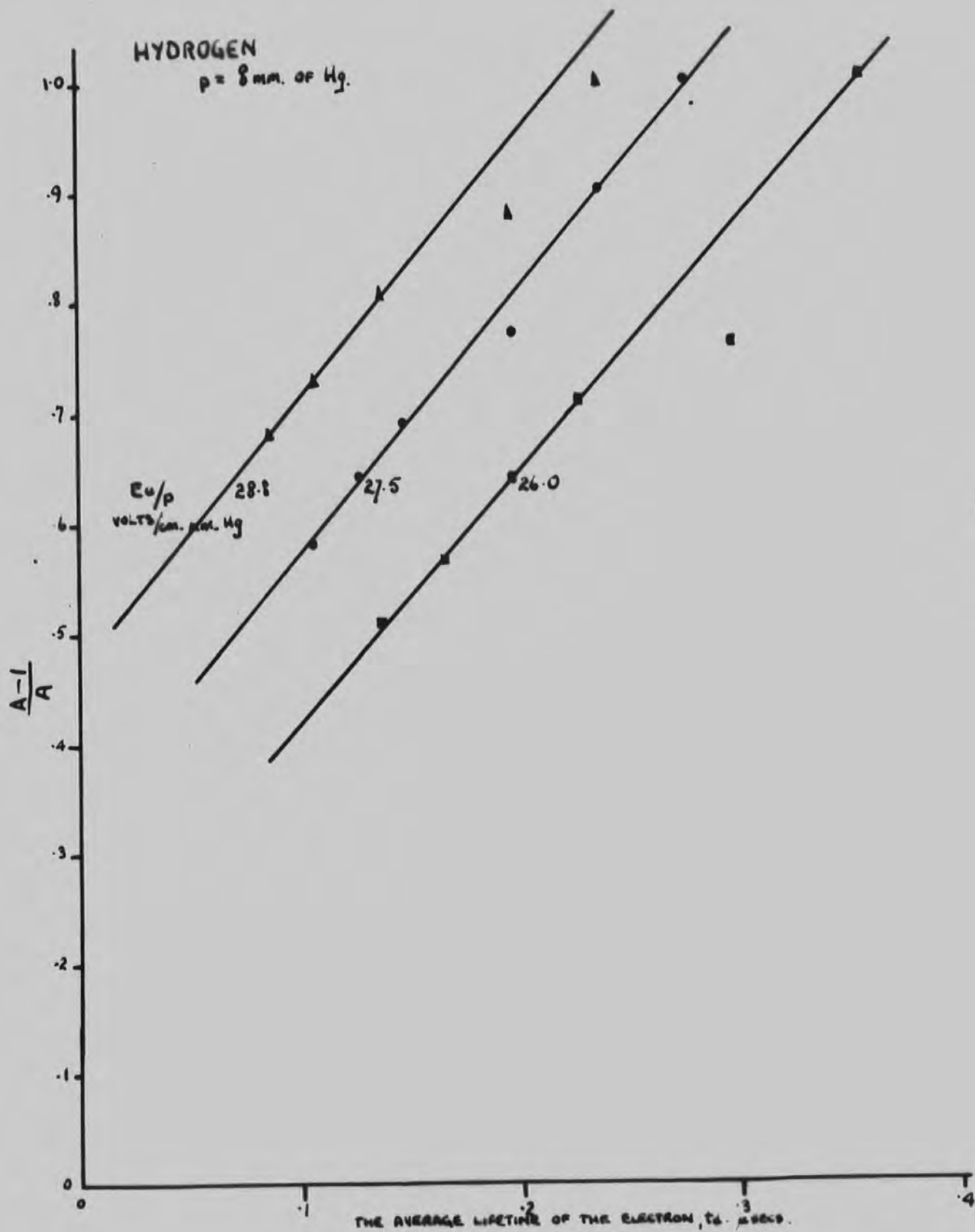


FIG. 14.4

A GRAPH OF  $(A-1)/A$  VERSUS THE ELECTRON LIFETIME FOR A PRESSURE OF 8 mm. OF Hg.

drift velocity determined from the mean value of the u.h.f. field,  $\alpha$  can be obtained and compared to the previously published values, Brown, 1958. The values of  $\alpha$  from the two sources are in Table 14.1 and seem to be in reasonable agreement considering the results are only preliminary.

In spite of the arguments and theoretical treatments outlined in this thesis it is not yet really clear what causes the drop in the current to the collecting electrode on increasing the u.h.f. field and how the drift field affects the lifetime of the electrons. It is becoming increasingly necessary to conduct experiments under similar electrical and pressure conditions but different gap widths and also to achieve the modulation and subsequent collection of the electrons. The former should especially help to indicate the cause of the current drop and the latter the effect of the drift field. This could be done by initially observing the transit time under the drift field alone (no u.h.f. field) which would be essentially a similar experiment to that of Bradbury and Nielson 1936, for low values of  $E/p$ . The u.h.f. field could then be applied and the effect on the transit time noted.

It is obvious that there is much more work to be done with the apparatus but it has been shown for the first time that the transition of a gas from the non-conducting to the conducting state under a u.h.f. field can be followed directly and it has been shown that the results so obtained are capable of being interpreted quantitatively.

TABLE 14.1

Hydrogen.

The average value of the u.h.f. field,  $E_a = \frac{2}{\pi} \cdot E_u$ .

$E_u/p$ v/cm.mm.Hg.	$E_a/p$	$\psi \times 10^{-6}$ ions/sec.	$w \times 10^{-6}$ cm./sec.	$p$ mm.Hg.	$\alpha/p \times 10^3$ ions/cm. mm.Hg. Experi.	$\alpha/p \times 10^3$ ions/cm. mm.Hg. Brown.
26.0	23.5	2.3	8.2		3.5	2.4
27.5	24.7	2.5	8.6	8	3.7	3.1
28.8	26.0	2.6	9.0		3.6	4.0
40.0	36.0	8.0	12.6		18.0	15.0
43.0	38.6	11.2	13.6		25.0	19.0
45.6.	41.0	15.8	14.5	3.5	27.0	21.0

The experimental results for  $\alpha/p$  are compared with those taken from Brown, 1958.

### ACKNOWLEDGEMENTS

The author is indebted to Dr. W.A. Prowse, his Research Supervisor, for his interest, assistance and criticism during the course of the work and to R.E. Long for the many helpful discussions.

He also wishes to thank Professor G.D. Rochester for his interest and advice and for the facilities made available at the Physics Department, South Road, Durham, and the Laboratory Staff for their constructive assistance.

Finally he wishes to express his gratitude to the British and Allied Electrical Research Association who provided a maintenance grant and contributed towards the cost of the apparatus.

### REFERENCES

- Biondi, M.A. and Brown, S.C., Phys.Rev. 79 946 (1950)
- Bradbury and Nielsen, Phys. Rev. 49 588 (1938)
- Braddick, H., 'The Physics of Experimental methods'  
Chapman and Hall (1954)
- Bruce, F.H., J.I.E.E. Pt.II 94 129 (1947)
- Brown, S.C., Handbuch der Physik, Vol. XXII. (1956)
- Brown, S.C., M.I.T. Tech.Report 283 June (1958)
- Brown, S.C., and Varnerin, L.J., Phys.Rev. 79 946 (1950)
- Clark, J., Ph.D.Thesis, Durham University. (1957).
- Crompton and Sutton, Proc.Roy.Soc. A 215 467 (1952)
- Fatechand, R., Nature London 167 566 (1951)
- Francis, C. and von Engel, H., Phil.Trans. 246 A 145 (1953-54)
- Fucks, W., Graf, L., Gurke, G., and Niesters H., (1957)  
3rd, Intern.Confer. Ion. in Gases, Venice.
- Gill, E.W.B and Donaldson, R.H., Phil.Mag. 12 719 (1951)
- Gill, E.W.B. and von Engel, H., Proc.Roy.Soc.A 192 446 (1948)
- Gill, E.W.B. and von Engel, H., Proc.Roy.Soc.A 197 112 (1949)
- Gutton, C., and H., Comptes Rendu 186 305 (1928)
- Herlin, M.R., and Brown, S.C., Phys.Rev. 74 291 and 902 (1948)
- Holstien, T., Phys.Rev. 69 50 (1946)
- Jones, C.V., E.R.A. Tech.Report. L/T334 (1956)
- Labrum, C.S.I.R., Australia. R.P.R.85 Dec. (1947)
- Lassen, Arch.f.Elek. 25 322 (1951)
- Llewellyn Jones, F., 'Ionization and Breakdown in Gases',  
Methuen. (1947)
- Llewellyn Jones, F., and Parker, A.B. Nature 165 960 (1950)

- Llewellyn Jones, F., and Parker, A.B. Proc.Roy.Soc. A  
215 185 (1952)
- Loeb, L., J.Franklin Inst. 205 305 (1928)
- Loeb, L., 'Fundamental Processes in Electrical Discharges in  
 Gases' John Wiley, (1939)
- Llewellyn Jones, F., and Morgan, G.D., Proc.Phys.Soc. B  
64 560 (1951)
- MacDonald, A., and Brown, S.C., Phys.Rev. 76 1692 (1949)
- MacDonald, A., Proc. I.R.E. March (1959)
- Margenau, Phys.Rev. 69 508 (1948)
- Maxwell, 'Electricity and Magnetism' Vol.II (1904).
- Monk, P.G. Thesis to be published. (1959)
- Paschen, F., Wied. Ann. 37 69 (1889)
- Paska. Ballistic Labs.Report. No.1944. (restricted (1955)  
 circulation)
- Penning, F., Naturwiss 15 818 (1927)
- Pim, J.A., J.I.E.E. 96 117 (1949)
- Prowse, W.A., J.B.I.R.E. 10 333 (1950)
- Prowse, W.A., E.R.A. Tech.Report. L/T358 (1957)
- Prowse, W.A., and Jasinski, W., Proc.I.E.E. Monograph 32 (1952)
- Prowse, W.A., and Clark J., Proc.Phys.Soc. LXXII 625 (1958)
- Reukema, L.E., A.I.E.E. 46 1314 (1927)  
47 38 (1928)
- Rogowski, Arch.f.Electrotech. 12 1 (1923)  
16 496 (1928)
- Thornton and Thompson, Jour. I.E.E. 71 1 (1933)
- Townsend, J.S., 'The Theory of ionization of gases by  
 Collision' Constable London. (1910)
- Townsend, J.S., 'Electrons in Gases' Hutchinson (1947)

## APPENDIX 1

### CALIBRATION OF THE DIRECT CURRENT MEASURING GALVANOMETERS.

The galvanometers  $G_1$  and  $G_2$  (Chapter IX) were calibrated roughly using a standard high resistance in series with a low source of potential.

Calibration of  $G_1$  (current leaving the filament), Tinsley galvo.  
Range. Sensitivity, amps/cm.

1	$1.06 \times 10^{-6}$
2	$1.5 \times 10^{-7}$
3	$4.8 \times 10^{-8}$
4	$7.0 \times 10^{-9}$

Calibration of  $G_2$  (current arriving at the collecting electrode)  
Range. Cambridge galvo.  
Sensitivity, amps/cm.

1	$4.8 \times 10^{-8}$
2	$2.7 \times 10^{-8}$
3	$5.4 \times 10^{-9}$
4	$1.1 \times 10^{-9}$

As the main interest lies in the ratio of two currents as measured on the same range ( $A = i/i_0$ ) the accuracy of the above calibrations need not be high and is in fact estimated as plus or minus 10%.

